5-2023

# The Fate of Fraxinus spp. in New Jersey : A Physioeconomic Evaluation of the Forest System and Infrastructure Implications

Erik W. Lyttek

# THE FATE OF FRAXINUS SPP. IN NEW JERSEY A PHYSIOECONOMIC EVALUATION OF THE FOREST SYSTEM AND INFRASTRUCTURE IMPLICATIONS

A DISSERTATION

Submitted to the Faculty of

Montclair State University in partial fulfillment

of the requirements

for the degree of Doctor of Philosophy

by

Erik W. Lyttek

Montclair State University

Montclair, New Jersey

Dissertation Chair: Dr. Pankaj Lal

MONTCLAIR STATE UNIVERSITY

THE GRADUATE SCHOOL

DISSERTATION APPROVAL

We hereby approve the Dissertation

THE FATE OF FRAXINUS SPP. IN NEW JERSEY A PHYSIOECONOMIC EVALUATION OF THE FOREST SYSTEM AND INFRASTRUCTURE IMPLICATIONS

of

Erik W. Lyttek

Candidate for the Degree:

Doctor of Philosophy

Graduate Program:

Environmental Management

Certified by:

[redacted]

Dr. Kenneth Sumner
Associate Provost for Academic Affairs and
Acting Dean of the Graduate School

5/12/23

Date:

Dissertation Committee:

[redacted]

Dr. Pankaj Lal
Dissertation Chair

[redacted]

Dr. Eric Forgoston

[redacted]

Dr. Ram Sewak Dubey

[redacted]

Dr. Onil Banerjee

# ABSTRACT

Though the impacts of pest infestation on forested ecosystems vary, the natural factors that facilitate outbreaks are of concern across multiple disciplines across the USA, affecting such diverse fields as economics, ecology, hydrology, atmospheric sciences, and pedology. Emerald Ash Borer (EAB) is a typical example of an aggressive invasive forest pest; it has proven difficult to eliminate, resistant to natural predators, and damaging to local flora. EAB has recently proliferated through the northern and mid-western forests of the USA, devastating the native population of ash trees (*Fraxinus spp.*), and has invaded an estimated 28% of all susceptible trees. In New Jersey alone, approximately 9% of forests are vulnerable to EAB attacks, potentially resulting in more than $2.7 billion in damages. The excessive cost of *Fraxinus* mortality presents serious implications for the state in the forestry and infrastructure sectors. Managing EAB is difficult, with critical uncertainties in the rates of infestation, mortality, and anthropogenically introduced controls. To address the imprecise future of *Fraxinus* under EAB predation we developed a set of novel models for exploring the spread of EAB and then further evaluated the potential risks to local electrical distribution infrastructure and ecosystem service provisioning. Through an original project that addresses this urgent, complex, and widespread challenge, utilizing New Jersey as a study area, we have i) developed a unique geospatial-based partial differential equation (PDE) model to predict EAB infestation through the forest system over a heterogeneous 2D landscape and estimate the mortality of both EAB, from introduced and native parasitoids, and *Fraxinus*, from EAB predation; ii) used an innovative tree fall risk structure to assess potential infrastructure impacts; and iii) examined ecosystem service losses caused by the infestation. We found that controlling the infestation requires early and intense introduction of parasitoids to maintain the forest structure. Failing to

do so will lead to millions of dollars of externalities in potential *Fraxinus* removals to protect critical infrastructure and the potential for increased erosion and sedimentation given the degraded state of the New Jersey Forest understory.

## ACKNOWLEDGEMENTS

I would like to acknowledge a great many people for the support and guidance necessary for this dissertation. This work would not have been possible without the guidance of Dr. Pankaj Lal, and without my doctoral committee consisting of Dr. Forgoston, Dr. Dubey and Dr. Banerjee. Additionally, without the assistance and companionship of my fellows I would have been unlikely to complete this work. The contributions of including Garrett Nieddu, Taylor Wieczerak, Gia Nguyen, Pralhad Burli, Archana Prasad, Meghann Smith, and many others were critical in both defining and finishing this project. The support of family and friends kept me moving forward and only slightly off-kilter, including Karl, Gary, Susan, Eugene, and Gracie Lyttek plus Benjamin Washechek among many others. Especially, I would like to thank my wife, Christina, without whose love and support I would not have been able to make it through some of the toughest and darkest days. I would also like to acknowledge Montclair State University, CESAC, and the NSF, all of whom partially funded this research.

# CONTENTS

## List of Tables

## List of Figures

# CHAPTER 1. INTRODUCTION

## 1 Emerald Ash Borer (EAB) Impacts on Ash Trees (*Fraxinus spp.*) In The United States- Complications and Impacts

Invasive species pose a significant threat to ecosystems through predation on native species, or by outcompeting native species for their niches. Approximately 50,000 invasive species have become established in the United States of America (USA), with related damages estimated at $120 billion per year (Pimentel et al., 2005). Current government policy around invasive species falls into two categories: preventing entry of a potential species and controlling the expansion of species already present. Several regulations have been implemented to manage invasive species, including the Lacey Act of 1900, Alien Species Prevention and Enforcement Act of 1992, Animal and Plant Health Inspection Service, and the Smuggling Interdiction and Trade Compliance Program (Animal and Plant Health Inspection Service, 2018).

Emerald Ash Borer (EAB), as an invasive species, has proven difficult to control. While this small beetle is benign in its natural Asian habitat, in the USA, it has caused significant harm to North American ash trees (*Fraxinus spp*. EAB, an Asiatic pest likely introduced from China in the mid-1990s, has already caused the death of millions of trees with a mortality rate greater than ninety percent in both timber and street trees (Poland et al., 2015). Collectively all standing *Fraxinus* were valued at up to $282.5 billion in the USA prior to infestation (Nowack et al., 2003; Poland et al., 2015). Though control of EAB is difficult, methods such as forest thinning, pesticide use, and firewood transport regulations have been considered in theoretical frameworks and implemented to some effect since the first infestation wave (McCullough et al., 2015; Mercader et al., 2011; Pugh et al., 2011; Siegert et al., 2015). Despite the ever-increasing range

of EAB, regulatory oversight is being discontinued in favor of methods aimed at limiting the effects of EAB infestation.

## 2 ENVIRONMENTAL AND ECONOMIC IMPACTS OF EAB

EAB's economic consequences present a significant liability for state and local municipalities, and time will only amplify this effect as the trees begin to age, decay and ultimately fall (Kovacs et al., 2011; Vanatta et al., 2012). *Fraxinus* trees, being a major element of the USA's rural and urban forests, are estimated to be worth at least $282.5 billion dollars (Nowack et al., 2003; Poland et al., 2015). More conservative reports from the Animal and Plant Health Inspection Service (APHIS) suggest that the total value of urban *Fraxinus* trees in the United States was somewhere between $20 and $60 billion dollars in 2006, due to being widely planted after mortality of other street tree species in the last century (Poland & McCullough, 2006). In addition, the United States Department of Agriculture (USDA) calculated the average total value of *Fraxinus* timber grown in the eastern United States at $25.1 billion per annum with approximately 8 billion *Fraxinus* trees present nationwide at the onset of EAB infestation (Nowack et al., 2003).

This high cost is due to several large ramifications from *Fraxinus* mortality, with the most obvious related to the loss of timber and products from EAB infestation (Poland et al., 2015). Beyond strict timber and biomass value, trees on urban and suburban property are valued because of their size, beauty, and other less fungible factors, like the reduction of the heat island effect, as opposed to the value of potential timber products (Arbab et al., 2022; Kovacs et al., 2011). This higher valuation for visible trees has led to some being protected by costly systemic insecticides (Poland et al., 2015). Before serious infestation damage began in New Jersey, there were an estimated 5.8 million dry tons of *Fraxinus* standing in the state (Crocker et al., 2017).

The *Fraxinus* population is set to decline rapidly with the onset of EAB infestation and State agencies will have to move forward in managing with the outfall for decades. Additionally, in areas where dead or dying trees are not removed, they are potentially a hazard to surrounding structures because of weakening timber that can easily and unpredictably fall (Audley et al., 2021; Oberle, Ogle, et al., 2018; Perry et al., 2018).

Another impact is the loss of ecosystem function due to decreased forest cover, carbon storage and potential runoff. Further, long-term effects such as mesophication, the ongoing shift of the Eastern hardwood forest to a less productive shade-tolerant system, could reduce ecosystem function into the foreseeable future (Dolan & Kilgore, 2018). Additionally, losses in the function of the water system, could mount substantially given the effects of previous insect outbreaks (Brantley et al., 2015). Numerous other negative outfalls from *Fraxinus* mortality will also accrue to one degree or another. Even lower infant birth weight has been related to local *Fraxinus* mortality to some degree, though this information is limited in its scope (B. A. Jones, 2018).

## 3 HISTORY AND MANAGEMENT OF EAB INFESTATION IN THE UNITED STATES AND CANADA

EAB was likely introduced to the Midwestern United States in the late 1990s and was first detected in Michigan in 1997 (Siegert et al., 2014). The continued spread of EAB has caused mass mortality up to 99% of *Fraxinus* with the survivors often being extremely fragmented (Poland et al., 2015). The natural spread rate of EAB is relatively slow, but is accelerated via anthropogenic spread, including inadvertent transport on wood products, vehicles and nursery supplies (Barlow et al., 2014; Buck et al., 2014; Evans, 2016). Several strategies have been presented by both public and private entities and evaluated as EAB management

options over the last two decades. These strategies include quarantine measures, trapping EAB adults, girdling *Fraxinus* as trap trees for EAB larvae, socially replacing and paying for private losses of affected trees, and the introduction of biocontrol agents to the forest system. However, the usage of these strategies has not been applied evenly across the USA with the most common method being the federal quarantine requirements and the next most utilized methods being biocontrol and trapping (Figure 1).

The federal quarantine program for EAB has been in effect since 2003 and has been further supplemented by various state and local budgets/initiatives (Diss-Torrance et al., 2018). The quarantine put control measures specifically on products that could carry EAB and enforced regulation on debarking timber before shipping outside the quarantine region, among other control measures. The quarantine was put in place once it was clear that EAB was firmly established while other options were explored (Animal and Plant Health Inspection Service, 2018). These efforts likely moderately delayed the spread of EAB by potentially limiting long range transmissions, which often caused jumps by hundreds of kilometers due to anthropogenic transport of infested material (Barlow et al., 2014; Buck et al., 2014; Poland et al., 2015).

Despite these measures, accidental releases occurred frequently and populations of EAB have established themselves as far away as Colorado and Georgia, far outside the natural range of *Fraxinus* in a highly isolated population of street trees. EAB has spread to over one quarter of the conterminous United States, making further quarantine an infeasible option (Animal and Plant Health Inspection Service, 2020; D. E. Jennings et al., 2016; Peterson & Diss-Torrance, 2012)**.** Without this control, the outlook for remaining *Fraxinus* is alarming. To control EAB without these extensive quarantine measures, current control efforts are now focused on the release of parasitoid wasps into infested North American forests. The hope is that these predators

will bring EAB into equilibrium with the remaining native *Fraxinus* allowing *Fraxinus* to maintain a foothold in the forest structure and adapt to the pressure of EAB over generations (Bauer et al., 2015; Liu et al., 2003, 2007). Biocontrol has had some impacts on EAB, but it remains to be seen if that will be sufficient to curtail the density and reproduction rate of EAB in North America (Animal and Plant Health Inspection Service, 2018; Burr et al., 2018; J. Duan et al., 2018).

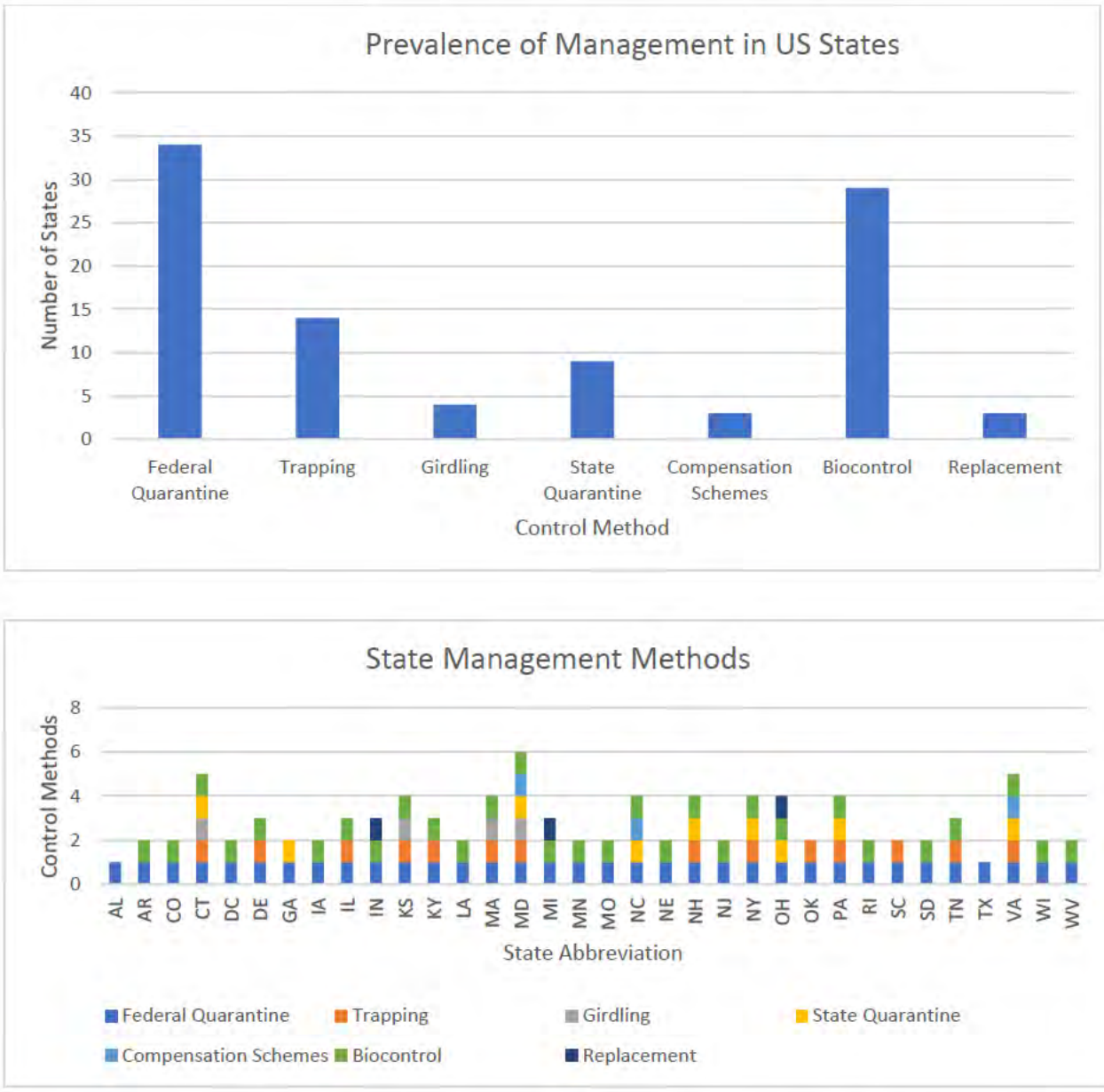


*Figure 1: Prevalence of Management Systems Across States. Sourced from State Department websites and published EAB management plans (Connecticut Department of Energy and Environmental Protection, n.d.; Delaware Department of Agriculture, n.d.; "Emerald Ash Borer Program," n.d.; Kansas Emerald Ash Borer Readiness and Response Plan, n.d.; Georgia Department of Agriculture, n.d.; Indiana Department of Natural Resources, n.d.; Iowa Department of Natural Resources, n.d.; Liu & Miller, 2014; Massachusetts Bureau of Forest Fire Control and Forestry & Massachusetts Department of Conservation & Recreation, n.d.; Meltzer, 2020; Michigan Department of Agriculture and Rural Development, n.d.; Missouri Department of Agriculture, n.d.; Nebraska Department of Agriculture, n.d.; New Hampshire Department of Agriculture Markets & Food, n.d.; New York State Department of Environmental Conservation, n.d.; Oklahoma Department of Agriculture & United States Department of*

*Agriculture, 2015; Parker-Renga & Peck, 2020; Pennsylvania Department of Conservation & Natural Resources, n.d.; Smith, n.d.; South Dakota Game, Fish and Parks, 2020; State of New Jersey Department of Agriculture, n.d.; Tennessee Department of Agriculture, 2018; Trickel, 2021; University of Arkansas Division of Agriculture Research and Extension, n.d., n.d.; University of Kentucky College of Agriculture, Food and Environment, n.d.; Virginia Department of Forestry, n.d.; West Virginia Division of Forestry, n.d.).*

Without a population of resistant trees or establishment of high predation of EAB by other species, EAB will remain one of the most damaging and highly invasive insect pests in North America (J. Duan et al., 2017; Kovacs et al., 2011; McCullough et al., 2015; Poland et al., 2015). Mass mortality of domestic *Fraxinus* populations has been the overwhelming result so far in the North American system since the introduction of EAB (Jennings et al., 2015; Morin et al., 2017; Poland et al., 2015). Since the mid-1990s (Siegert et al., 2014), EAB has been spreading across North America from the Midwest and central Canada, and is now spreading aggressively through the Eastern seaboard, causing billions of dollars in damages just from the loss of landscaping trees alone, spiking municipal budgets and causing negative impacts to real estate prices (Evans, 2016; Hauer & Peterson, 2017; Kovacs et al., 2011; Pugh et al., 2011). *Fraxinus* mortality has resulted in an estimated $282.5 billion in potential damages to the productive quality of hardwood forests across the USA and Canada (Evans, 2016; Hauer & Peterson, 2017; Kovacs et al., 2011; Pugh et al., 2011). Additionally, the pest poses additional risk for both Western and Eastern Europe, as EAB has recently been introduced to Europe and has proven damaging to the local *Fraxinus spp.* population. It has already caused significant issue in European Russia and many other parts of Eastern Europe and has been listed in the European Union as a priority quarantine pest (Orlova-Bienkowskaja & Bieńkowski, 2018, 2020).

## 4 BIOCONTROL AS A CONTROL MECHANISM OF EAB

With the repeal of the quarantine measures in place, more emphasis in recent years has been placed on managing EAB infestation as opposed to controlling their spread (Animal and Plant Health Inspection Service, 2018; J. Duan et al., 2018). The goal is to bring EAB into equilibrium with the local forest system and allow *Fraxinus* to slowly regrow into the forest after the initial wave of the infestation. There is some merit to this hypothesis as there are instances of North American native *Fraxinus* surviving in the native range of EAB in Northeastern China as introduced trees and landscape trees (J. Duan et al., 2011).

Through extensive testing both in EAB's native environment and controlled conditions in North America, several different species of wasps, known to prey on EAB life stage cycles almost exclusively, have been tested and determined safe for release in North America (Liu et al., 2007; Parisio et al., 2017). These parasitoids have been released in various combinations across the USA. Not all species can be released in all locations due to their varied environmental tolerances. In our study area, the species being used are *Spathius galinae, Tetrastichus planipennisi*, and *Oobius agrili*. *Spathius galinae* has shown lower rates of establishment and persistence in trials but remains viable and a key component due to its ability to prey on EAB larvae that other species cannot. This enhanced ability is due to a longer ovipositor than *Tetrastichus planipennisi* allowing it to parasitize all EAB regardless of tree size, while *Tetrastichus* is constrained to EAB larvae on smaller trees (Diameter at Breast Height (DBH)<20cm) due to bark thickness (J. Duan et al., 2018). *Oobius agrili* is even more constrained compared to the other two species, as it is a strict egg parasitoid. Despite these limitations, *Oobius agrili* has shown promise in several post-release surveys (J. Duan et al., 2019). Additionally, there are recorded instances of native predators opportunistically preying on

EAB. For example, various woodpecker species have been known to prey on EAB in the later stages of infestation; but this has little effect on managing the pest as the trees are already well past recovery when this becomes a serious EAB mortality factor (D. E. Jennings et al., 2016). Some native wasps have been recorded preying on EAB in the Northeast and Canada; *Phasgonophora sulcata* was recorded parasitizing EAB larvae up to a rate of 40% in some cases in 2015 (Roscoe et al., 2016).

## 5 AFTERMATH OF INFESTATION BY EAB AND POTENTIAL FOR REGROWTH OF *FRAXINUS SPP.*

Biocontrol methods may take many years to firmly establish and spread to protect the local tree species (J. Duan et al., 2018), which leaves many of the remaining trees in a position where they will fail before the system balances out. This gap between treatment and result places the impetus of landscape level *Fraxinus* regrowth on the seed bank and regeneration of stump sprouts, similar to many previously extirpated species (Kashian, 2016).

Studies have shown that despite EAB related mass mortality, stump sprouting and regrowth are common in the core of the EAB mortality region and in open-grown *Fraxinus* that receive significant light at ground level (Robinett & McCullough, 2019; Siegert et al., 2021). In Kashian et al. (2018), a follow-up study on the persistence of *Fraxinus* in the core of the infested region in southeastern Michigan, *Fraxinus* was persistent only in areas where the canopy had been significantly impacted by the death of overstory *Fraxinus.* This opened canopy allowed significant light to reach the forest floor and enabled shade-intolerant genera, like *Fraxinus*, to regrow. However, other multi-year studies at other sites show that stump sprouts are not reaching maturity and are failing as the seed bank is slowly exhausted (Burr et al., 2018; Kashian, 2016; Robinett & McCullough, 2019; Siegert et al., 2021). This led to greater rates of mesophication

in these mixed forests due to the formation of small forest gaps in the canopy that are seemingly insufficient for the regrowth of shade-intolerant species like *Fraxinus* (J. Duan et al., 2018).

This continued decline in the diversity and structure of the highly productive deciduous Eastern forests of North America has been progressing for decades due to shifts away from an open, fire-driven structure and towards a less productive, closed multi-layer system (Dolan & Kilgore, 2018; Nowacki & Abrams, 2008). In areas with low density of *Fraxinus*, like the study area, forest recovery to the previous species composition is unlikely once the initial cohort of trees have died. The failure to recover in these forests will have an unquantified ecological impact on species diversity and density in the Eastern United States as productivity shifts (Dolan & Kilgore, 2018; Goins et al., 2013; Kutta & Hubbart, 2018; Nowacki & Abrams, 2008). This long-term impact brings the focus to introducing parasitoid wasps in a way that maximizes their potential to reduce EAB damage, while *Fraxinus* within mixed stands are still standing. So far, surveys on the released parasitoids have shown highly variable local success with current release patterns in North America and we need to understand these dynamics to inform release and recovery guidelines (J. Duan et al., 2019; D. E. Jennings et al., 2018; D. E. Jennings et al., 2016; Margulies et al., 2017; Parisio et al., 2017).

## 6 STUDY AREA

We centered our study in Northern New Jersey as the leading edge of the EAB infestation was just entering New Jersey at the beginning of this study and even now is dealing with the fallout as patches of trees die out. Northern New Jersey was chosen because of several factors, one the forest has a scattered population of *Fraxinus* through the canopy; second, the geographic vicinity to the granting institution of this degree, and third, the urbanized character of the region that will increase the possibility for negative externalities. Overall, *Fraxinus* made up about 10%

of the forest canopy in New Jersey in 2018 and was scattered evenly throughout the canopy primarily in the Northwest of New Jersey (Figure 2). These trees will not likely be harvested due to the lack of a domestic forest industry as timberland is only partially privately owned and is not often utilized for timber (Crocker et al., 2017). This lack of utilization distances the local markets from more immediate repercussions, weighting the impacts more heavily to change in forest quality than timber production. Additionally, the state is heavily populated even its rural areas, which leaves it more vulnerable to negative externalities from infrastructure damage leading to continued debate on removal vs. replacement efforts (Arbab et al., 2022; Bíl et al., 2017; Hughes et al., 2021; Poulos & Camp, 2010).


*Figure 2: Map of* Fraxinus spp. *Distribution in New Jersey. Compiled in ArcGIS by Erik Lyttek with original data sourced from Wilson et al. 2012. Units Presented are in square meters per hectare.*

## 7 RESEARCH OBJECTIVES

This research addresses three primary objectives: i) the effectiveness of biocontrol as EAB spreads through the forests; ii) a combined methodology to address the spread of EAB damages from *Fraxinus* fall rates on incident infrastructure; and iii) impacts on local services and ecosystem quality stemming from losses in the forest (Figure 3).

In chapter 2, we developed a fine resolution spatiotemporal model to assess EAB in New Jersey forests. Various types of models have proved to be an invaluable tool to aid managers' attempts to control outbreaks (Anderson & Dragicevic, 2016; BenDor & Metcalf, 2006; Cuddington et al., 2018; Mercader et al., 2016; Pitt et al., 2009; Prasad et al., 2010). Here we

focus on the county level spread to assess the effectiveness of current biocontrol options (Jennings et al., 2018).

In chapter 3 we address the looming threat to infrastructure from mortally injured *Fraxinus*, we evaluated the Northwestern counties of New Jersey for the potential of damage to electric distribution infrastructure from *Fraxinus* mortality and fall (Balducci et al., 2006; Warwick et al., 2016). We integrated a GIS estimate for powerline position and length as a function of space and integrated it with conditions associated with *Fraxinus* fall. We used this result in a cost benefit analysis to show the relationship between *Fraxinus*, power infrastructure and cost.

Chapter 4 provides a comprehensive overview with an ecosystem service evaluation, we have integrated an InVEST-based ecosystem mapping methodology with the results from the EAB-*Fraxinus* PDE model(Brown & Quinn, 2018; Hamel et al., 2015; Hamel & Bryant, 2017). Through this we address the looming possibility of increased mesophication and the more immediate concerns about forest productivity in the region for water quality, nutrient export and sedimentation (Hamel & Bryant, 2017; Polasky et al., 2011; Sims et al., 2013). By completing this project, we have aimed to address gaps in invasive species management and spatial theory while working to minimize the negative externalities from EAB-related tree loss in the North America.

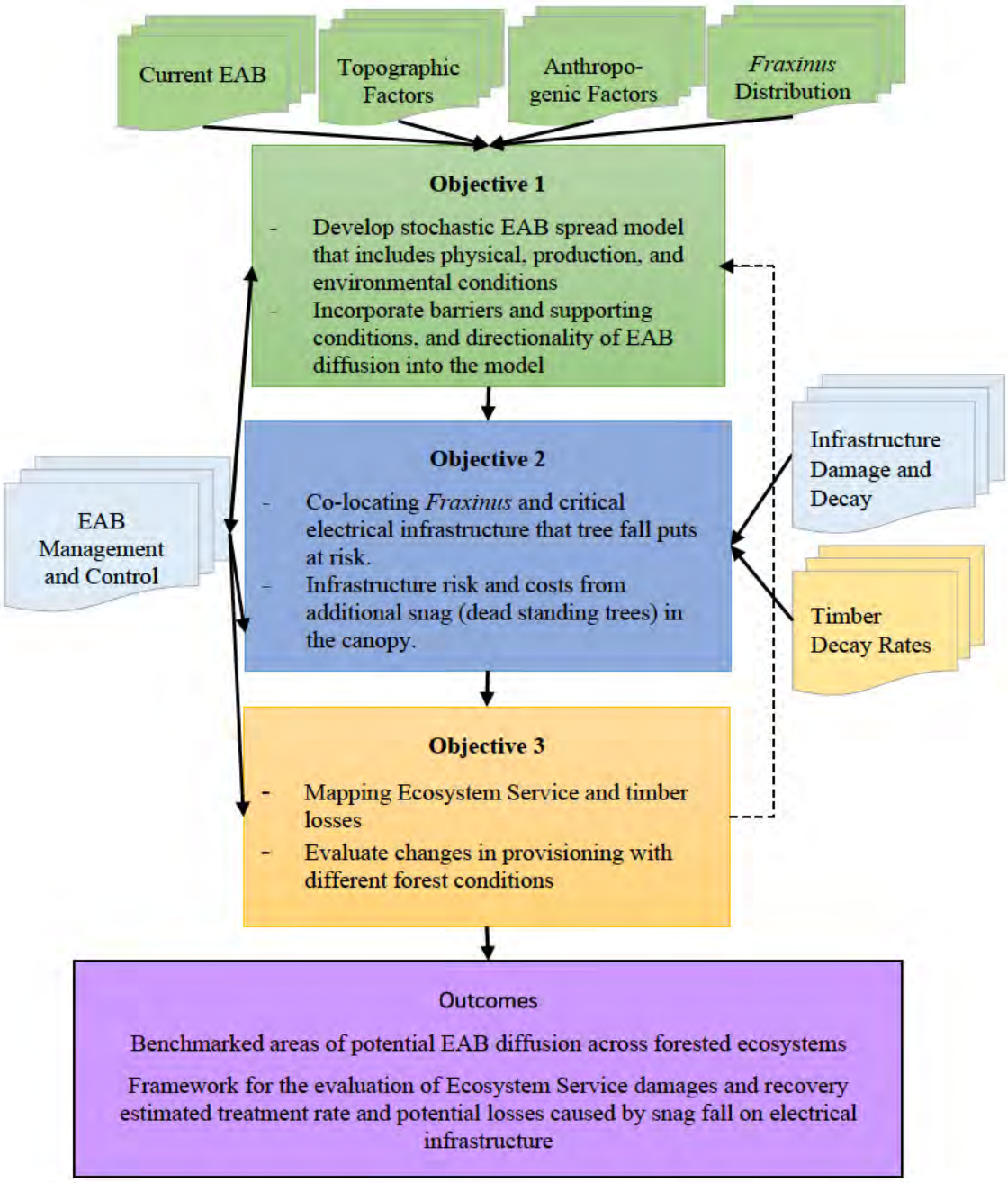


*Figure 3: Project Outline and Objectives*

# CHAPTER 2. EAB SPREAD AND PARASITOID DYNAMIC MODELING IN NORTHERN NEW JERSEY

Emerald Ash Borer (EAB) has severely impacted the ecosystems and economies of North America by devastating the local *Fraxinus* population. To assess potential bio-control scenarios and methods we have developed a dynamic partial differential equation (PDE) model with stochastic introductions of EAB to simulate their spread, growth, and impact on *Fraxinus*. Due to EAB, mesophication is being accelerated in deciduous North American forests and losses of *Fraxinus* are accumulating. Current USA government policies regarding EAB management are focused on biological control as a method to preserve *Fraxinus* in the forest structure. However, the variability in the effectiveness of biological control, outside of the native environment of EAB, could lead to the inability of *Fraxinus* to recover. Poor *Fraxinus* recovery is validated by the results of our model, which show that forests only recover if bio-control vectors are introduced when EAB does not have a strong regional presence. With current policies in place, it is likely that continued introductions of parasitoids will be largely ineffective if not deployed to follow the leading fringe of the infestation where populations are still weak and isolated.

EAB, an invasive forest pest, is responsible for billions in damage to ash trees (*Fraxinus spp.*) in the USA and Canada. The losses to forest structure and landscape values will have decades-long impacts. To control EAB, East Asian parasitoid wasps are being introduced to reduce populations, but their long-term effectiveness is uncertain. To address the gap in parasitoid deployment and to increase the chance of success of this intervention strategy, we have developed a PDE model to assess a variety of control scenarios. Our model results show the biocontrol program leaves local *Fraxinus* without a clear path to recovery when intervention is delayed by just a few years. Model results suggest that the poor recovery of *Fraxinus* in mixed

forests pose a significant barrier to regrowth across the original range of *Fraxinus* without swift action. The loss of overstory *Fraxinus* shows a potential obstacle in the primary mission to preserve *Fraxinus* in the forest system. By prioritizing early establishment of parasitoids, we show that *Fraxinus* is able to persevere with a regional endemic population of EAB. In our model, we examine a heterogeneous *Fraxinus* distribution and the behavior of EAB populations under parasitism at observed and theoretical rates in a simulated environment. We find that EAB populations, if allowed to reach epidemic levels, did not decline significantly enough upon introduction of parasitism to allow the survival of any mature *Fraxinus*. This model result emphasizes the necessity of prioritizing release and establishment of parasitoids in large regions with low to moderate EAB populations, rather than focusing on site-based mitigation efforts.

## 1. INTRODUCTION

EAB is an East Asian wood boring beetle that preys primarily on trees in the genus *Fraxinus*. EAB feeds on the fringes of *Fraxinus* leaves as an adult and as a larva it feeds on the inner bark of the tree. With large populations of EAB, this feeding strategy causes a failure in the *Fraxinus* vascular system and a subsequent die back of the tree from the canopy down, usually resulting in mortality (BenDor & Metcalf, 2006). In its natural habitat, local *Fraxinus spp.* have co-evolved with EAB and so are not in significant danger of severe infestation unless there is another significant source of stress (J. Duan et al., 2013, 2017). Additionally, numerous species have evolved to prey upon EAB in its native range. This intense predation of EAB has allowed even vulnerable North American members of the *Fraxinus* genus to survive in the native range of EAB where they are shielded both by resistant trees and significant EAB mortality (Buck et al., 2014; J. Duan et al., 2018). Current policies hope to successfully introduce some of this biological control system to support North American *Fraxinus* and to control EAB populations

(J. Duan et al., 2018; Liu et al., 2007). This interplay of factors led us to develop a model for the spread and development of EAB under variable levels of parasitoid predation.

EAB predation is defined by both native and exotic species(J. Duan et al., 2018; Lyons, 2015). Before the introduction of exotic parasitoids, North American native species, such as parasitoid wasps supplemented by various woodpecker species, were not sufficient to effectively limit EAB growth (BenDor et al., 2006; Jennings, Duan, Bauer, et al., 2016; Poland et al., 2015). However, the exotic parasitoids introduced to the North American hardwood ecosystem are still an uncertain solution due to issues monitoring their populations to ensure establishment and spread (J. Duan et al., 2019; D. E. Jennings et al., 2016; Quinn et al., 2022). While some initial data has come out due to post-release site sampling and multi-year forest transect monitoring, samples are varied and inconsistent across introductions and samples as parasitoid recovery methods evolve and become more effective over time (J. Duan et al., 2018; M. I. Jones et al., 2019; Quinn et al., 2022). Methods for sampling are understandably difficult to verify; EAB itself is often difficult to note until later stages of infestation, even more so for the parasitoids that prey upon it (D. E. Jennings et al., 2016; Poland et al., 2015; Prasad et al., 2010). Jones et al. (2019) and Quinn et al. (2022) confirmed parasitoid spread along sampled transects. This research confirmed that EAB parasitoids exhibit the ability to travel with the EAB wave to some degree, but the rates are variable and often at a significant lag (M. I. Jones et al., 2019; Quinn et al., 2022). The former study confirmed the spread of only one species, *Tetrastichus planipennisi*, and a multi-year lag to the detected EAB wave, while the second study confirmed the spread of two species several years after introduction and only to 14km from release sites. The latter study reported similar average rates of predation along their sampled transects, though with higher variability for one sampled species. These are two isolated studies; without the widespread

ability to accurately track parasitoids, which have swiftly become the primary EAB mitigation strategy in the USA (Animal and Plant Health Inspection Service, 2018, 2020), modeling their interactions proves to be a necessity. While more accurate data on the spread and dispersal of EAB parasitoids will be forthcoming in the next years, the infestation wave will likely have continued its spread and will have already encompassed the majority of the range of *Fraxinus* leaving any conclusions on the appropriate application and dispersal of reared parasitoids too late (Gould et al., 2020; Poland et al., 2015).

Currently four species of parasitoid wasps are being introduced that have demonstrated limited, or no, predatory inclination toward other species in North America. Among these, three are being actively released in the Northeastern region of the USA as control measures: (1) *Oobius agrili* (an egg parasitoid), (2) *Tetrastichus planipennisi* (a larval parasitoid) and (3) *Spathius galinae* (another larval parasitoid). Hundreds of thousands of wasps have been and continue to be released across North America every year, with a focus on releases in areas that are currently experiencing the epidemic stage of infestation (Gould et al., 2020). These releases add a new layer into the balance equation for EAB reproduction and *Fraxinus* decline, but with limited information on the spread and effectiveness of these parasitoids, they cannot be simulated as a discrete agent in a modeling environment. We have developed our model to address the introduction of these new uncertain parasitoids on a landscape scale to help further and understand the current federal policy for introducing parasitoids for EAB control. This policy is currently focused on establishing parasitoids, but exposes current forest stands of *Fraxinus* to heavy infestation, which could lead to the collapse of these stands if parasitism cannot bring EAB populations into equilibrium (Dolan & Kilgore, 2018; D. E. Jennings et al., 2016).

Our model framework directly addresses the issue of parasitoid release and parasitism rates to evaluate the growth and recovery of *Fraxinus* populations (Kashian, 2016). There have been numerous previous efforts to model EAB, which have focused on the ability of EAB to infest new regions, evade quarantine efforts, and cause economic externalities among other topics (Ali et al., 2015; Anderson & Dragicevic, 2016; BenDor & Metcalf, 2006; Kovacs et al., 2011; Mercader et al., 2016; Prasad et al., 2010). Methods used have been varied and have been specialized to address specific concerns of the time. Initial modeling efforts towards EAB, like other invasive pests, was focused on predicting potential locations of spread, based on limited data on the pest itself. These efforts continued through much of the initial stages of EAB's spread across the USA and made use of simple diffusion and kernel models at first (BenDor et al., 2006; Muirhead et al., 2006) and later shifted to more complex models calibrated specifically on the ability of human interaction to spread the pest along transport networks (Prasad et al., 2010; Yemshanov et al., 2012). These models did not need to integrate all of the biological information about EAB and *Fraxinus* to achieve their goals. Additionally, they were unconcerned with measuring the decline in the canopy and focused on spread and shorter term population dynamics (Mercader et al., 2016; Prasad et al., 2010).

After largely focusing on the regional spread of EAB, and with many regions now buckling under the weight of this new invasive pest, modeling efforts shifted towards simulating interventions at the smaller experimental plot to the local scale, often covering only a town or city park, and the potential response of EAB to treatment and control and the forest canopy over a few square kilometers at most. Examples of model frameworks that have been utilized at this extent include agent-based models (Anderson & Dragicevic, 2016), mechanistic simulations (Mercader et al., 2016) and multi-patch stochastic models (Ali et al., 2015). These models all

worked to bring context to the problem of managing EAB actively in small spaces and with direct interventions such as the introduction of a parasitoid in Anderson & Dragicevic, (2016), who used an agent-based model to simulate the interactions of EAB, *Fraxinus* and a single parasitoid over the area of a city park. However, this simulation had to be severely curtailed due to computational and data collection limitations. Mercader et al. (2016) and Ali et al. (2015) are similarly limited due to their respective constructions (Ali et al., 2015; Mercader et al., 2016). Limitations in the former include, a mechanistic description of short range EAB interactions with active control measures, girdling and insecticide treatment, while the latter simulates control methods for reducing firewood transport, a vector for EAB transmission, between locations. In the author's opinion these frameworks have served their purpose well, but for the task of preserving *Fraxinus* under almost constant predation in a wide-ranging forest system by using parasitoids that are still poorly understood in their capacity and speed we need a new framework that emphasizes the statistical likelihoods of EAB spread and allows for parasitoid predation at a wide range of rates at the landscape scale. We have entered a place where we understand the problem intimately, but not the solution currently being implemented. A different method, such as an agent-based model, would address the concerns with available data over the small-scale, but that is not feasible at the landscape scale due to excessive computational requirements when dealing with billions to trillions of individual EAB. Additionally, the years of studies needed to understand the dispersal and survival of all implemented parasitoids are in their very first stages and will likely not be published until they are of little use in North America (Anderson & Dragicevic, 2016; J. Duan et al., 2019; M. I. Jones et al., 2019; Quinn et al., 2022). With the situation shifting from active to passive control regimes, (Animal and Plant Health Inspection

Service, 2020) a different modeling context is needed to contextualize the widespread use and integration of passive control in the forest system as a whole as opposed to the micro-scale.

We use a PDE model where adult EAB diffuse across the region of interest with random dispersal of satellite populations across a range of *Fraxinus* densities to demonstrate the effects of EAB and parasitoid spread on *Fraxinus* survival. This model structure allows us to track the size of both adult and immature EAB populations and how they interact with *Fraxinus* and the effects of parasitoids at both the local and regional level. PDE models have been found to be exceptionally useful as data quality increases (Gilbert et al., 2004). Early experiments with a leaf mining insect, *Cameraria ohridella,* in Eastern Europe showed that a stratified dispersal function most closely approximated the recorded spread of this insect across the region when compared with a simple diffusion and a leptokurtic dispersal model (Gilbert et al., 2004). A similar model was applied to the spread of the invasive Argentine ant, *Linepithema humile*, in New Zealand (Pitt et al., 2009). This study led to the beginnings of an adaptable mechanistic spatially explicit model with integrated landscape generator and metrics. This model was constructed with the goal of being an adaptable model system with numerous plug-in potentials (Lustig et al., 2017). The strength of models, like this, is that it allows for the integration of numerous biological and supplementary systems while remaining tractable.

Another well-known problem is the spread and dispersal of the aggressive mountain pine beetle (MPB), *Dendroctonus ponderosae,* which causes mass mortality of pine, *Pinus spp.*, in Western North America (Powell et al., 2018). To track MPB, Powell et al. (2018) used a similar stratified diffusion model to Pitt et al. (2009), altered to track the influence of the Allee effect. The Allee effect is a determinate on the ability of MPB to successfully attack a tree and reproduce, and these dynamics were verified by aerial photography of the densely invaded stands

of pine. Unfortunately, due to the diffuse nature of *Fraxinus*, it is impossible to verify EAB spread with similar methods.

To overcome the issues surrounding EAB we first used GIS data from the Forest Inventory and Analysis program (FIA) to create the base layer of the model and create a heterogenous environment based on actual forest structure (Wilson et al., 2012). This environment does have the drawback of no possibility of aerial tracking due to the diffuse nature of *Fraxinus* where in the majority of cases it is a minor component of the canopy (Kashian, 2016; Powell et al., 2018; Wilson et al., 2012). We track EAB through a two-stage life cycle from larvae through adult and assess its impacts on *Fraxinus* stands. However, simple diffusion of EAB adults does not accurately capture their biology. To account for differential spread we have a variable diffusion coefficient based on the health and density of the local *Fraxinus*. EAB are less likely to pass by a forest dense in *Fraxinus*, and will also be more likely to have overall reduced spread if there is a large amount of stressed *Fraxinus* and vice versa (Mercader et al., 2009; Siegert et al., 2010; Tluczek et al., 2011). Finally, parasitism would prove challenging to justify in other model structures given the sparse level of data that has been collected regarding the spread and the responses of EAB to parasitoids and their response to EAB in an unfamiliar environment. Predictions from this model can help facilitate informed decision-making regarding best management practices to implement parasitoid control methods and to perform accurate economic analysis.

A source of concern with PDE modeling methods is the issue of compounding error in PDE models over long simulation periods as each previous step influences the next (Stępniak & Jacobs-Crisioni, 2017). Additionally, it does not fully account for EAB's tendency to make mid- to long-range jumps beyond the leading edge of the infestation. We addressed this trait of EAB

by introducing stochastic long range spread events parameterized according to a dendrochronological study for EAB infestations from the original infestation site (Siegert et al., 2014). Stochastic factors impacting diffusion have been found to be an appropriate tool for mapping insect spread when large numbers of individuals are present and the result becomes more chaotic (Pitt et al., 2009; Yemshanov et al., 2009).

The success or failure of EAB parasitoids in increasing *Fraxinus* survival will determine the future of this species in North America. Parasitoid success has shown substantial sensitivity to the introduction time (J. Duan et al., 2018; Knight et al., 2013). Maximizing the potential of a full *Fraxinus* recovery will be dependent on increasing predation of EAB to such levels that the remaining EAB preying on *Fraxinus* are not significant enough to cause mass mortality (Berry et al., 2017; Gould et al., 2020). We evaluated this model at two scales in areas of Northern New Jersey: (1), a single small county with known infestation point and date, and (2), three larger northwestern counties of the state, which have experienced a much more general and widespread infestation pattern, to demonstrate the extensibility of our model framework.

## 2. METHODOLOGY

We have developed a reaction-diffusion PDE model in a heterogeneous system that integrates EAB diffusion with *Fraxinus* density and stress. EAB diffusion among an adult subclass and consumption of *Fraxinus* by a larval EAB subclass occurs over a four-month period, known as the “on-season,” while the remaining eight months, known as the “off-season” are characterized by EAB larva dormancy, adult mortality, and some regrowth of *Fraxinus*. During the off-season, EAB larva consumption is discontinued to mimic EAB overwintering under the bark of host *Fraxinus* (Poland et al., 2015). For tractability, the study area is divided

into cells measured in square meters; all values in the model are adaptable to different cell sizes and inputs, but are parameterized with 100 square meter cells (Lyttek et al., 2019).

Given the relationship of EAB to its immediate environment, we integrate the dynamic spread of EAB into the system. We allow EAB adults to spread through the forest system, influenced both by the biological limits of EAB, as well as the impacts of the forest system on EAB's spread. EAB spread is defined this way as several previous researchers have noted that the quantity and quality of *Fraxinus* have a strong influence on the speed and direction of EAB spread (Mercader et al., 2009, 2011; Siegert et al., 2010). We define the spread and diffusion of EAB adults in the active season as:

$$\frac{\partial \mathrm{E_a}}{\partial \mathrm{t}} = D_u A_s \left(\frac{\partial^2 E_a}{\partial x^2} + \frac{\partial^2 E_a}{\partial y^2}\right) - \Omega E_a + RL, \quad (1)$$

where $E_a$ is the population density of EAB adults, $D_u$ governs the diffusion of EAB, $A_s$ alters the rate of diffusion at each location as a function of the quantity of *Fraxinus* (Appendix 1.4), Ω is a testing mortality factor for EAB adults, $R$ is the random risk for additional populations, and $L$ is the rate at which new EAB adults are introduced to a region. Additionally, $x$ and $y$ are respectively the latitudinal and longitudinal spatial variables, while $t$ is the time variable in months.

The presence of EAB adults, then results in the continuation of the species with a larval EAB class. This class of EAB is the one that damages *Fraxinus* and in the next season becomes the next generation of EAB adults. On-season growth of EAB larva is modeled as the system of equations,

$$E_l(t_i) = E_l(t_i) + min\left(\bar{G}P_{oa}E_a(t_i), \bar{C}A(t_i) - E_l(t_i)\right),$$

*( 2)*

$$\frac{dE_l}{dt} = -\omega E_l - P_{mp}E_l$$

*( 3)*

where $E_l(t_i)$ is the population density of EAB larva at the current timestep. Additional EAB are added at a rate $\bar{G}P_{oa}E_a(t_i)$ up to a limit of $\bar{C}A(t_i) - E_l(t_i)$, where $\bar{G}$ is a growth constant for EAB, $E_a(t_i)$ is the EAB adult population present, $P_{oa}$ is the rate of parasitism by the egg parasitoid *Oobius agrili* (Table 1), $\bar{C}$ is an EAB larva crowding constant, and *A* is the density of *Fraxinus*. Equation (2) serves to add the minimum number of EAB larva to the system by comparing the growth due to incident EAB adults and the carrying capacity of the system. We assume that all additional EAB larva are added at the beginning of the timestep and then experience mortality through time according to eq. (3). In eq. (3), $E_l$ is the larval population and time, *t*, is defined in months, ω is a random mortality factor and $P_{mp}$ is the parasitism rate caused by both *Tetrastichus planipennisi* and *Spathius galinae* (Table 1). These two species are combined due to their similar predation styles. *Tetrastichus planipennisi* is highly effective at parasitizing EAB on trees with thin outer bark and *Spathius galinae* is much more effective on the thicker bark layer of older trees, but both prey on maturing EAB larvae (J. Duan et al., 2017; Murphy et al., 2017).

*Table 1: Ranges of Predation Rates from Parasitoids*

| Parasitoid | Standard | High | Low | Source(s) |
|---|---|---|---|---|
| *Oobius agrili* ($\boldsymbol{P_{oa}}$) | *0.225-0.495* | *0.225-0.62* | *0.12-0.495* | (J. Duan et al., 2018) |
| *Tetrastichus planipennisi* and *Spathius galinae* ($\boldsymbol{P_{mp}}$) | *0.14521-0.50182* | *0.14521-0.83268* | *0.02027-0.50182* | (J. Duan et al., 2018; J. Duan et al., 2019) |
| *Phasgonophora sulcata* ($\boldsymbol{P_{ps}}$) | 0.32±0.02 | 0.34±0.02 | 0.30±0.02 | (Roscoe et al., 2016) |

Now that the EAB side of the model system is defined, the next step is to define the system to simulate the *Fraxinus* that are affected by EAB larva. The temporal evolution of *Fraxinus* is dependent on the abundance of EAB, the state of the stand and the estimated room available to grow given by the observed canopy cover. The equation for *Fraxinus* growth is defined by,

$$\frac{dA}{dt} = \begin{cases} \hat{G}_1 \mathrm{A} - \hat{\mathrm{C}}\mathrm{F_c}\mathrm{A}^2 - \mathrm{CE_l A} & \frac{\mathrm{A}}{\mathrm{A_{(1)}}} \geq 0.1\mathrm{F_c} \\ \hat{G}_2 \mathrm{A} - \hat{\mathrm{C}}\mathrm{F_c}\mathrm{A}^2 - \mathrm{CE_l A} & \frac{\mathrm{A}}{\mathrm{A_{(1)}}} < 0.1\mathrm{F_c} \end{cases}, \quad (4)$$

where *Fraxinus* trees do not spread outside their cells and are assumed to grow and regenerate according to the growth rate $\hat{G}_1$ or $\hat{G}_2$ depending on the state of the stand, either maturing stands ($\hat{G}_1$), or significantly damaged stands ($\hat{G}_2$), $\hat{\mathrm{C}}$ is the crowding rate for Fraxinus sourced from the Forest Vegetation Simulator northeastern USA variant (Dixon & Keyser, 2016), where the density of *Fraxinus* is limited by the carrying capacity $\frac{\widehat{G_1}}{\hat{C}F_c}$ when *t* approaches infinity. Crowding is modified by $F_c$, which describes the local canopy cover, as an approximation for forest cover (U.S. Geological Survey, 2019). The growth rate $\hat{G}_2$ assumes that trees that have been

excessively damaged are able to exhibit aggressive stump sprouting and that there is no crowding out by different species, which allows *Fraxinus* the most optimal expected chance of recovery and resilience (Kashian, 2016). *Fraxinus* is reduced due to consumption by EAB larva with a rate *C* normalized by the density of *Fraxinus*. By normalizing consumption according to the density of *Fraxinus*, we integrated the crowding EAB experiences more directly given the algebraic population updating we utilized. This derivation for the consumption coefficient *C* abstracted the biology of EAB, but allowed for the incorporation of crowding as seen on overcrowded specimens in both lab and field data (J. Duan et al., 2013). Equations (1-4) describes the situation during the active season of the year, but during the off-season, we consider EAB adults to die-off leaving only the larval stage and *Fraxinus* as actively simulated elements.

During the off-season, the governing equations are given by eqs. (5-8),

$$\frac{dE_l}{dt} = 0, \tag{5}$$

$$E_a = 0, \tag{6}$$

$$\frac{dA}{dt} = \begin{cases} \hat{G}_1 \mathrm{A} - \hat{\mathrm{C}} \mathrm{F_c} \mathrm{A}^2 & \frac{\mathrm{A}}{\mathrm{A}_{(1)}} \geq 0.1 \mathrm{F_c} \\ \hat{G}_2 \mathrm{A} - \hat{\mathrm{C}} \mathrm{F_c} \mathrm{A}^2 & \frac{\mathrm{A}}{\mathrm{A}_{(1)}} < 0.1 \mathrm{F_c} \end{cases},$$

, (7)

and

$$E_{a\left(\frac{t_0}{T_1}\right)} = E_{l\left(\frac{t_{12}}{T_0}\right)}(1 - P_{PS}).$$

*(8)*

The off-season equations are simpler as EAB larva are dormant under the bark of host trees, reducing their consumption rate to zero. Additionally, we assume that during the off-season EAB do not reproduce, but upon emergence in the following *T*, experience a spatially variable mortality rate of $P_{ps}$, as measured for the native parasitoid *Phasgonophora sulcata* in North American forests. Native species have been observed preying on EAB. Many of these species do not cause significant impacts, or are linked to mortally damaged *Fraxinus* and so do not a play a significant role in controlling EAB, as is the case with woodpeckers (Jennings, Duan, Bauer, et al., 2016). In our model we integrate a recently studied northern species of parasitoid wasp, *Phasgonophora sulcata*, to account for native mortality factors. *Phasgonophora sulcata* has been shown to have a substantial impact on EAB mortality throughout the range of *Phasgonophora sulcata* range (Gaudon et al., 2018; Lyons, 2015; Poland et al., 2015; Roscoe et al., 2016). Often other mortality factors for EAB are similar in degree and extent to it across most of North America, including woodpeckers, other parasitic wasps and natural resistance, but these are implicit within our crowding ($\bar{C}$) and fecundity ($\bar{G}$) rates in eq. (2) (Gaudon et al., 2018; Lyons, 2015; Poland et al., 2015). A summary of units and sources is found in Table 2, additional information on the derivation and model structure can be found in Appendix 1.

*Table 2: Truncated List of Derived Parameters and Sources. Diffusion was simulated across a range that was used in all simulations and multiple runs varied the rate of parasitism, Fraxinus growth varied between mature specimens and sapling level growth depending on if the stand had been severely damaged by EAB. The two growth coefficients simulate the sprout back effect that has been observed in other states where stump sprouting has proved to be common and vigorous (Robinett & McCullough, 2019).*

| PARAMETER | NAME | UNITS | SOURCE |
|---|---|---|---|
| $D$ | Diffusion Rate | $\frac{m}{T}$ | (Mercader et al., 2009; Siegert et al., 2010) |
| $D_U$ | Diffusion Coefficient | $\frac{m^2}{t}$ | (Mercader et al., 2009; Siegert et al., 2010) |
| $A_S$ | Combined Stress Factor | $\frac{A_b}{A_{sf}}$ | (Mercader et al., 2009, 2011; Siegert et al., 2010) |
| $R$ | Risk | *Binary* | (Ali et al., 2015; Mercader et al., 2016; Siegert et al., 2014) |
| $L$ | Introduction Rate | $\frac{E_a}{t}$ | (Siegert et al., 2014) |
| $\overline{G}$ | EAB Growth | $\frac{\text{inl}}{\text{ina} \cdot \text{t}}$ | (McCullough & Siegert, 2007; Mercader et al., 2016) |
| $\overline{C}$ | EAB Crowding | $\frac{\text{in}}{\text{m}^2\text{BA}}$ | (J. Duan et al., 2013; McCullough & Siegert, 2007) |
| $\widehat{G_{1-2}}$ | *Fraxinus* Growth | $\frac{1}{t}$ | (Schlesinger, 1990) |
| $\widehat{C}$ | *Fraxinus* Crowding | $\frac{\text{ha}}{\text{m}^2 \cdot \text{t}}$ | (Dixon & Keyser, 2016; Gould et al., 2020) |
| $F_C$ | Forest Cover | $\frac{1}{\%}$ | (U.S. Geological Survey, 2019) |
| $C$ | EAB Consumption | $\frac{\text{ha}}{\text{inl} \cdot \text{t}}$ | (McCullough & Siegert, 2007) |

Parameterization of the model was based upon experimental results from regions of the USA already affected by EAB. *Fraxinus* density data for Essex, Warren, Sussex and Morris Counties, in Northern New Jersey are based upon 2009 data from the Forest Inventory and Analysis Program (FIA) (Wilson et al., 2012), while canopy cover was sourced from the

National Land Cover Database (U.S. Geological Survey, 2019). Growth over the lifetime of *Fraxinus* was simplified into a pair of growth factors based upon the growth of *Fraxinus* from establishment to failure and the growth of pole size timbers and saplings respectively (Dixon & Keyser, 2016; Schlesinger, 1990). The carrying capacity of *Fraxinus*, $34.44\frac{m^2}{ha}$ was sourced from the northeastern variant of the forest vegetation simulator (FVS) (Dixon & Keyser, 2016). EAB growth was approximated as $12\ (\pm 0.57)$ EAB born per year per individual based on multiple sources (McCullough & Siegert, 2007; Mercader et al., 2011, 2016). The average distance diffused under ideal circumstances was estimated to be 27.027 meters per year using Mercader's (2009) negative exponential function. To account for differential flight distances by EAB adults, 80 different diffusion simulations with a range of diffusion coefficients (*D*) varied based on a linear spread distance between 5m and 805m (separated by 10m increments) were performed. The theoretical flight diffusion could then be further extended by site conditions up to 8-kilometers when *D* is 805m and *Fraxinus* is not present because of the influence of the $A_s$ variable. *D* is the precursor to $D_{u,}$ which is measured in linear distance and years, rather than $D_u$ which is measured in months and area. EAB larva carrying capacity on *Fraxinus* was found to be $88.9\ (\pm 4.6)$ beetles per square meter of *Fraxinus* surface area based on the experimental results of McCullough et al. (2007).

To set our starting state we used an estimate of Fraxinus populations calculated in 2012 by Wilson et al. (2012). Though this sample point is aging, the estimated change in *Fraxinus* populations between 2009 and 2019 for our study area, are on the order of 5-10 percent, using Statewide inventories, which is very little considering the intrinsic error involved in forest inventory data. Additionally, the overall trend for the inventory is very flat, exhibiting more oscillation than strict growth or decline (Figure 4).

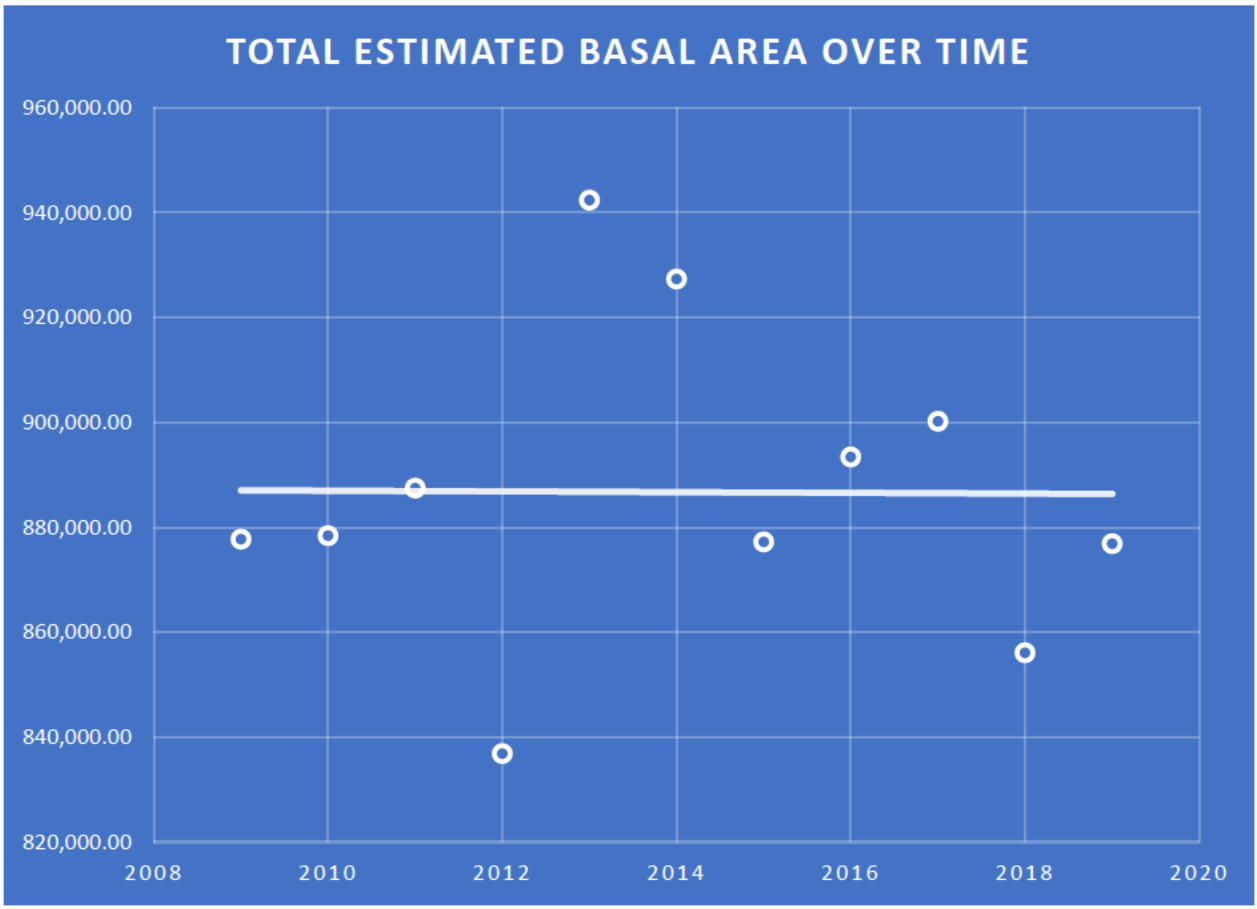


*Figure 4: The Overall Trend in Assessed* Fraxinus *Populations from 2009 to 2019. The trend for the assessed quantity of* Fraxinus *has remained almost flat for the last decade. This graph shows the total Basal area assessed for New Jersey in square feet between 2009 to 2019. Basal area is the assessed cross-sectional area for a tree or forest.*

## 3. RESULTS AND DISCUSSION

We tested numerous scenarios in our model to assess the role of EAB population and the impact of timing on parasitoid effectiveness. We found that timing of EAB parasitoid introduction proved to be more influential towards overall management of EAB damage and *Fraxinus* mortality than the parasitism rate of the parasitoids themselves. When infestations are identified early on and biocontrol is quickly deployed, there is higher likelihood for *Fraxinus* success as well as an increased time span before EAB could reach densities that cause *Fraxinus* population collapse. The variables for the different scenarios include the rate of parasitism and

the year of establishment. The parasitism was varied between average, high and low estimates, while the year parasitism was introduced was varied between the first year the seventh year and the eleventh year.

In Table 3, we include a range of outcomes from scenarios on the introduction of parasitoids to counter EAB in the forest system. Without any parasitism, EAB quickly overwhelms the local *Fraxinus* and eliminates it (Scenario 1). Overall, these results indicate that situations in which EAB parasitism is below average can prevent immediate extirpation of local *Fraxinus*, but does not prevent its eventual collapse, just provides a slower decline (Scenario 4). As the effectiveness of treatment increases, EAB populations never reach levels that cause a decline in the forest system with EAB populations measured in the thousands to millions rather than billions compared to no parasitism (Scenario 2-3). However, as the introduction time of parasitism begins later and later the effectiveness also declines with results beginning to approach uncontrolled EAB (Scenarios 8-10). This trend becomes problematic when compared with the results from Scenarios 5-7, where parasitoids are introduced after EAB have been present for seven years and then linearly rise to full strength over 4 years to mimic monitored releases of parasitoids, which are released when there is a small dense core of EAB that can be parasitized (J. Duan et al., 2017; Gould et al., 2020; Margulies et al., 2017; Parisio et al., 2017). These scenarios show poor results for *Fraxinus* survival unless rates rise to the high end of estimates (Scenario 6).

*Table 3: Primary Scenario Results in End State. Scenario 1 is the control, while the remaining nine scenarios are permutations on two variables related to parasitism. The first term is the year in which parasitism is established (Year 1, 7 and 11 of the simulation). The second is the rate of parasitism once the parasitoids are established which are referenced in Appendix 1, Table 15.*

| Scenario | Variation | EAB Year 21 (ln) | *Fraxinus* Year 21 ($m^2$ BA) |
|---|---|---|---|
| Scenario 1 | No Parasitism | $5.37e^9$ | $5.23e^3$ |
| Scenario 2 | Average | $9.09e^6$ | $2.12e^5$ |
| Scenario 3 | High Rates | $5.23e^3$ | $2.12e^5$ |
| Scenario 4 | Low Rates | $3.37e^9$ | $1.29e^5$ |
| Scenario 5 | Average Rates Year 7 With Establishment | $3.05e^9$ | $6.87e^4$ |
| Scenario 6 | High Rates Year 7 With Establishment | $2.92e^8$ | $1.76e^5$ |
| Scenario 7 | Low Rates Year 7 With Establishment | $3.74e^9$ | $2.16e^4$ |
| Scenario 8 | Average Rates Year 11 | $2.23e^9$ | $4.32e^4$ |
| Scenario 9 | High Rates Year 11 | $1.13e^9$ | $8.58e^4$ |
| Scenario 10 | Low Rates Year 11 | $3.24e^9$ | $1.3e^4$ |

Figures 5 and 6 show the marked difference between controlling EAB population early and letting it grow before any controls are implemented. To evaluate the persistence of *Fraxinus* under the slow growth of EAB, we have also simulated the standard rate of parasitism starting at year 1 for a 100-year cycle. This test showed that even over this longer timescale EAB was not a significant threat to *Fraxinus* as EAB population growth was not sufficient to cause harm to the *Fraxinus* population.

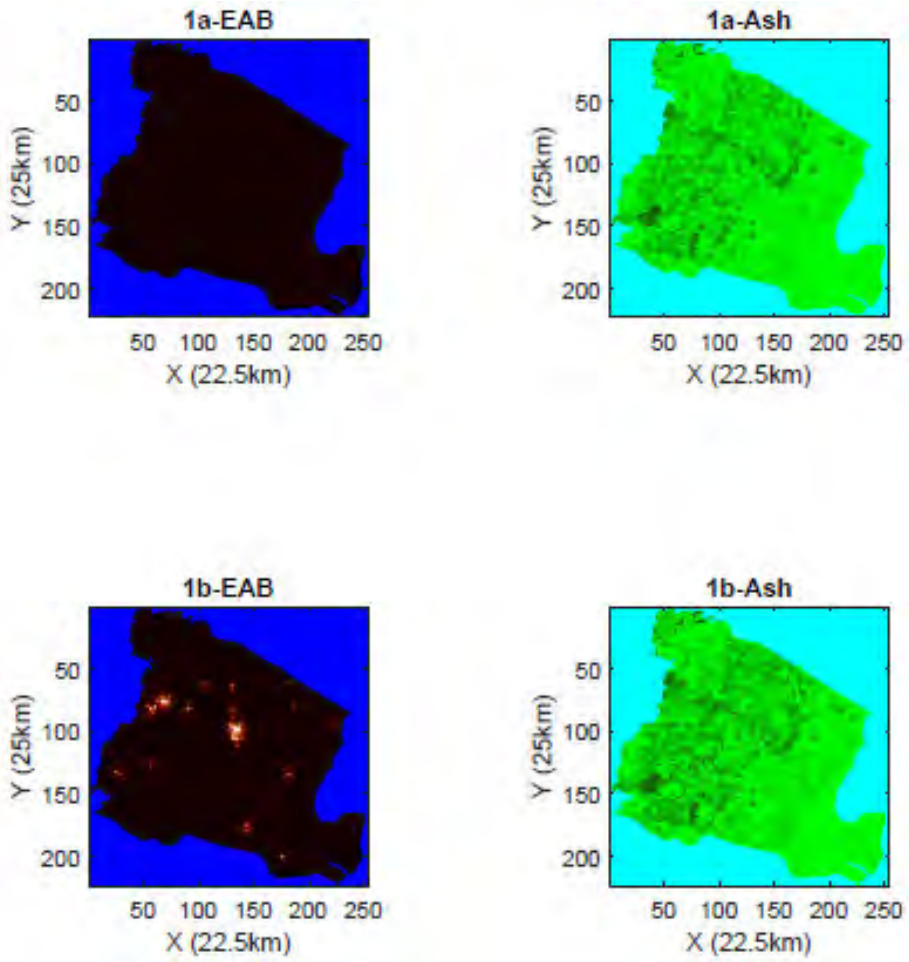


*Figure 5: EAB and* Fraxinus *Populations Under Average Parasitism Introduced in Year 1 After 10 years(a) and 20 years(b). With first year introduction of parasitism, the system is stable with a barely growing population of EAB. On the left, brighter orange areas indicate growing EAB populations. On the right, the related Fraxinus in the forest structure is denoted in the dark green.*

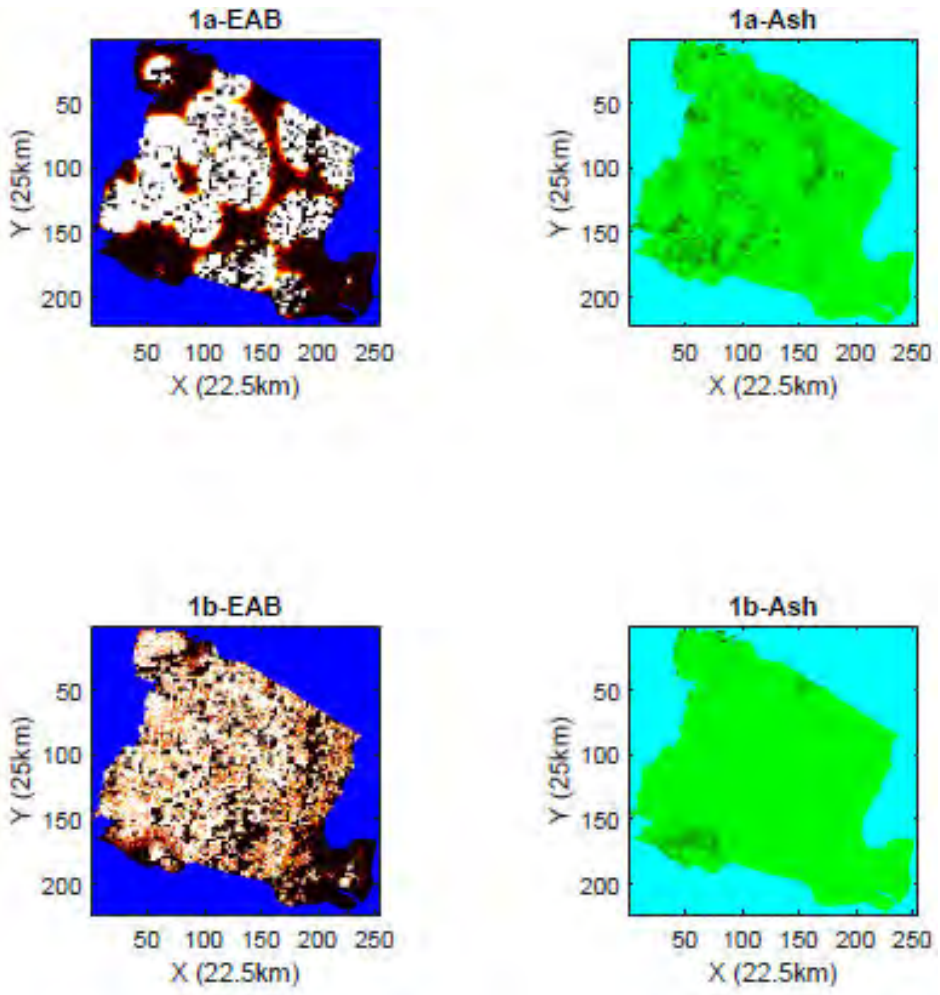


*Figure 6: EAB and* Fraxinus *Populations Under Average Parasitism Introduced Year 11 After 10 Years(a) And 20 Years(b). The figure shows the simulation after 10 years (a) and at the end of 20 years (b), when parasitism is introduced after 11 years of EAB infestation. The result is overall* Fraxinus *population collapse. On the left, brighter orange areas indicate growing EAB populations. On the right, the related Fraxinus in the forest structure is denoted in the dark green.*

Moving the results from a spatial plot to an annual sum and combining with an additional fifteen iterations, we make a line plot of sixteen simulations, each of which has a different number and location of EAB introductions, we see the relationship between introduction time and outcome even more clearly (Figures 7-9). When average rates start at year 1 (Figure 7), we see that EAB is almost nonexistent when scaled next to populations with later introductions and

the baseline of no parasitism (Scenarios 1-4). A similar pattern is seen under high rates of parasitism (Figure 8).

There is a shift in the overall trend at lower levels of parasitism (Figure 9). *Fraxinus* is still declining in the cases where only low rates of parasitism are implemented, even with first year introduction. Even though *Fraxinus* is declining by the end of the simulation, there is still a substantial forest compared to the baseline, where all *Fraxinus* has been extirpated. There is still a chance of recovery as opposed to later introductions, where there is truly little left to recover.

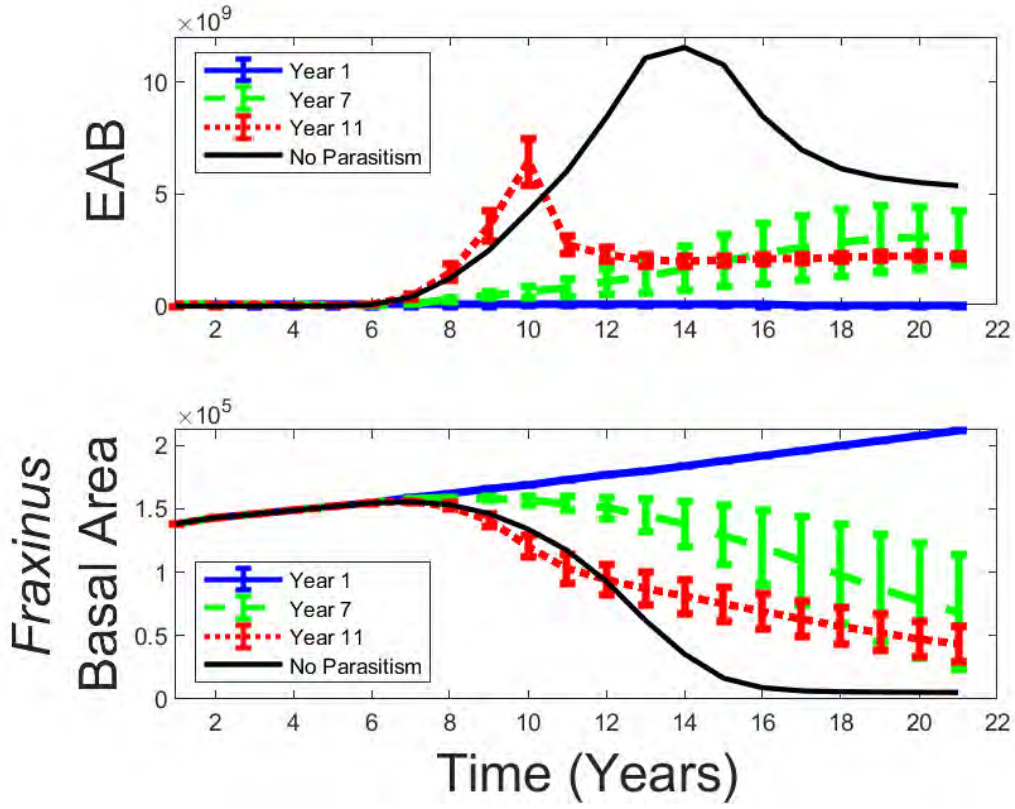


*Figure 7: Influence of Introduction Time on EAB and* Fraxinus *Populations Under Average Parasitism Rates. The black line indicates the no control scenario (Scenario 1) which leads to the almost complete extirpation of* Fraxinus*, whereas when the introduction time is closer to the initial infestation, we see improved outcomes for* Fraxinus.

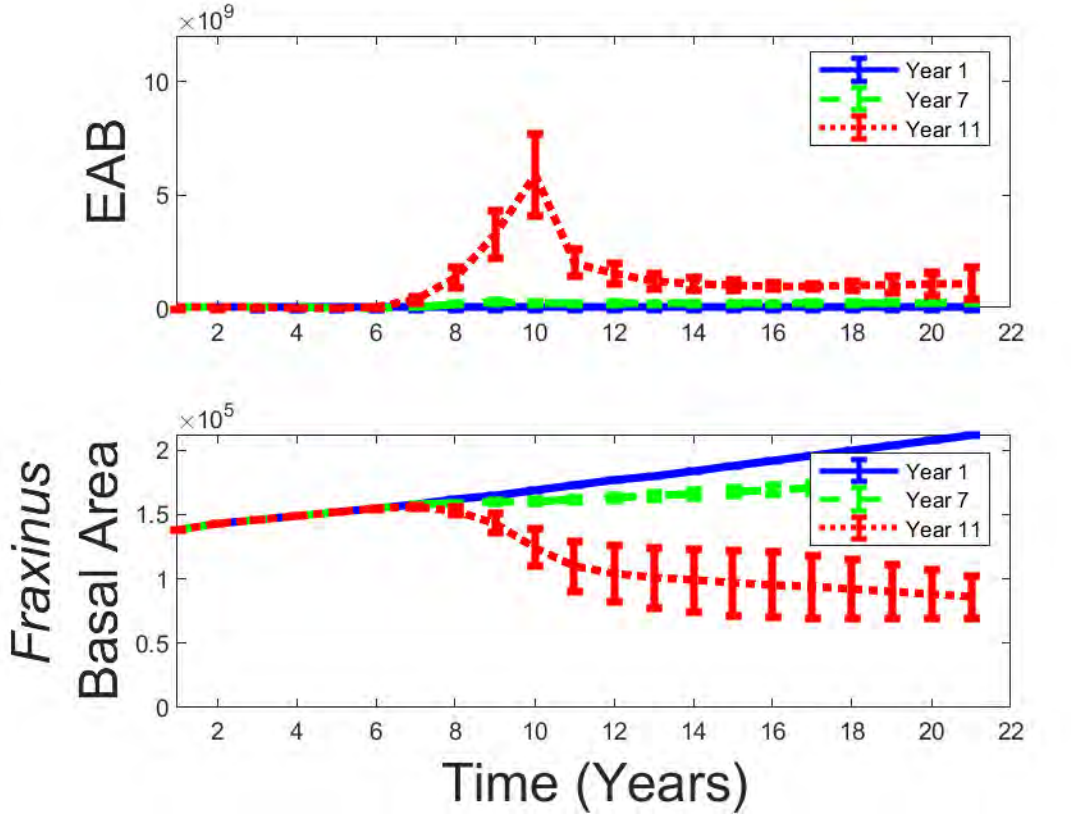


*Figure 8: Influence of Introduction Time on EAB and* Fraxinus *Populations Under High Parasitism. Compared to the average rates in Figure 7, parasitoids at these rates do not let EAB severely impact Fraxinus unless introduction is stalled until year 11.*

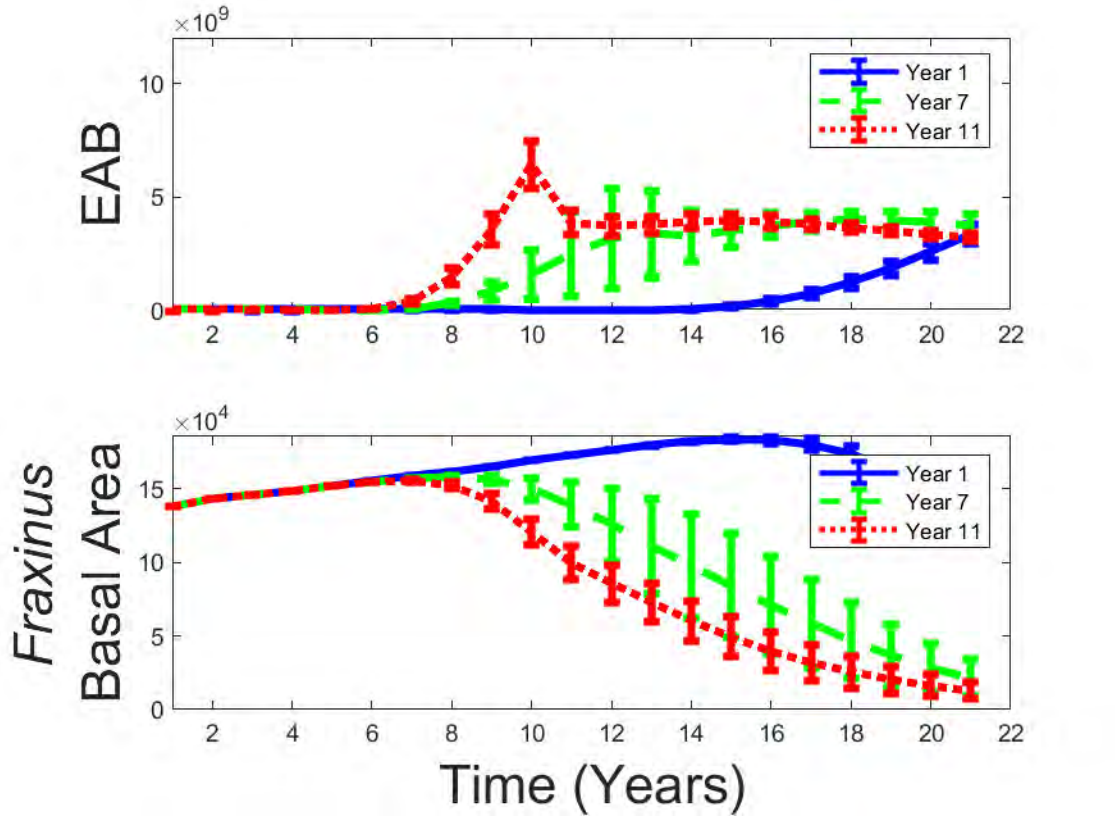


*Figure 9: Influence of Introduction Time on EAB and Fraxinus Populations Under Low Parasitism.*

The lag time associated with the establishment of parasitoid wasps has been noted in numerous sources (J. Duan et al., 2019; D. E. Jennings et al., 2016; D. E. Jennings et al., 2016; D. Kashian et al., 2018), and indicates that biocontrol introduction timing is even more critical for preserving *Fraxinus* than Scenarios 2-4 indicate. A lag of more than seven years between when EAB has first entered a region and when control measures are implemented could make the effort almost useless to preserving the current forest structure.

*Fraxinus* will not recover without early intervention and the earlier interventions are better for *Fraxinus* outcomes. In effective scenarios, there are high rates of parasitism coupled with early intervention measures, and EAB infestation impacts are not significant for a century (Figure 10). When we extend the time horizon to a century there is some level of abstraction in

population dynamics, as levels of EAB this low may be low enough to be unable to reproduce and so completely collapse, this level of population dynamics is not simulated here, so populations are able to maintain themselves without the requirement for sufficiently dense populations.

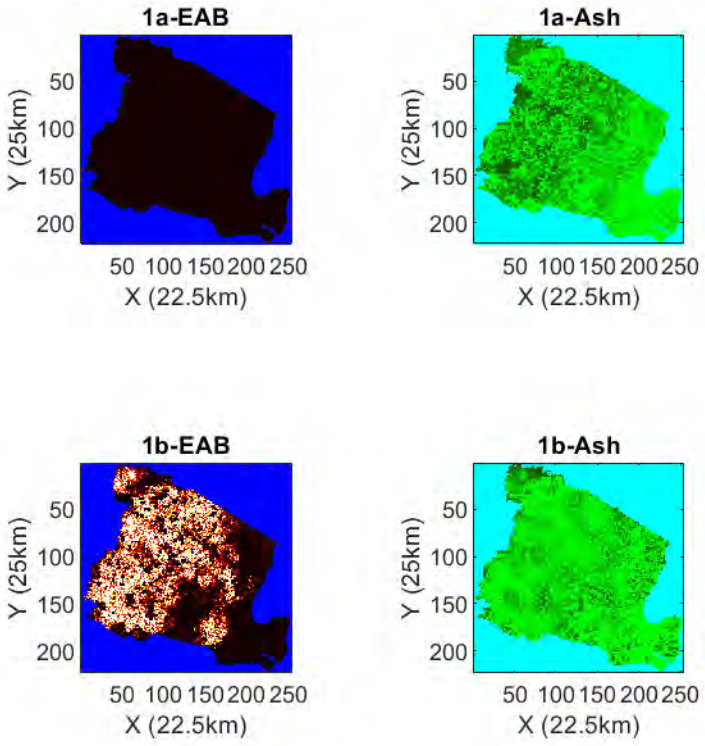


*Figure 10: Influence of Introduction Time on EAB and* Fraxinus *Populations Under High Parasitism Introduced Year 1 After 50 Years(a) And 100 Years(b). The figure shows the simulation after 50 years (a) and at the end of 100 years (b), when parasitism is high. The result is that the EAB population slowly grows and eventually still causes* Fraxinus *mortality, but takes an order of magnitude longer, which could be enough time for* Fraxinus *to adapt. On the left, brighter orange areas indicate growing EAB populations. On the right, the related Fraxinus in the forest structure is denoted in the dark green.*

Compared to high and average rates, low rates of parasitism cause uncontrolled EAB growth, even under situations in which introduction happened close to the time of infestation. While it is an improvement over baseline, the trend of *Fraxinus* basal area is still clearly

downward. Current policy is to introduce parasitoids in areas with heavy, confirmed EAB infestations to ensure the establishment of the bio-control vectors; however, according to our results, this is a dangerous gamble if infestation levels are too far progressed. Failure of *Fraxinus* is not appreciably slowed unless introduction of control vectors happens earlier in the infestation cycle, and if the parasitoids are evenly distributed through the infected area. In our model the parasitoids are applied at all points across the landscape during a single timestep. This uniform application is a limitation from the limited flight, spread and effectiveness data on parasitoids used in this study. If parasitoids could be effectively simulated similar to EAB's parameterization, parasitoids would likely be even slower at curtailing EAB growth and spread due to the additional lag time from the spread of the parasitoids, as similar experiments have shown that some species can spread with EAB, but likely at a lag of some years (M. I. Jones et al., 2019; Quinn et al., 2022). To preserve Fraxinus and curtail the worst effects of EAB, introductions of parasitoids should be executed in regions where the infestation is as new and recently detected as possible, as after several years there is little likelihood in parasitoids being an effective treatment for EAB infestation.

Our results indicate that over long enough timescales, even elevated exotic, and native parasitism still results in a growing population of EAB. However, such diffuse populations would collapse as they became more diffuse and isolated, additionally maintaining these high rates with such a diffuse population of EAB is unlikely. The unlikelihood of maintaining these rates is low as numerous establishment studies for species of parasitoids have highly variable rates of effectiveness and spread, which could still allow for pockets of EAB to grow (Abell et al., 2014, 2016; J. Duan et al., 2019; D. E. Jennings et al., 2016; M. I. Jones et al., 2019) . This means that even with native parasitism it will be a long-term solution; EAB continues to grow,

but at a rate that allows trees to reproduce and potentially adapt to the issue without further intervention (J. Duan et al., 2017). Other mortality and control factors not simulated here have been observed but have limited impact on population dynamics. Some observed factors include predation by native woodpecker populations and native *Fraxinus* resistance to EAB, where the former only results in significant EAB mortality at the end of the epidemic wave, and the latter is compensated for with our EAB growth term (J. Duan et al., 2013; D. E. Jennings et al., 2016; D. E. Jennings et al., 2015; Murphy et al., 2018).

The limitations from these control factors indicate that the current practice of releasing small numbers of EAB parasitoids in areas already heavily infested with EAB may not be enough to preserve breeding stock of currently mature trees. If the region is already heavily infested, introduction criteria should be regionally defined with management efforts focused on regions that have not yet lost a substantial portion of their *Fraxinus* stock. While this approach is potentially more intensive due to requiring more widespread dispersal of parasitoids to more isolated populations of EAB, it has the potential of saving the current stock of trees in the upper canopy. Alternatively, if there is no way to facilitate the introduction of parasitoids into satellite populations due to budgetary, tracking, or other constraints, introductions should be focused on regions where potential *Fraxinus* mortality is significant enough to allow for regrowth and recovery similar to that which has been observed in some parts of the Midwestern USA, where *Fraxinus* is a major canopy component (D. M. Kashian et al., 2018; D. M. Kashian, 2016). These results are repeated by running the same parameterization over a larger region adjacent to the one depicted above. The larger region is represented by the three Northwestern counties of New Jersey (Warren, Sussex, and Morris), where a substantial portion of *Fraxinus* extant in New

Jersey is present. This region is experiencing an earlier state of the infestations than the rest of New Jersey and the local *Fraxinus* could be preserved.

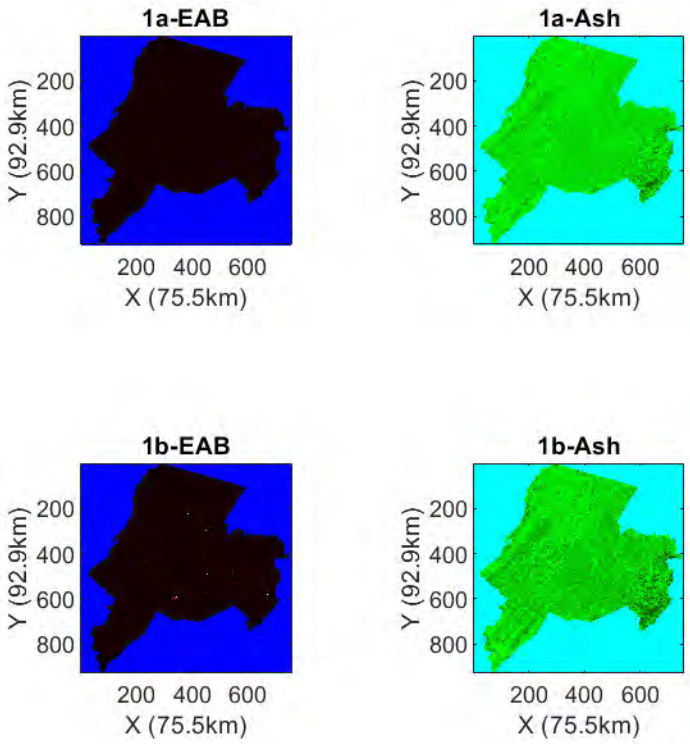


*Figure 11: Normal Parasitism Starts Year 1 Large Area Realization Years 10(a) and 20(b). On the left, brighter orange areas indicate growing EAB populations. On the right, the related Fraxinus in the forest structure is denoted in the dark green.*

When parasitism starts early in the infestation wave, we see that the state of the forest is good after 20 years (Figure 11), but when parasitism is delayed even when highly effective, we see a stark decline in the forest (Figure 12). It should be noted that these larger scale runs were reaching the limitations of computational feasibility with the model's current structure, with

processing times almost unreasonable using the available resources of the Montclair State University's High-Performance Computing (HPC) system. Using 81 nodes out of 120 available with 1 node for each diffusion coefficient for EAB, the model maintained runtimes in excess of 1 month even after significant optimization for data transfers. With greater computational resources, more testing at this scale could be accomplished.

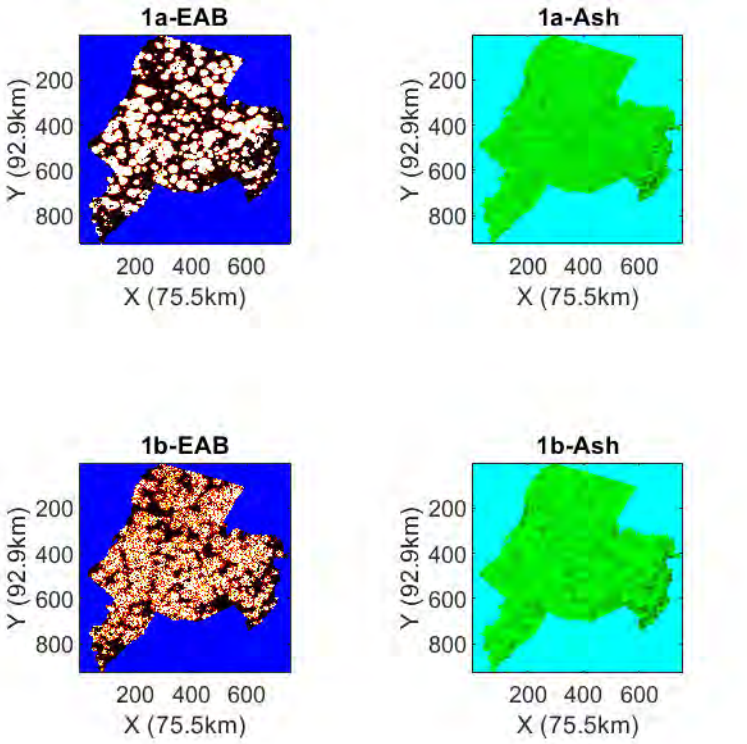


*Figure 12: High Parasitism Starts Year 11 Large Area Realization Years 10(a) and 20(b). On the left, brighter orange areas indicate growing EAB populations. On the right, the related Fraxinus in the forest structure is denoted in the dark green.*

## 4. CONCLUSIONS AND FUTURE STUDY

Further extension of this and similar models may be useful once additional, more detailed data on parasitoid spread and diffusion with EAB have been gathered. This model is applicable beyond the North American sphere, as Europe has begun testing potential control options for

EAB in their own growing epidemic. The current primary limitation with this model to the application of EAB spread is the assumption that parasitoids are evenly distributed and do not require additional travel time in between EAB populations. While this is confirmed to some extent for *Tetrastichus planipennisi*, it has not yet been confirmed for the other species of parasitoid (J. Duan et al., 2019; M. I. Jones et al., 2019; Quinn et al., 2022). If the control methods were even slower at controlling EAB than simulated, then the window to successfully preserve *Fraxinus* is even narrower than anticipated with results approaching the low end of our simulations. EAB continues to be a growing threat; while North America enters the final stages of EAB dispersion, Eastern Europe is experiencing the earlier stages of infestation. They will continue to face EAB pressure into the future, making continued study and control of EAB necessary on a global scale as control measures are implemented in new regions (Orlova-Bienkowskaja & Bieńkowski, 2018, 2020).

PDE modelling using GIS data as an input is applicable to many invasive species that are in the process of reaching an endemic phase within their respective environments. Once climactic concerns are eliminated or integrated, the primary concern related to an entrenched invasive population is population control below epidemic levels. Population maintenance prevents the worst of the damage, as the invasive species fills out its new niche. Controlling well-entrenched invasive species requires control to be established such that it can come into equilibrium with the environment in which it has been introduced.

# CHAPTER 3. ESTIMATION OF *FRAXINUS* IMPACTS ON ELECTRIC DISTRIBUTION INFRASTRUCTURE STABILITY FROM SNAG FALL

## 1. INTRODUCTION

New Jersey is a state with a high degree of urbanization and development. This development has led to an extensive electric grid built through densely forested areas. The mass mortality of *Fraxinus* due to EAB is directly leading to an ongoing surge in the number of snags. Snags, dead standing trees that either stand independently or slouch onto neighboring trees, pose an extant threat to nearby infrastructure. In our case we study power infrastructure, as these are a public service with long ranging impacts if damaged, but other stationary infrastructure, such as buildings, can be damaged by tree fall (Larsen et al., 2018). These trees become more brittle with age, leading to increased risk and frequency of outages caused by tree fall as well as increased risk of property damage. New Jersey is currently in the process of upgrading the current electric distribution network to decrease reliance on fossil fuel and increase dependency on cleaner sources in the process known as electrification. These efforts look to increase the height of the electric distribution lines and so the resiliency of the grid. This increase in height could reduce the risk of snag fall on powerlines by raising them above more of the canopy. We demonstrate a yearly risk assessment methodology for *Fraxinus* snags using an integrated GIS and applied regression model framework under two distribution network parameterizations. We apply this framework to three northern New Jersey counties (Warren, Sussex, and Morris). This area is managed by one utility, New Jersey Central Power and Light, and is home to most of the *Fraxinus* extant in the State.

With increasing climate variability and the movement of exotic pests and diseases, the rate of forest mortality has become a hotly debated issue globally due to an ever-increasing

number of feedbacks and impacts (Harmon & Bell, 2020). EAB, as one such pest, has proven just as varied in its impacts. For example, treefall is often influenced by wind, but the situation is more nuanced than simply increasing the rate of fall and potential damage. In cases where entire stands are damaged and destroyed, the strength of the prevailing wind has a strong influence on the likelihood of the trees falling (Audley et al., 2021; Oberle, Ogle, et al., 2018). However, when given snags are scattered throughout a forest rather than homogenous stands, we see wind speeds have much less impact on fall rate (Oberle, Ogle, et al., 2018; Perry et al., 2018). The lack of wind influence means that in the case of *Fraxinus* the normal method of using wind speed and catastrophic event risks to estimate damage from treefall is not appropriate.

Hardening the electric grid against snag fall may prove effective at preventing losses and unnecessary expenses. There are two potential ways that this hardening may be achieved: through regular trimming and cutbacks along electric distribution lines (to prevent dead, or dying, trees from directly contacting the lines) or by improving the infrastructure to reduce snag damage. Currently, many New Jersey electric utilities are planning (or are in the process of planning) to upgrade their electric distribution network from the current 26 kilovolt (kV) capacity distribution lines to 69kV lines as part of their efforts to match the projections from the New Jersey Energy Master Plan (New Jersey Board of Public Utilities (NJBPU) et al., 2019). This distribution service upgrade is being done to both strengthen the resiliency of the state to wind events in the coastal areas, as well as increase the capacity of the grid to allow for increased adoption of electric dependent technologies, like electric vehicles (EVs). As an added benefit, this upgrade in electrical capacity also increases the average height of distribution level electric poles from 30 feet to 65 feet with all power lines being placed at least 50 feet above ground level. This results in an increase of a minimum of 20 feet over current height, which could

significantly reduce the likelihood of a snag being within critical range of the powerline to cause an outage. Increased minimum height of the electric lines is a central part of our scenario analysis.

Previous studies on the impacts of snags on infrastructure focus on small neighborhood to city level impacts, and rely on intensive sampling for the course of the study through on-the-ground measurements and methods (Bíl et al., 2017; Hughes et al., 2021; Poulos & Camp, 2010). Through our analysis, we hope to provide further justification for both line maintenance schedules and the extension of electrical infrastructure upgrades at the regional level (Public Service Electric & Gas Co. (PSE&G), 2007).

### 1.1 Infrastructure Risk Modeling

Rating infrastructure according to natural risk factors is not uncommon but can be problematic due to intensive sampling methods that are often employed. This problem with infrastructure rating is especially true for electric distribution infrastructure that are often suspended in the tree canopy, and so are at elevated risk from nearby snags, even to a portion of a nearby tree. It is critical to maintain trees, shrubs, and other vegetation near and around electric distribution lines to prevent excess outages. By allowing trees and other vegetation to encroach upon these essential infrastructures, the possibility for failure of the system during storms or even normal events is affected. The risk of tree falls can potentially cut power to residents for extended periods of time, which can have even greater economic impacts than just the damage to the system itself. However, given the intensity of the simulation and the lack of information on switches in the grid, we do not incorporate knock-on economic losses in our methodology (Balducci et al., 2006; Larsen et al., 2018). Removing all trees along rights of way is improbable

given the sheer length of distribution lines, the cost to landowners, and the character of the region (Hughes et al., 2021).

Numerous methods have been suggested to monitor this issue. One of the most common methods involves using intense tree surveys along small sections of infrastructure networks (Poulos & Camp, 2010). Others have used statistical and spatial data for a set region such as a city or county under normal disturbance regimes over the course of years to decades to identify high risk zones; data from these analyses may then be extrapolated for surrounding regions (Bíl et al., 2017). Monitoring methods also exist at the micro-scale to focus on strengthening the infrastructure itself and assess how often maintenance needs to be performed to prevent losses using physical properties of the landscape and the state of the local infrastructure. This level of simulation can lead to good outcomes on that scale but is limited in scope due to the intense data collection requirements (Hughes et al., 2021).

### 1.2 Fall Rates of Snags

According to Coder (2014), the primary method by which wind causes trees to fall is by blowing through the upper canopy, causing a rotational force on the trunk of the tree, and pulling up on the root plate, which leads to treefall. The process in which wind can damage trees is a combination of both the weight of the tree, the quality of the local soil, and the wind that is impacting the tree. However, wind-damage is not correlated strongly with the fall rate of snags in the Eastern United States of America (USA). Wind-damage is correlated with other well-known snags in Northern Canada and the Western USA, where the mortality of one species results in much broader impacts to the canopy, such as large tracts of western pine species killed by mountain pine beetle (Audley et al., 2021; Oberle, Ogle, et al., 2018).

Oberle, Ogle, et al., (2018), constructed a multiple logistic regression analysis parameterized based on Forest Inventory and Analysis (FIA) snag data over the course of a decade. In their analysis, they found that air temperature, diameter at breast height (DBH), trees per hectare (TPH), and the region of the country were significant in determining when a snag would fall. Their method was able to predict which snag would fall 75 percent of the time over a five-year period. The largest influencing factors in their analysis for snag-fall were air-temperature followed closely by the species' wood durability and the specimen's DBH.

With the impending loss of *Fraxinus* across the Northeastern USA, residents will need to brace for the budgetary impact this will have. This project addresses one aspect of these costs, specifically the vulnerability of electrical distribution infrastructure to the decay and fall of *Fraxinus*.

## 2. METHODOLOGY

For yearly snag falls and damages, we have adapted a logistic regression model by Oberle et al. (2018) and collaborated with the original authors by coupling it with the EAB spread model developed in Chapter 2. Together, these parts are used to i) estimate the rate of snag fall in the study area and ii) estimate the rate at which utilities could see additional service interruptions. The interruptions then necessitate additional charges due to line clearing and repair in Northern New Jersey, where the landscape is heavily forested and populated.

To estimate the rate of snag introduction, we track the mortality of *Fraxinus* caused by EAB in an altered form of eq. (4) from Chapter 2, where we discount the influence of *Fraxinus* . The damaged timber is saved by year as an output from the EAB spread model in square meters of basal area per hectare. Mortally damaged *Fraxinus* timbers become the source of new snags

that we track as they fall. These new snags are assumed to belong to the first decay class due to being previously healthy trees (Table 4).

*Table 4: Decay Classes of Snag Trees from the Forest Inventory Analysis, Department of Forestry*

| DECAY CLASS | DESCRIPTION (MCROBERTS ET AL., 2005) |
|---|---|
| **1 ($ST_A$)** | All limbs, pointed top, 100% bark, intact sapwood, height intact. |
| **2 ($ST_B$)** | Few limbs, top may be broken, some bark and height loss, sapwood decay. |
| **3 ($ST_C$)** | Limb stubs, broken bole, bark, and sapwood sloughed, broken top. |
| **4 ($ST_D$)** | Few stubs, bole broken/rotten, 50% bark, sapwood sloughed. |
| **5 ($ST_E$)** | No stubs, broken and rotten bole, 20% bark, sapwood gone, rotten 50%. |

Over time these new snags fall and could damage existing infrastructure, but predicting when they fall is not a trivial matter. First, a sample of snag *Fraxinus* was extracted from the Forest Inventory and Analysis program (FIA) database. Once we had prepared the sample and removed irrelevant observations, we had a sample size of 2677 individual *Fraxinus* samples, with 1857 of them being repeat observations from the Northeast that had fallen naturally after becoming snags and used this data to train a system of equations to describe the lifecycle of a *Fraxinus* snag as it decays and eventually falls (Forest Inventory and Analysis, 2022). We adapted the model structure from Oberle et al., (2018), using additional data released that has since become available which allows for a maximum of four resampling periods to the same tree. TPH and DBH were used as additional site factors for the spatial model due to the small target region relative to the wide sampling distance between Forest Inventory Analysis (FIA) test plots (Table 4). Due to how the sample data for decay is defined, it was necessary to take a categorical approach as the FIA records the qualitative description of snag condition as listed in Table 4.

Once the trees have fallen, we then expect that a proportion of these trees will become hazards and fall on electric distribution infrastructure according to their height and the distance from the distribution infrastructure. The saved basal area per hectare from eq. (4) is split into individual trees based on the size distribution of *Fraxinus* in New Jersey's state inventories (Crocker et al., 2017; Forest Inventory and Analysis, 2022; Woudenberg et al., 2010). The height of the fallen *Fraxinus* is estimated from all *Fraxinus* that have been recorded by the FIA in the northeast. The height of the sample is related to their DBH which can be compared with New Jersey's state inventories (Forest Inventory and Analysis, 2022).

In order to estimate the location and length of the relevant distribution infrastructure, the locations of transformers submitted for the New Jersey Department of Environmental Protection (NJDEP) Solar Capacity project in 2016 were used as a starting point (Bureau of Climate Change and Clean Energy, 2021). The transformer locations were associated with their local road network sourced from the USA Census TIGER/line roads database (Bureau of Transportation Statistics et al., 2016). With the transformers associated with their local roads the points were connected by lines according to the road network associations.

Then using the estimated number of fallen trees and the distribution network, the number of hazard trees that intersect any distribution infrastructure and potential costs are calculated. To do this we assume the tree has an equal chance to be in any part of the local forest and have the potential to fall and intersect the distribution infrastructure located there as a function of the amount of infrastructure present. Further, the taller the tree is, the more likely that it could hit the infrastructure, as it can be further away and still be a hazard when it falls. This damage then has a resultant cost from either preventative maintenance on the hazard tree or repair of the distribution infrastructure.

In all, this makes seven primary steps in our methodology, which we expand on in following sections. First, we solve for the basal area of dead snags in each location using an altered EAB spread model form Chapter 2. Second, we find the distribution of size classes for different tree sizes using New Jersey State Forest inventories. Third, we estimate the height of each size class from recorded FIA tree heights. Fourth, we estimate the transitions between decay classes using categorical methods trained on FIA and apply it to our EAB killed *Fraxinus*. Fifth, we estimate the length of powerlines and poles in the study area using GIS data on transformer locations. Sixth, we solve for the probability that any one of the falling trees intersects with the distribution infrastructure. Seventh, we estimate the cost of this intersection either in terms of preventative maintenance, or repairs.

### 2.1 Fraxinus Snag Generation

To track the accumulation of snags and the decay of *Fraxinus* in our forest system, we set the accumulation of snag basal area (BA) in the first decay class as equal to the consumption of *Fraxinus* by emerald ash borer (eq. (4)) from Chapter 2. The equation was altered slightly to mirror EAB biological constraints rather than spread and we re-ran the model system for the three northern counties of Morris, Sussex, and Warren in New Jersey where there is still extant *Fraxinus*. The altered equations for the model are as follows,

$$\frac{\partial ST_a}{\partial t} = CE_l, \tag{9}$$

$$\frac{\partial \mathrm{A}}{\partial \mathrm{t}} = \begin{cases} \hat{G}_1 \mathrm{A} - \hat{\mathrm{C}} \mathrm{F_c} \mathrm{A}^2 - \mathrm{CE_l} & \frac{\mathrm{A}}{\mathrm{A_{(1)}}} \geq 0.1 \mathrm{F_c} \\ \hat{G}_2 \mathrm{A} - \hat{\mathrm{C}} \mathrm{F_c} \mathrm{A}^2 - \mathrm{CE_l} & \frac{\mathrm{A}}{\mathrm{A_{(1)}}} < 0.1 \mathrm{F_c} \end{cases}, \tag{10}$$

where for eq. (9), $ST_a$ is the standing *Fraxinus* timbers which are created at the rate of *Fraxinus* consumption by EAB (*C*) and the local population of EAB larva ($E_l$). For eq. (10), all variables are the same as eq. (4), but *A* is removed as a variable from the consumption term being expressed as $CE_l$ rather than $CE_lA$, to allow EAB to be only constrained by their biology rather than approaching zero consumption as *Fraxinus* approaches zero. In this study we are less concerned with the population dynamics of EAB and focus on the temporal distribution of *Fraxinus* snags; therefore, we do not consider the amount of local *Fraxinus* as a factor in the consumption of *Fraxinus* by EAB. This reparameterization type shows limited differences to the baseline. Below, we have a comparison between these two parameterizations over sixteen runs for Essex County with the same inputs, but varied EAB introductions similar to Chapter 2 (Figure 13). A full description of the derivation differences between these two models can be found in Appendix 2. The difference is expressed such that *Fraxinus* declines somewhat faster than the model used in Chapter 2 but expresses the same basic curve shape with similar error from introduction variation.

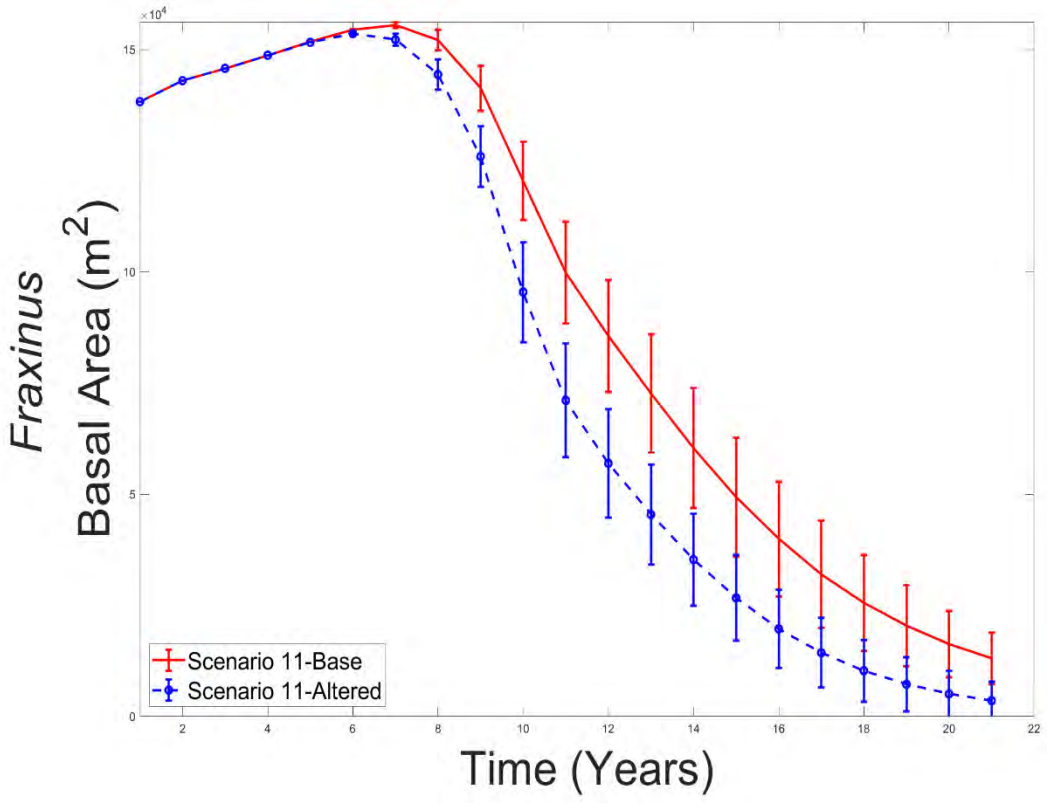


*Figure 13: Differences in* Fraxinus *Trajectory Between Consumption Coefficients. Scenario 11-Base is the same as presented in Chapter 2, while Scenario 11-Altered has the altered consumption coefficient discussed in equation (10). The altered consumption coefficient results in a slightly faster decline in* Fraxinus *as well as a lower end state when compared to Scenario 11-Base.*

## 2.2 Size Class Distribution Estimation

With the calculated BA of snags using the altered EAB spread model in the previous section, the relative proportion of BA that is in each diameter at breast height (DBH) size class of *Fraxinus* in the study area is calculated from state inventories. Ten years (2009-2019) of *Fraxinus* abundance data from the FIA are used to estimate the proportion of basal area that is due to each recorded class of DBH size class of *Fraxinus* on Forest Land in New Jersey (Crocker et al., 2017; Forest Inventory and Analysis, 2022; Woudenberg et al., 2010). This results in the distribution displayed in Figure 14. The distribution shows that, for example, any unit of BA,

approximately 15% will fall into the 14-inch DBH size class. These data allows us to assign basal area to all size classes of trees according to their relative abundance in our target forests. As trees get larger, they individually contribute more to the BA, but are also significantly rarer and so have a higher sampled error between inventory years that is not seen in smaller specimens.

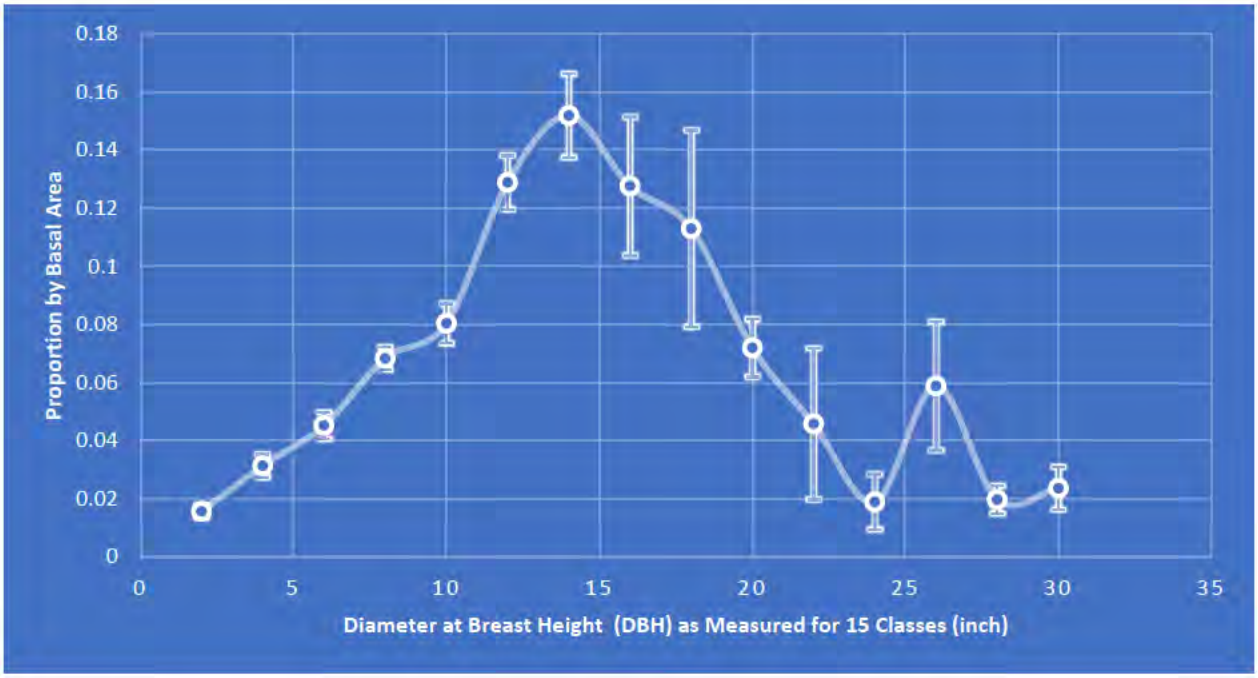


*Figure 14: Proportion of* Fraxinus b*y Size Class for* Fraxinus *from 2009-2019*

***2.3 Fraxinus Height Regression based on DBH***

With the distribution of *Fraxinus* DBH from the previous section, the next step is to estimate their height relative to their diameter. The height of *Fraxinus* is dependent on the region being studied, so in order to estimate the height *Fraxinus* snags, all live *Fraxinus* that were sampled by the FIA from 2000-2020, which totaled over 30,000 trees, from the surrounding states were utilized to plotted their height versus their DBH (Forest Inventory and Analysis, 2022). This sample was taken from New Jersey and surrounding States, including Pennsylvania,

New York, Delaware, and Connecticut (Figure 15). These data are somewhat disparate with only one explanatory factor, but fit did not improve upon including other data that could be spatially referenced for our study area. Testing with other recorded parameters, such as site elevation and site conditions, did not provide any additional insight to the height of *Fraxinus*, so without justification for multivariate analysis, DBH was maintained as the sole predictor of height (Figure 15).

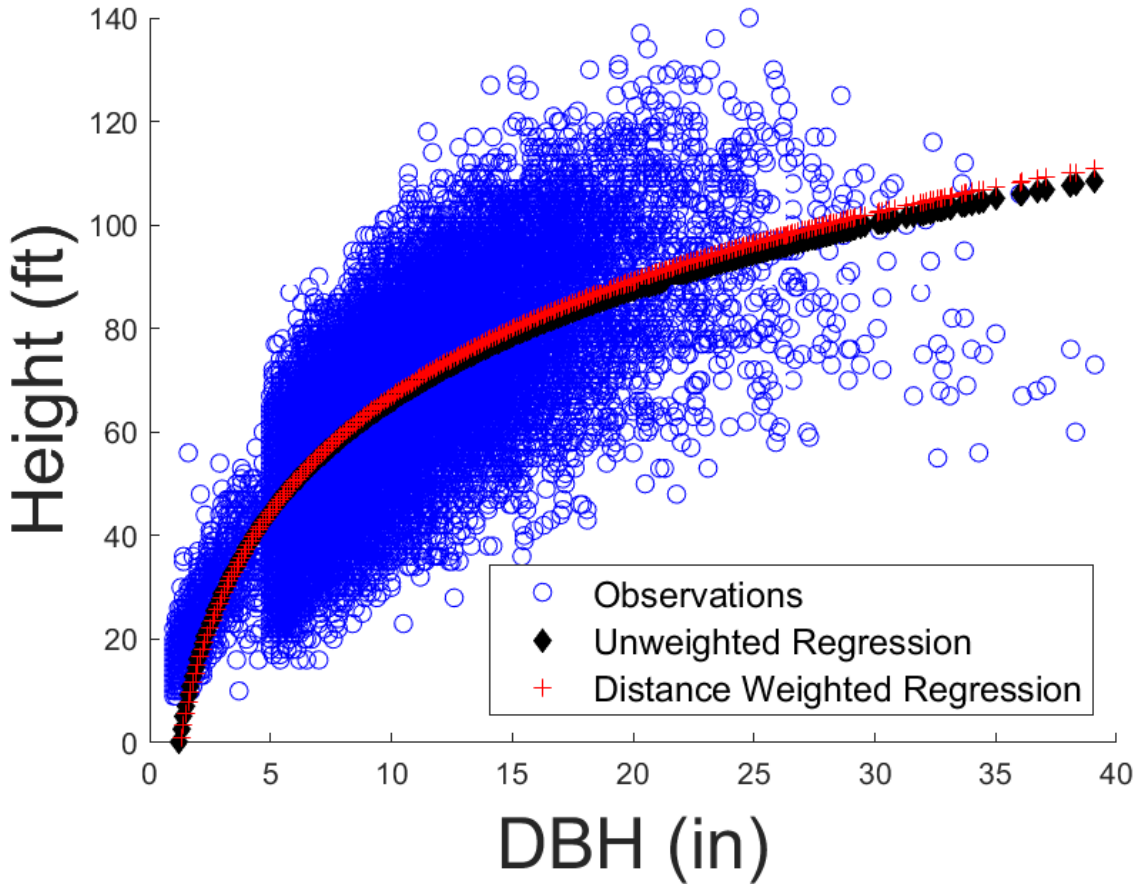


*Figure 15:Distribution of Samples and the Curve of Best Fit Between DBH and Height. Samples are widely dispersed, but do not show significant trends with other traceable variables*

*precluding the ability to do a multivariate analysis. Further multivariate analysis could be attempted with known sample plot locations.*

After testing for multiple fits, we eventually calculated a log linear regression for the size of *Fraxinus* in our study area and found a fit with a ±9.31-foot error, when the samples were weighted based on their distance to our study area. That is, the further samples were from the geographic center of the study region in Northern New Jersey, the lower the weight they had in the regression. This distance was kept coarse using decimal degrees as the distance, as plot locations and exact distance for the samples is imprecise to protect the locations of the FIA plots and prevent tampering (Forest Inventory and Analysis, 2022). We found

$$Ht_{(ft)} = 32.26\log(DBH_{in}) - 7.37, \quad (10)$$

where $H_t$ is the height in feet and $DBH_{in}$ is the diameter at breast height in inches. The Mean Squared Error (MSE) of the regression was 86.70 with an error parameter of ±9.31. An unweighted distribution where all samples are weighted identically in the regression performed significantly worse, with a MSE of 144.71 (Figure 15).

### 2.4 Decay Rate and Fall chance

The residence time and decay state of *Fraxinus* snags influences how quickly dead snags fall. With increasing decay, the snag has a higher chance of falling. With the results of the three previous sections, the next step is focused on describing how *Fraxinus* decay through time. The sample period was limited to the years 2000-2020, as earlier data did not thoroughly sample snags and later data had not been resampled. We sourced these data from the same USA States that we used for height, New Jersey, Pennsylvania, New York, Delaware, and Connecticut (Forest Inventory and Analysis, 2022). Once we had cleaned the FIA data from 2000-2020 of

any snag *Fraxinus* that had been artificially removed, or otherwise compromised we evaluated them using the five FIA decay classes (Table 5).

This sample comprised a robust 2677 individual records, with 1857 of them being repeat observations. When trees are not sampled in the next period it is assumed that the tree has fallen based on FIA sampling protocols (Woudenberg et al., 2010). To compensate for inconsistencies in the data, some limits and assumptions were made. First, *Fraxinus* was only allowed to advance decay classes, as a small number of samples were noted to revert decay classes on follow-up inspections, becoming less decayed over time, which is impossible. Additionally, the sample treats inventory resample periods as equivalent for all snags records. The measurement times varied in some cases and, while resampling usually occurred every five years, a small portion was resampled on a four- or six-year timescale. However, we treat the transition matrix as an approximation for a five-year resurvey interval, as that was by far the most common interval with the four and six-year intervals happening in a minority of cases.

Concatenation of this sample results in a transition matrix where trees are held to either their current decay class, transition to a more advanced state of decay, or fall between sample periods (Table 5). Where if the average tree, for instance, starts the period in decay class 1, it will have a probability of 0.526 of falling by the next resampling period and a probability of only 0.028 of remaining in decay class 1 by the next resampling period. This transition matrix was used to define a Markov Chain process for a system of equations that will be used to define the transition of *Fraxinus* under varying site conditions. We train our system of equations using a random walk process according to a Markov Chain Monte Carlo process (MCMC). The model is

trained in rJAGS and is built out of 15 individual equations (Depaoli et al., 2016; Plummer, 2003).

*Table 5: Transition Matrix for Decay Classes*

| DECAY CLASS | 1 | 2 | 3 | 4 | 5 | FALLEN |
|---|---|---|---|---|---|---|
| **1** | 0.028 | 0.197 | 0.229 | 0.020 | 0.000 | 0.526 |
| **2** | 0.000 | 0.164 | 0.218 | 0.034 | 0.002 | 0.583 |
| **3** | 0.000 | 0.000 | 0.173 | 0.043 | 0.008 | 0.776 |
| **4** | 0.000 | 0.000 | 0.000 | 0.096 | 0.007 | 0.897 |
| **5** | 0.000 | 0.000 | 0.000 | 0.000 | 0.030 | 0.970 |

The system of equations was defined as a combination of logistic regressions and SoftMax categorical regression formulas. SoftMax categorical regression is an extension of logistic regression when there are more than two outcomes possible, but the result is still discrete. First logistic regression is the classification into either the 'positive' category or 'negative' category. The logistic equation is defined as

$$\sigma(z) = \frac{1}{1+e^{-(\beta z)}}, \tag{11}$$

where $\sigma(z)$ is the probability of an outcome under condition $z$, which could be one or multiple conditions which are believed to relate to the outcome and β is a trained parameter for condition $z$, that weights the impact of $z$. Logistic equations are used to calculate the probability of an event when the output has only two outcomes, as is the case when decay is in the last stage and *Fraxinus* will either fall or remain standing. For the remaining decay classes there are more than two potential states at the next sample period, so they are categorized as SoftMax categorical regressions, which is defined as,

$$\sigma(z)_i = \frac{e^{\beta z_i}}{\Sigma_{j=1}^{K} e^{\beta z_j}},$$

*( 12 )*

where *K* is the number of potential output categories, *z* is the input condition and *j* is 1 and β is a trained weight parameter (Wolfe et al., 2017). SoftMax is used to define all other relationships in our system of equations, with 14 individual equations, each with their own trained β weight parameters.

Given the small study region and small sample of interest, we focused on DBH and TPH as additional site factors. The average of the sample was taken to mean no effect and variation from the mean were evaluated. Other factors that could be considered if the model was expanded to a larger area could include the mean annual temperature (MAT) and the physiographic class of the sample sites; these were not considered significant due to the study area not having a variable MAT and physiographic class was not considered due to the lack of site data from the FIA and how physiographic classes could be condensed into widely recorded land use land cover classes.

In this case there are a total of three input parameters. First, the current decay class of the snag ($D_{c_n}$). Second, we have the diameter class of the tree ($D_c$), which could influence the tree to either stay standing or fall. Third we have the trees per hectare ($TPH$), which could influence the tree to either remain standing, or fall. For both $D_c$ and $TPH$, the null effect is defined as the average of the sample and any deviation from there is considered the potential influence. The initial amount of timber in the first $D_{c_1}$ is defined as the sum of all mortality in each year from eq. (9).

When training the model the focus is on the transition to the next state for a particular sample. Decay out of a class ($D_{c_n(t)}$) and into another decay class ($D_{c_m(t)}$) in the trained model is defined as,

$$D_{c_m(t+5)} = D_{c_n(t)} \left( \frac{e^{\beta D c_m + \beta_1 D_c + \beta_2 TPH}}{\Sigma_{j=1}^{K} e^{\beta D c_j + \beta_1 D_c + \beta_2 TPH}} \right),$$

*( 13 )*

where $D_c$ is the diameter class of the *Fraxinus*, *n* is the initial decay class being evaluated, *m* is the decay class whose transition is being evaluated, *t* is the initial year, *TPH* is the trees per hectare in that sample location, *K* is the number of decay classes, $\beta$ is the trained parameter for transitioning between decay classes *n* and *m*, $\beta_1$ is the trained parameter for the influence of size class and $\beta_2$ is the trained parameter for the influence of trees per hectare. Equation (13) means that the amount of *Fraxinus* BA in decay class *n* that will enter class *m* at time *t*+5 is proportional to the amount present now according to SoftMax regression. The structure of the regression is identical for all cases except for decay class 5 as since there are only two potential outcomes the logistic regression is used, but influencing variables remain identical.

The model was trained in rJAGS using the Gibbs sampling algorithm, a variation of the Metropolis-Hastings algorithm for Markov Chain Monte Carlo (MCMC) systems (Depaoli et al., 2016; Plummer, 2003). The model trained three Markov chains simultaneously and after a 1000 step burn-in to account for noise in the first steps of the Markov Chains, 20,000 samples were extracted and the mean of best fit chain taken to define our model system. The best fit was determined by visual inspection when compared with the original sample distribution. The results of this process are displayed in Table 6, where trained weight parameters for each potential transition and site factors are displayed. Site factors are only displayed in terms of

whether they influence the possibility of the specimen to fall or remain standing to reduce the number of parameters that needed to be trained.

*Table 6: Selected Beta values for the Transition of* Fraxinus *between Decay Classes. The code attached to the beta value refers to the initial state and the end state. For instance, beta.12 indicates the beta coefficient for the transition of timber from decay class 1 into decay class 2.*

| | MEAN | STANDARD DEVIATION | NAÏVE STANDARD ERROR | TIME-SERIES STANDARD ERROR |
|---|---|---|---|---|
| **beta.12** | 1.978183 | 0.29461 | 0.0012028 | 0.0071085 |
| **beta.13** | 2.129820 | 0.29206 | 0.0011923 | 0.0072076 |
| **beta.14** | -0.351238 | 0.42597 | 0.0017390 | 0.0071344 |
| **beta.15** | -80.970151 | 58.79299 | 0.2400214 | 0.4011628 |
| **beta.1f** | 2.966160 | 0.28302 | 0.0011554 | 0.0070137 |
| **beta.23** | 0.277871 | 0.13035 | 0.0005321 | 0.0011083 |
| **beta.24** | -1.598005 | 0.23596 | 0.0009633 | 0.0014912 |
| **beta.25** | -5.229981 | 1.26970 | 0.0051835 | 0.0080808 |
| **beta.2f** | 1.278972 | 0.11052 | 0.0004512 | 0.0009751 |
| **beta.34** | -1.422282 | 0.23587 | 0.0009629 | 0.0014378 |
| **beta.35** | -3.285867 | 0.54935 | 0.0022427 | 0.0031250 |
| **beta.3f** | 1.518051 | 0.11513 | 0.0004700 | 0.0007073 |
| **beta.45** | -3.134961 | 1.33008 | 0.0054300 | 0.0089360 |
| **beta.4f** | 2.293788 | 0.29657 | 0.0012107 | 0.0016414 |
| **beta.5f** | 4.047865 | 1.29729 | 0.0052962 | 0.0081469 |
| **beta.DBHf** | -0.026615 | 0.07674 | 0.0003133 | 0.0007314 |
| **beta.DBHs** | 0.190139 | 0.08749 | 0.0003572 | 0.0008317 |
| **beta.TPHf** | -0.187436 | 0.07059 | 0.0002882 | 0.0006126 |
| **beta.TPHs** | 0.004739 | 0.08236 | 0.0003362 | 0.0007240 |

The site factor parameters show that in general, larger snags are more likely to transition to a more advanced decay class (with a beta.DBHs significantly greater than zero) but are no more likely to fall (beta.DBHf). Snags in denser stands are no more likely to transition to a higher decay class (beta.TPHs) but are less likely to fall (beta.TPHf is significantly less than zero). Additionally, for each decay class there was a far higher probability to transition into the fallen decay class than there was to remain in one of the standing decay classes with large positive numbers for each parameter associated with tree failure (Table 6: beta.1f, beta.2f, beta.3f, beta.4f, and beta.5f).

### 2.5 Distribution Infrastructure Location and Trees per Hectare Estimation

The final two factors to estimate are: (1) trees per hectare (TPH) as stand density is a significant factor in determining how fast trees fall and (2) the length of electric lines in the distribution network, which is at risk from treefall (Hughes et al., 2021; Oberle, Ogle, et al., 2018). To estimate the TPH we used the Forest Cover variable from Chapter 2 and multiplied the forest cover percent by an average of 1400 TPH. The number 1400 TPH was sourced from a combination of the average of New Jersey State Inventories and the FIA sample data for *Fraxinus* from the entire sample region (Crocker et al., 2017; McRoberts et al., 2005).

We estimated the length of powerlines in each cell where *Fraxinu*s was located by first georeferencing the locations of transformers submitted for the New Jersey Department of Environmental Protection (NJDEP) Solar Capacity project in 2016 (Bureau of Climate Change and Clean Energy, 2021). The estimation of electric distribution lines was developed using New Jersey Department of Environmental Protection Geographic Information System digital data, but this secondary product has not been verified by NJDEP and is not state-authorized or endorsed.

The transformers were then referenced to the local road network sourced from the TIGER/line shapefile and translated into strings of points to allow ordering transformers along the length of each road (Bureau of Transportation Statistics et al., 2016). The referenced transformers were then connected to measure the approximate length of the distribution network in the study area (Figure 16). This approximated distribution network is not perfect information as it does not connect the network across roadway intersections, but other mapped distribution networks are not available for the study area and given the method involved, likely slightly underestimates the actual network. However, it is a good coverage, and approximates the distribution network for the purposes of costs incurred by treefall. The distribution is displayed in Figure 16 and shows significant coverage in the Southern and Eastern portions of the study area. The height of the distribution network is defined as 35 feet which is the average height of distribution power lines in the region, but with expected upgrades due to electrification we also consider a height of 60 feet (Public Service Electric & Gas Co. (PSE&G), 2007; Warwick et al., 2016).

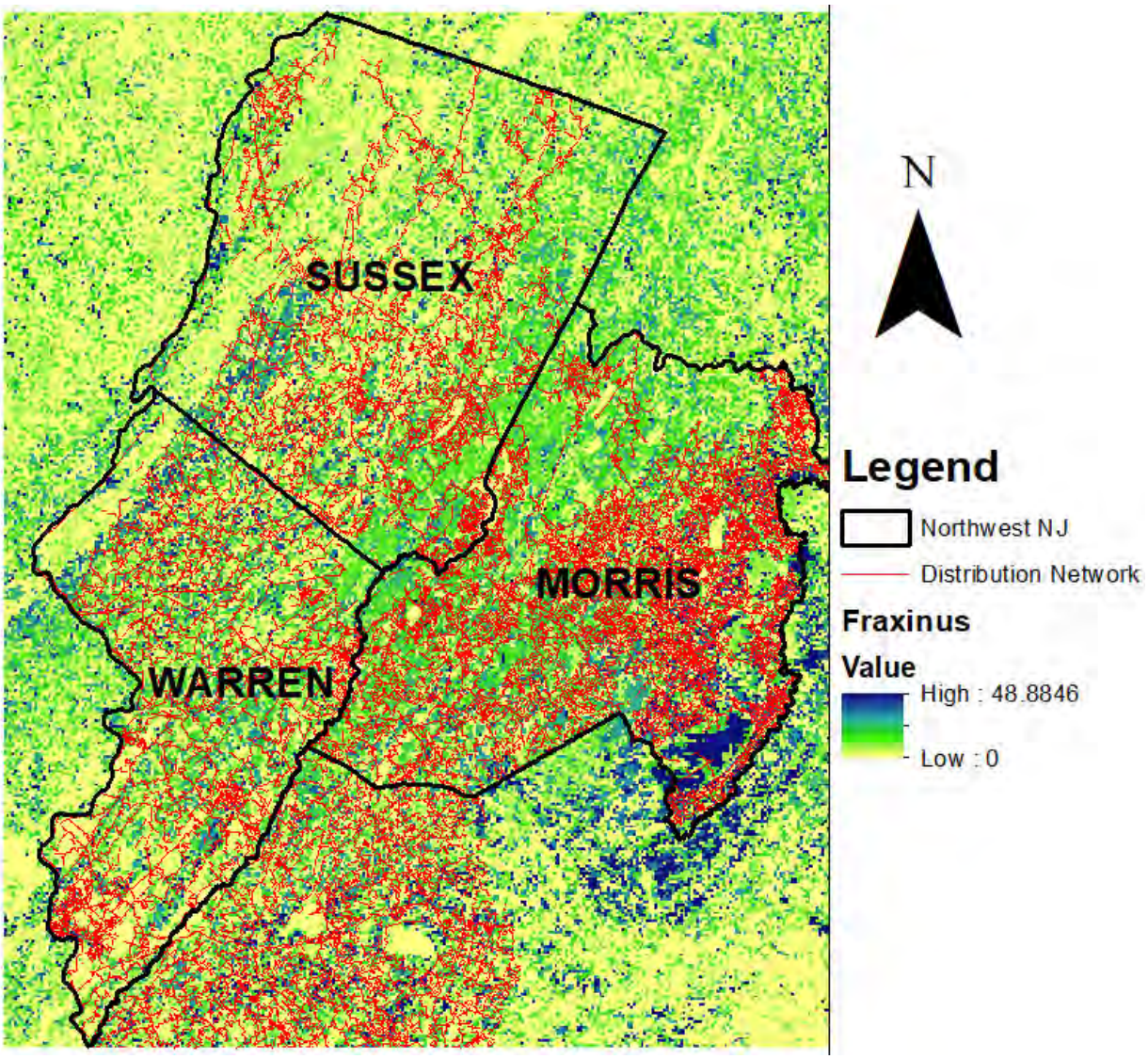


*Figure 16: Map of Northwestern New Jersey and the Associated Fraxinus and Electrical Distribution Infrastructure*

### 2.6 Modeling Fall Risk

At this point, there are five prepared inputs for the methodology, including (1) the distribution of standing dead *Fraxinus* per year due to EAB infestation, (2) the height of the standing dead *Fraxinus*, (3) the transition probabilities between the decayed and fallen classes of

*Fraxinus*, (4) the estimated length of the local power distribution network, and (5) the height of the distribution network.

First, we construct a set of equations to relate the expected proportional fall of *Fraxinus* to our spatial data such that,

$$D_{c_n x(t+5)} = D_{c_n(t)}\left(1 - \sum_{m=n+1}^{K} \frac{e^{\beta D_{c_m} + \beta_1 D_c + \beta_2 TPH}}{\sum_{j=1}^{K} e^{\beta D_{c_j} + \beta_1 D_c + \beta_2 TPH}}\right),$$

*( 14 )*

where $D_c$ is the diameter class of the *Fraxinus* basal area, *n* is the decay class being evaluated, *x* indicates this is the amount of *Fraxinus* remaining at *t*+5 from the original amount, *m* is *n*+1 as long as it is less than *K*, *t* is the year of input data from section 2.1 being evaluated, *TPH* is the estimated trees per hectare in that location, *K* is the number of decay classes, $\beta$ is the trained parameter for transitioning between decay classes, $\beta_1$ is the trained parameter for the influence of size class and $\beta_2$ is the trained parameter for the influence of trees per hectare. Equation (14) means that the amount of *Fraxinus* BA in decay class *n* at time *t*+5 is proportional to the amount present now, times one minus the sum of the proportions of BA in decay class *n* at time *t* that are advancing to a more advanced decay class. This is step one as any classes in less advanced states of decay will feed into the system adding material to the decay class *n* such that the system of equations equals,

$$D_{c_n(t+5)} = D_{c_n x(t+5)} + \sum_{m=1}^{n-1} D_{c_m(t)} \frac{e^{\beta D_{c_m} + \beta_1 D_c + \beta_2 TPH}}{\sum_{j=1}^{K} e^{\beta D_{c_j} + \beta_1 D_c + \beta_2 TPH}},$$

*( 15 )*

All terms are the same as eq. (14), except for *m*, which here is defined as all classes that are less than *n*. Overall, eq. (15) means that part of each decay class *m* at time *t* transitions into decay

class *n* at *t*+5. Transitions into the fallen class were taken from each decay class on each transition and stored by year and diameter class such that,

$$D_{c_f(t+5)} = \sum_{n=1}^{f-1} D_{c_n(t)} \frac{e^{\beta D c_f + \beta_1 D_c + \beta_2 TPH}}{\Sigma_{j=1}^{K} e^{\beta D c_j + \beta_1 D_c + \beta_2 TPH}}. \quad (16)$$

Equation (16) means that the fallen class in the next period equals the sum that fall from each standing decay class. This system of equations is used to process all the spatial data for the study area out 40 years from the EAB spread model start time. We chose 40 years as this time period to evaluate as it allows an additional 20 years beyond the end of the EAB model for the decay and fall of *Fraxinus* that were affected in the final year of the EAB spread model.

After snag fall has been projected the next step is to determine which snags could cause damage to distribution infrastructure. The predicted *Fraxinus* mortality is combined with the length of the electric lines present to estimate the number of *Fraxinus* that will probabilistically fall on the electric lines.

The topographical relationship between *Fraxinus* snags and assume that on average equal numbers of trees will be on level terrain compared to the distribution infrastructure and so topography is not considered in height calculations. The probability of a tree falling towards or away from distribution infrastructure is set as a binary outcome and any more detailed probabilities would require specific knowledge of the conditions around the distribution infrastructure. Cases where distribution infrastructure is taller than the potential hazard tree are not evaluated because there is no risk.

To calculate the number of potential hazard trees, we calculate the ratio of basal area in a size class ($D_c$) over the basal area of one tree in that size class ($BA_c$). The number of fallen trees

that impact distribution infrastructure is defined a proportion of the area *P* that contains both hazard *Fraxinus*, $\frac{D_{c_{(t)}}}{BA_c}$, and length of distribution lines, $G_l$ combined with the distance from distribution infrastructure, *Fraxinus* of a certain height can be $D_g$.

To define the distance, $D_g$, we use the height of the distribution grid, $H_g$, and the height of the tree, $H_t$. These two heights form two legs of a right triangle when we assume that the average slope between the *Fraxinus* snag and distribution infrastructure is zero. We utilize the Pythagorean theorem to solve for the distance between the pole and the tree such that the tree forms the hypotenuse.

In all, this relationship is defined as

$$F_{\mathrm{r_c}} = \begin{cases} 0 & H_c < H_g \\ 0.5\left(\frac{D_{c_{(t)}}}{BA_c} \cdot \frac{\left(G_l\sqrt{H_c^2 - H_G^2}\right)}{P}\right) & H_c > H_g \end{cases} \quad (17)$$

where $F_{\mathrm{r_c}}$ is the number of trees falling on a powerline for a size class of trees, 0.5 is the random chance that a tree in the danger area falls towards the powerline, $D_{c(t)}$ is the basal area that has fallen in one size class, $BA_c$ is the average basal area per tree in each size class, the ratio $\frac{Dc(t)}{BA_c}$ defines the number of trees in size class *c* at time *t*, $G_l$ is the length in meters of the local electric lines, $H_c$ is the height of diameter class *c*, $H_g$ is the height of the electric lines and *P* is the area of a pixel, in this case a square hectare. Equation (15) reads that the number of treefalls for size class *c* at time *t* is equal to half the number of fallen trees times the length of the grid times the absolute value of the square root of the height of the tree class squared minus the height of the electric grid squared over the square meters in one pixel, *P*.

## 2.7 Economic Costs of Treefall

Costs for a tree falling on a powerline are counted as a direct cost between $4,508 and $13,518 based on the cost for a new mile of traditional overhead power lines and the assumption that the damage compromises the line between two utility poles, usually a length of between 100 and 300 feet depending on site conditions in 2022 dollars (Warwick et al., 2016). This cost does not consider overtime, or the urgency of the remedial work.

The cost of removing a tree is set between $1,166 and $3,499 for normal operations and management (O&M) tree removal in 2022 dollars. Precise estimates are not available for the cost of tree removal due to the nature of the work so this cost is estimated from local contractors estimation (Amazing Tree Services, 2017; Moosewood Tree Service, 2017). In the case of line repair and tree removal we assume that costs will approach the low end of presented costs due to economies of scale and to not overstate the issue. The cost of the upgrade to higher power electric distribution infrastructure is significant at approximately $238,000 per mile, but will be done at some point in the future due to increasing electrification of the State through the 69kV initiative (Public Service Electric & Gas Co. (PSE&G), 2007; Warwick et al., 2016). This means that decreased incidence of costly treefall events given 15-foot higher line height area is an ancillary benefit of a policy that is already being enacted. We employ a discount rate for four cost scenarios of 3% for a public good that is not expected to :

$$C_t = \frac{F_{r_c} C_s}{1.03^t}$$

*( 18 )*

where $C_s$ is the estimated economic costs of this system by using the number of incident trees, $F_{r_c}$, described in Section 2.5 times the four potential cost above and the years since the initial fall to calculate the present value of either the removal, or topping, of incident trees.

## 3. RESULTS AND DISCUSSION

Our initial results show the importance of spatial simulation to determine the costs of EAB infestation on the electrical grid. When all vulnerable trees die in year one and enter the first decay class, it results in high costs (Table 7, Scenario 1), with a stepping pattern due to the 5-year updates (Figure 17); error is ±30% due to uncertainty of the tree heights, other factors, like the uncertainty with fall rates, result in far less error (Table 7, Scenario 1 versus Scenarios 2 & 3). Despite the uncertainty from tree heights, the impacts to current infrastructure (Table 7, Column 3) are decidedly outside the range of the upgraded infrastructure (Table 7, Column 4) and while the upgrade of the infrastructure reduces costs significantly, the most effective method is to mitigate the threat by identifying and removing all potentially dangerous trees near powerlines. The magnitude of these costs is also significantly impacted by the discount rate, which almost halves the impact of snags if the mortality is delayed till the twentieth year of the simulation (Table 7, Scenario 4). Spatial scenarios (Table 7, Scenarios 6-9) have much higher costs because of the growth of *Fraxinus* that occurs before mortality and have interesting properties that come out once we look at their temporal characteristics compared to the fixed introduction scenarios (Table 7, Scenarios 1 & 5).

*Table 7: Summary of Results from Costs Due to Incident Trees in Millions of 2022 Dollars. High estimates where incident trees impact the grid are displayed first and costs where the trees are topped, or trimmed, are displayed second within parentheses.*

| SCENARIO | PARAMETERIZATION | CURRENT INFRASTRUCTURE COST OVER 40 YEARS | UPGRADED INFRASTRUCTURE COST OVER 40 YEARS |
|---|---|---|---|
| **S1: IMMEDIATE MORTALITY YEAR 1** | All *Fraxinus* present in the survey fails in Year 1 and begins decaying | $1,455 ($233) | $376 ($60) |
| **S2: IMMEDIATE MORTALITY YEAR 1 MINUS BETA** | Sensitivity to decreased beta values from S1 | $1,443 ($231) | $373 ($60) |
| **S3: IMMEDIATE MORTALITY YEAR 1 PLUS BETA** | Sensitivity to increased beta values from S1 | $1,461 ($235) | $378 ($61) |
| **S4: DELAYED MORTALITY YEAR 20** | All Mortality is delayed till year 20. This delay is to check the impacts of discounting. | $829 ($133) | $215 ($34) |
| **S5: EVEN MORTALITY (5 YEARS)** | All *Fraxinus* fails evenly over the course of five years. No growth. | $1,372 ($220) | $354 ($57) |
| **S6: SPATIAL 10** | Simulated damage by EAB. Seed 10. | $1,937 ($311) | $501 ($80) |
| **S7: SPATIAL 50** | Simulated damage by EAB. Seed 50. | $1,945 ($312) | $503 ($81) |
| **S8: SPATIAL 100** | Simulated damage by EAB. Seed 100. | $1,945 ($312) | $503 ($81) |
| **S9: SPATIAL 150** | Simulated damage by EAB. Seed 150. | $1,945 ($312) | $503 ($81) |
| **S10: SPATIAL 100+NO REGROWTH** | Spatial simulation of spread without sprouting factor | $1,798 ($288) | $465 ($75) |

Once we introduce the variable of time to our results, we see how the costs are really incurred strongly in first few years after the dead timber is introduced. Scenario 1 shows a strong

stepping pattern as all timber is updated in the same year, with almost half of the costs already incurred five years of the mortality (Figure 17).

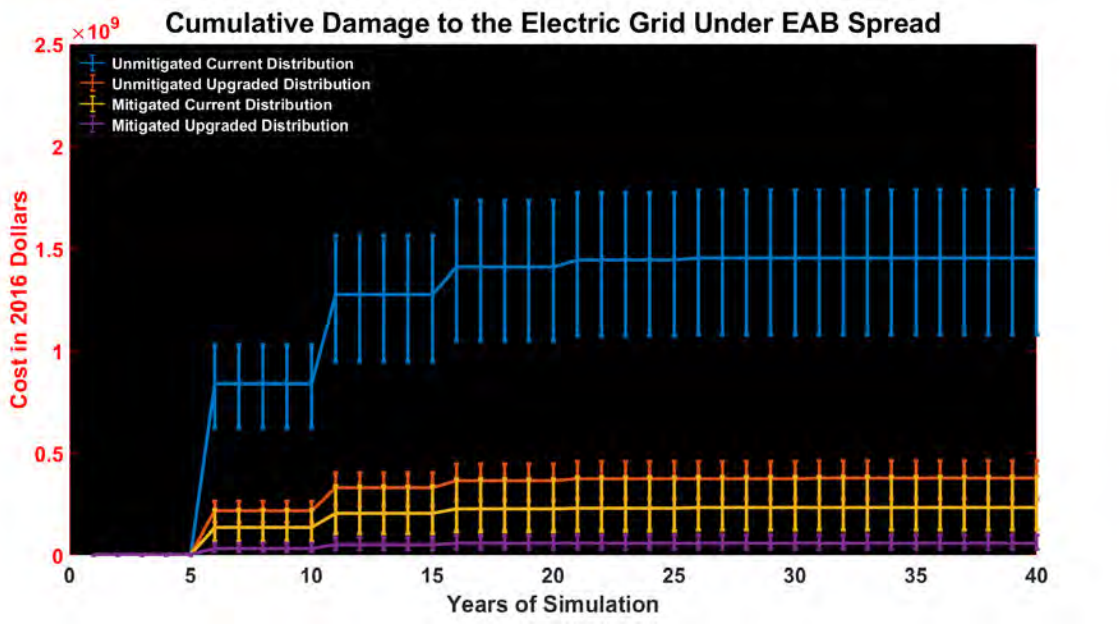


*Figure 17: Cumulative Costs in Scenario 1. All trees currently in place are assumed to enter the first decay class immediately. Starting in year 1. Because of the pattern of our sample the decay classes are updated every fifth. Year, leading to a spike at year five and every following fifth year. Mitigation refers to whether* Fraxinus *are assumed to be removed before damage occurs.*

Once we start to spread the mortality over multiple years, as in Scenario 5, it smooths the cost curve, but shows a similar end cost, with discounting not making a large distance in the result. The total result is similar immediate mortality, being just slightly lower due to discounting. This reinforces the result of scenario 4 in that the timing of Fraxinus mortality influences costs if there is a long enough lag (Figure 18).

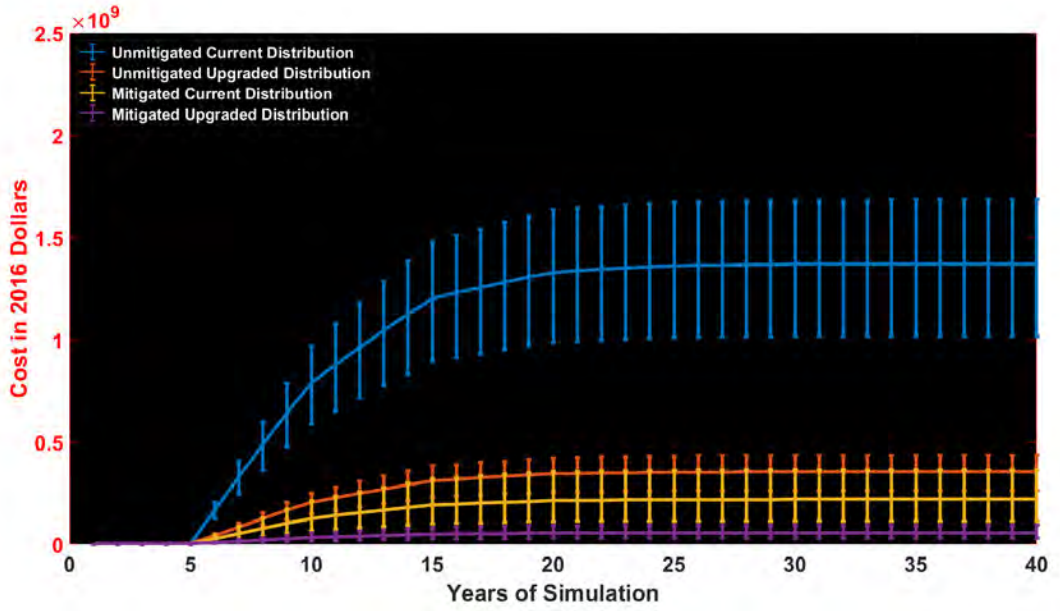


*Figure 18: Staggered Introduction of Mortally Damaged Timber over 5 Years. This introduction results in a much smoother cost curve over an immediate mortality scenario.*

These scenarios set our baseline; we then used four realizations for the spread of EAB in the study region under no parasitism. These realizations exhibit behavior somewhere between the 20 year and immediate mortality scenarios, but with higher costs due to the simulated growth of *Fraxinus* leading to higher costs. This growth outpaces the discounting of future costs despite mass mortality of *Fraxinus* not occurring until year 12-13 of the simulation. The greater magnitude of the result is caused by the aggressive regrowth and resprouting that is assumed in the EAB model for damaged *Fraxinus* (Figure 19). All four of these scenarios have extremely similar results which shows that damages are not highly dependent on the distribution of EAB due to random placement.

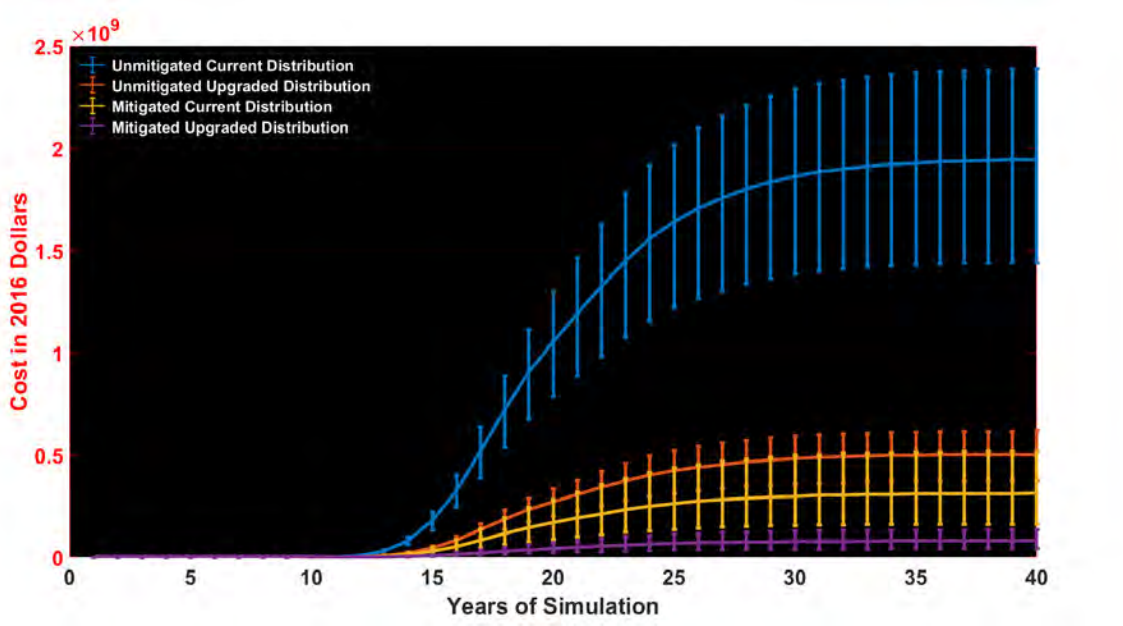


*Figure 19: Cumulative Costs using EAB Spread Modelling as the Input. The spread of EAB results excess* Fraxinus *mortality in year 13 leading to a steep cost curve and prohibitive costs due to regrowth of* Fraxinus.

In Scenario 10, we expand on these results and instead only allow *Fraxinus* to grow at its normal rate, leading to overall lower costs. This variation on the previous scenario was used to assess the affect that new growth from EAB killed stands of *Fraxinus* were having on the magnitude of the result. By eliminating sapling class growth, there was a ~15% reduction in cost across all treatments, which showed that the regrowth of *Fraxinus* was a significant contributor to elevated costs in previous scenarios. In reality, regrowth from stump sprouts and the seedbank, would not be a significant risk as all *Fraxinus* would be in the sapling class for the foreseeable future(Figure 20).

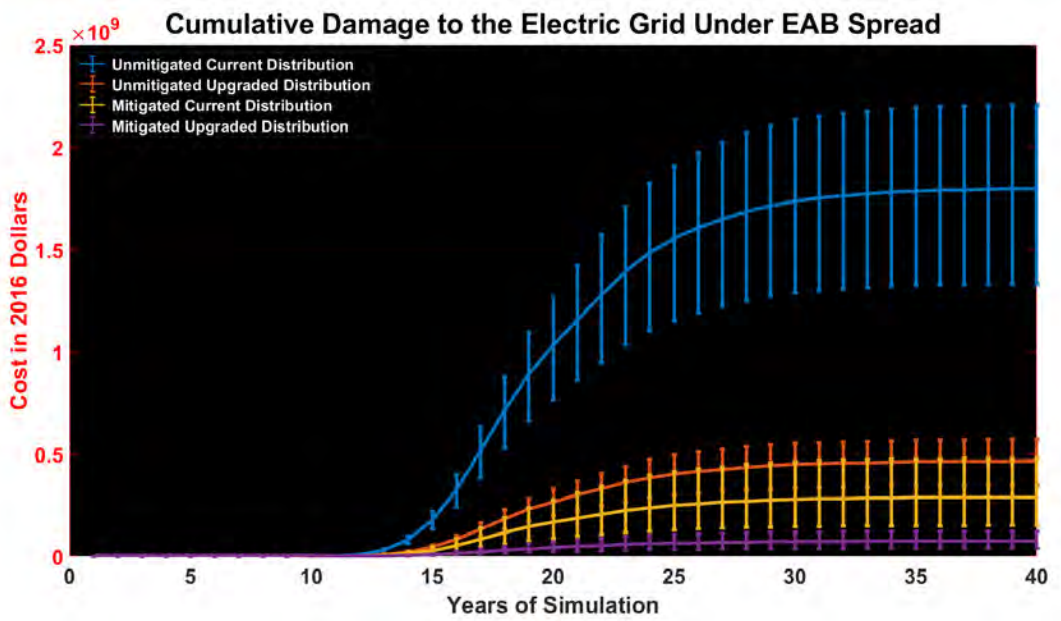


*Figure 20: Cumulative Costs using EAB Spread Modelling and Limiting Regrowth of* Fraxinus. *The spread of EAB results in a spike of* Fraxinus *mortality in year 13 leading to a steep cost curve, but without aggressive sprouting we see a much smoother curve for costs. This scenario shows costs more akin to the initial estimates with immediate mortality, with a reduction of $150 million over Figure 19.*

Between scenarios, we see a wide range of potential costs for the 9,800 kilometers of electric lines in the study area. Costs for an individual location range from $0 up to $406,000 ($214,000 when mitigated) for the current electrical infrastructure. With this wide range of results, we wanted to investigate what trend the inputs might have on the results. That is whether the length of the powerline, or the local basal area of *Fraxinus* influences costs more. After testing fits for the data, our results showed that the relationship between total cost is strongly linear with the product of the meter length of electric lines and the basal area of *Fraxinus* (Figure 21). The positive relationship between these three factors is somewhat expected, though still surprising given the highly varied input data involved that just two factors are the primary

drivers for cost. The scenario plotted does have influence on the slope of the line, but not on the linear trend which is observed across all scenarios.

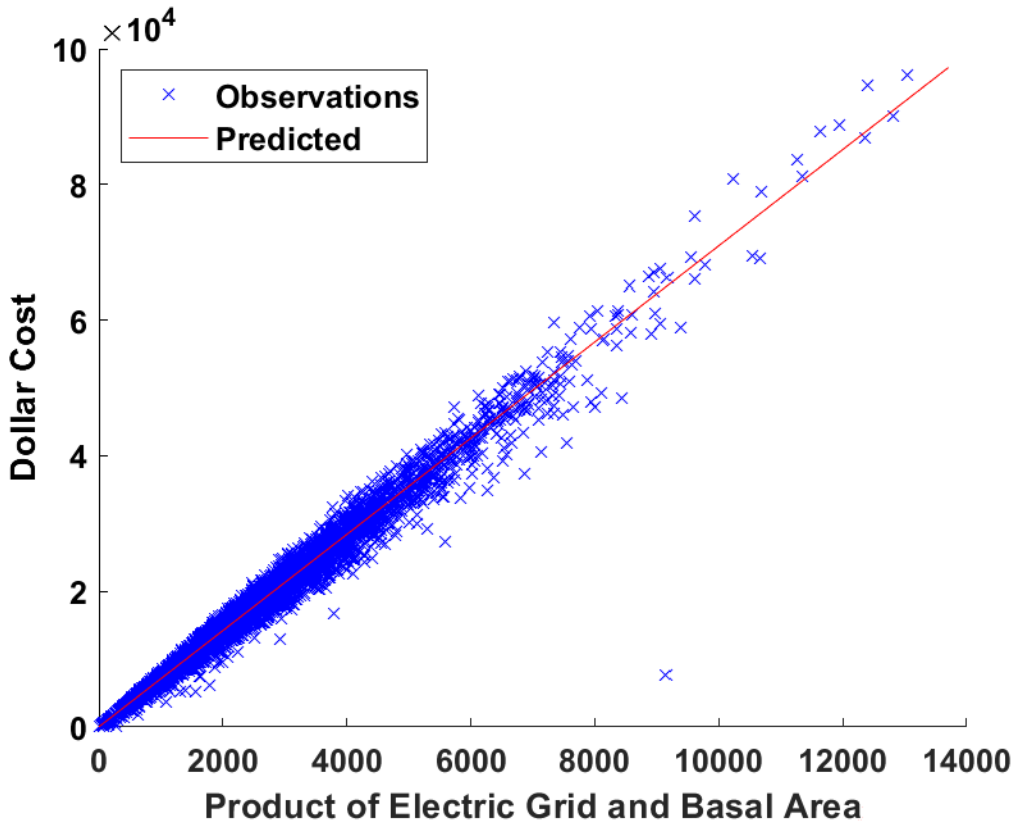


*Figure 21: Trend Between the Dollar Cost (2022) and the Input Product for Mitigated Locations in the Spatial 100 Scenario. By taking the product of every point where both* Fraxinus *and electric lines are present and plotting them versus the cost, we see that the data is strongly linear in our current model.*

To make upgrading the electrical infrastructure feasible based strictly on reduced *Fraxinus* snag damage, the cost savings will have to exceed $147.88 per meter of electric grid present based on the average upgrade cost. We can see that if there is little to no line maintenance for dead and dying trees, the average case will almost cover the costs of upgrades to the grid. As without line maintenance average costs for the current electric distribution infrastructure is just over $190 and drops to just over $50, which means just over $140 of benefit (Table 8). However, if the trees are trimmed the mitigated benefit is much lower, with only ~$40

of avoided cost per meter of powerlines. This potential savings is significantly below covering the cost of electrical infrastructure upgrade and means that if the lines can be properly maintained, upgrading the distribution network will not be justified at large by *Fraxinus* fall rates, but would still cover nearly one-quarter the costs on average of upgrading the distribution lines.

*Table 8: Average Cost per Meter by Treatment. The first column contains dollars per meter of electric grid associated with* Fraxinus spp. *when the infrastructure has been upgraded and the second column represents dollars per meter of electric grid associated with current infrastructure. Values in parentheses are related to infrastructure maintenance, while values outside parentheses are indicative of infrastructure repair.*

| SCENARIO | UPGRADED INFRASTRUCTURE | CURRENT INFRASTRUCTURE |
|---|---|---|
| **S1: IMMEDIATE MORTALITY YEAR 1** | $38.35 ($6.15) | $148.26 ($23.79) |
| **S6: SPATIAL 10** | $51.07($8.20) | $197.43 ($31.70) |
| **S7: SPATIAL 50** | $51.28 ($8.23) | $198.24 ($31.83) |
| **S8: SPATIAL 100** | $51.28 ($8.23) | $198.24 ($31.83) |
| **S9: SPATIAL 150** | $51.28 ($8.23) | $198.24 ($31.83) |
| **S10: SPATIAL 100+NO REGROWTH** | $47.40 ($7.61) | $183.27 ($29.41) |

## 4. CONCLUSIONS AND FUTURE STUDY

Our methodology for *Fraxinus* snag fall was particularly enlightening on the degree of damage that EAB is capable of and helps to identify locations that are of special concern. With the mortality and decay of *Fraxinus* continuing apace, there is significant impetus for a detailed survey of electric distribution lines to prevent outages. Our model has demonstrated when and

where these costs occur and while not perfect it does serve as framework to evaluate potential costs across a wide spatial area. Costs, that with current parameterization, are excessive and for some locations the cost for *Fraxinus* management is greater than the cost to upgrade to a taller more robust grid, though in most cases were better served by standard line management practices, if they are completed in time.

This methodology was only limited by its data, focused primarily on the height of *Fraxinus* and the cost estimates for repair and distribution. If precise plot locations for the FIA samples could be obtained for a future study, then much more could be done to attempt fine-tuning the height regression. Machine learning with LiDAR data has been shown to be an efficient solution for these data gap and could bring some definition to the problem involved if FIA data can be given as input (Wang et al., 2021). This extension could also improve our knowledge on the general distribution and structure of *Fraxinus* in the forest structure, allowing even greater accuracy for both this study and providing a unified method for the future. The repair and distribution estimates can be improved with input from stakeholders in the field, either through survey or further direct discussion.

# CHAPTER 4. EAB RELATED MORTALITY IMPACTS ON ECOSYSTEM SERVICES OF HOST FORESTS

## 1. INTRODUCTION

Extirpation of *Fraxinus* will cause disruption to local ecosystems and interruptions in ecosystem services (ES) from impacted forests. ES are the unpaid services and goods that are provided by the landscape without significant anthropogenic maintenance. Services provided include resource provision, water filtration, sediment/nutrient cycling, urban cooling, oxygen production among many others (DeSantis et al., 2013). These services provide the underpinning to economies around the world (Rastetter et al., 2021).

The loss of *Fraxinus* in the Northeastern Forest system of the United States of America (USA) has been noted to have far ranging impacts, but here we focus on landscape level impacts within the first years after extirpation from the forest system. Losses in urban systems are well-studied and have been discussed at length by previous studies and are not discussed here (Arbab et al., 2022; Bushaj et al., 2021; Poland & McCullough, 2006; Selbig et al., 2022).

Forests provide key resources that help local economies. First is the provisioning of raw materials in the form of timber and other forest products; this is not of significant concern in the study area as the timber industry in the State of New Jersey is not a major industry. Forest products are generally not harvested or are exported to neighboring states for processing on the rare occasion they are harvested. This lack of harvest is despite the fact that upwards of 80% of New Jersey's forest can be defined as timberland, as they have been all almost uniformly maturing into late stage growth with limited harvests despite abundant material present (Crocker et al., 2017).

The focus for measurable impacts then is on non-use services. These include: 1) water yield, the ability of land to yield usable fresh water on an annual or seasonal basis (Brantley et al., 2015; Fissore et al., 2012; Selbig et al., 2022); 2) the nutrient delivery ratio (NDR), the ability of the landscape to filter and store necessary nutrients and impound them (Harmon & Bell, 2020; Sims et al., 2013) and 3) sediment delivery ratio (SDR), the ability of the land to hold sediment in place and prevent erosion into water bodies (Hamel & Bryant, 2017). Losses in these core services could threaten the stability of the forested region responsible for supplying much of the drinking water in the State of New Jersey.

We evaluate these key ecosystem services over the course of EAB infestation. Through this method we can estimate the mitigation, or other methods that might be required to minimize the negative externalities from *Fraxinus* mortality in the study area.

ES have been studied as they apply to *Fraxinus* for many years, with various impacts and issues surrounding *Fraxinus* mortality becoming known over decades of study. Potential ES impacts include the extirpation of *Fraxinus* dependent species, a surge in wood feeding insects from the surge of fallen timber, and the expansion of other invasive plant species making use of disturbed canopy gaps (Baron & Rubin, 2021). However, simulations of these effects on the ecosystem would not be readily apparent at the scale of our study because of their highly site-specific nature. The history of ecosystem service evaluation has been extensive however, so it would be remiss not to cover the progression of this field.

It will be years before we fully understand the impacts of *Fraxinus* mortality. Long-term studies about the changing balance in forests will be necessary to define their successional dynamics and changing services. A real concern is the accelerated mesophication of the entire East Coast, with climate change and invasive species slowly eliminating the shade-intolerant

overstory leaving shade-tolerant genera in place. Especially since *Fraxinus* mortality often does not usually open the canopy enough to encourage shade-intolerant species (Rastetter et al., 2021).

A commonly assessed service is carbon storage and sequestration, which is the productive ability of the landscape to store gaseous carbon as biomass. The loss of *Fraxinus* will account for a loss of sequestered carbon by upwards of 225 million metric tons in the USA (DeSantis et al., 2013). However, further research on the subject minimizes the risk from this release of carbon in our study area. First, the decay of large woody material takes significant time, especially since *Fraxinus* is a hardwood species classified as somewhat resistant to decay slowing the annual release from killed trees (Oberle, Covey, et al., 2018). Second, modeling using Midwestern states as proxy showed substantially increased productivity in forests post EAB invasion when *Fraxinus* is not a majority component of the forest; the extra light liberated from the canopy leads to increased growth by neighboring trees until the canopy is filled in again and carbon storage recovers (DeSantis et al., 2013). These two factors preclude the study from taking carbon losses as a major ecosystem service disruption, as the disruption is quickly recovered.

However, other potential ES have received little attention, with little done to monitor their shifts due to *Fraxinus* mortality. These results on ancillary services do show one thing, long-term effects are not expected to persist longer than a few decades. It is expected that ecosystem function will return to near baseline as trees recover and fill the gap within 30 years post invasion. This view is supported, as there have been other observations of induced growth from the relatively small gaps in the forest canopy from *Fraxinus* mortality (Flower, Knight, Rebbeck, et al., 2013; Goins et al., 2013). While on average this was not high enough to

completely compensate for the losses, it did allow compromised forests with low densities of *Fraxinus* to reasonably recover in just a few years (Flower, Knight, & Gonzalez-Meler, 2013). This result backs up more recent results which showed significantly better recovery post-EAB with higher species diversity. The expected recovery does reduce our expected long-term impact in the Northeast somewhat due to the diversity of species present, but represents another step towards a uniform and less productive canopy (Granger et al., 2019).

Even over the short term there will still be a substantial impact in the near to mid-term, as *Fraxinus* mortality is often synchronous across large areas (Abell et al., 2016; Kashian et al., 2018; Siegert et al., 2014). Additionally, beyond provisioning ecosystem service changes, there are a host of smaller services that research has shown to have potential impacts from *Fraxinus*. Potential impacts that will require further research once short-term measures are justified include; human infant birth weight, soil biome, nutrient cycling regimes and the extinction of dependent insect species (B. A. Jones, 2018; B. A. Jones & McDermott, 2015; Perry et al., 2018; Rastetter et al., 2021; Ricketts et al., 2018).

While long-term impacts may be few, there are lines in current research that show potential shifts in the soil make-up. A study in New Hampshire found limited changes in soil respiration and demography at least shortly after *Fraxinus* mortality in forests where *Fraxinus* is a limited component of the forest canopy (Matthes et al., 2018). This research indicates, that at least in the short-term, soil carbon storage may not be significantly impacted in our study area, which has a similarly sparse distribution of *Fraxinus* (Matthes et al., 2018). This hypothesis is supported by the result from Ricketts et al. (2018), which only showed slight differences in the sub-surface biota between *Fraxinus* and non-*Fraxinus* forest plots. However, there was another more significant long-term impact. With *Fraxinus* mortality, Ricketts et al. (2018) found in test

plots that nutrient cycling for sulfur, phosphorous, and carbohydrates was higher than in similar forest communities without *Fraxinus*. One genera of acid loving bacteria was found to be more common in non-*Fraxinus* plots. The loss of this genera resulted in a significant difference in subsurface nutrient balance (Ricketts et al., 2018). Even after the forest recovers, there may be a significant enough disruption in nutrient cycling to justify further study (Ricketts et al., 2018).

In our study area, research has already focused on the large population of urban *Fraxinus.* In New Jersey the cost for replacing and treating the large quantity of street trees was deemed untenable compared to increased treatment and management over a 20 year timescale (Arbab et al., 2022). This bank of trees, if successfully treated, could provide a genetic bank for the State as biocontrol and other measures begin to spread, but also increases the mortality of biocontrol agents (Flower et al., 2018; Steiner et al., 2019). Additionally, in an urban setting, trees are even more valuable than in the wider landscape, in terms of their water retention capacity, with an individual mature tree being able to intercept an average of 6376 liters (L) of water per tree (Selbig et al., 2022).

In the core of the infestation in Northeastern Michigan, a decade after EAB had extirpated all vulnerable *Fraxinus*, only about 25% of infested *Fraxinus pennsylvanica* stumps exhibited any stump sprouting. Additionally, little to no seed production was evident, leaving one orphaned cohort of *Fraxinus* struggling in the understory. Given EABs continued presence in the region, it is doubtful whether there will ever be a full recovery in this region at anywhere near pre-infestation levels (Kashian, 2016; Kashian et al., 2018; Siegert et al., 2021). This lack of *Fraxinus* recovery indicates that lost services specific to this genus will not be recovered over time, but other services will be if other tree species are present.

To assess the losses in landscape ecosystem services gap that will be felt over the region, we use the Natural Capital Project's InVEST model (Natural Capital Project, 2022). InVEST is an accepted method for ecosystem service assessment under varied impacts (Hamel & Bryant, 2017; Polasky et al., 2011; Zarandian et al., 2017). We are utilizing the Nutrient Delivery Ratio (NDR), Sediment Delivery Ratio (SDR), and Annual Water Yield Models for three Northwestern New Jersey counties where *Fraxinus* is a strong component of the forest system. Other models offered by InVEST include impacts from carbon sequestration to habitat quality, and while there will be impacts in these fields due to *Fraxinus* mortality, they are either inconsequential according to the literature, or so unknown that they are impossible to quantify as a service without significant local data collection.

## 2. METHODOLOGY

Land use land cover (LULC) is the most common aspect that needs to be defined after the loss of *Fraxinus.* LULC refers to the anthropogenic, or natural landcover that is in a geographic space. Each LULC code simulated must be defined in terms of its effect on ES; a full list of LULCs simulated and the associated variables organized by model can be found in Appendix 3: Table 17. In our analysis, we keep the primary LULC static through time to isolate the impact of the loss of *Fraxinus* without including any shifts in the base LULC. Instead *Fraxinus* loss results in a slightly different land cover defined as the original land cover and the associated quantiles of *Fraxinus* loss, which will be covered in more detail in future sections (Table 9). These adjusted LULCs are defined by a shifted set of variables depending on the percentage loss of trees from the initial state to the present state. Shifts in ES provisioning have been observed in cases of similar disturbances to the forest structure, first with an expected increase in Annual Water Yield (Brantley et al., 2015; Ren et al., 2021) and second with decreased filtration of nutrients and

sediments as the soil surface is exposed to weathering (Wang et al., 2021). We incorporate these into our adjusted variables, as either a barren or shrubby site condition occupying the lost forest area. By adjusting the LULC values from the baseline condition to a barren or shrubby condition we simulate for the losses in provisioning water and constraining sedimentation and nutrification from this land area after the extirpation of *Fraxinus*.

We defined our biophysical tables by literature review from previous InVEST based studies that were in the same region as our study. While this is not perfect information due to regional differences, as there is a massive range of values that have been parameterized in even a relatively small area of North America with LULC variables that are well over an order of magnitude in difference (Bai et al., 2019; Berg et al., 2016; Brown & Quinn, 2018; Hamel et al., 2015; Walston et al., 2021). To this end, we adopted Brown & Quinn's (2018) parameterization, as it was the most amenable to our situation and set of land covers as well as being in a similar, though more southerly, Appalachian context compared to other available research.

Tables 17 in Appendix 3 includes a code for the LULC followed by the relevant information for each potential LULC. The Water Yield model's biophysical table includes vegetated status as a yes/no statement, the estimated root depth associated with the land cover in mm and a value $k_c$. The $k_c$ term is the cover coefficient that depends on the primary vegetative state of the site which was also compared with the recommended source from InVEST's documentation. The SDR model included only two factors the USLE Cover Factor (*C*) and the USLE Practice Factor (*P*). *C* indicates the land cover types, forest, agriculture or other, while *P* indicates the tilling, or land management practice with higher values of *P* indicating more conservative practices. Finally, the NDR model includes factors for the nitrogen and phosphorous loads/retention efficiency for each land cover types as kilograms per year.

Additionally, the NDR model includes terms for the critical length for both phosphorous and nitrogen. The critical length indicates the assumed distance a nutrient is transported before being at least partially arrested by the land cover. Outside of deriving the parameters from detailed studies on water cover that are usually unavailable, this is assumed to be the length of one cell, or in this case 100m, which is the InVEST default when local studies are not available.

### 2.1 Parameterization of the Models

To make use of the biophysical tables in a spatial context, we must define the environment that provides ecosystem services. Terrain height, watershed boundaries and other inputs are all required by InVEST to assess ecosystem services. We summarize the sources and definitions of this spatial data in Appendix 3: Table 16. In this section we define the spatial inputs and factors utilized in each of the three models.

First, inputs that were required by all models included LULC, watershed boundaries, annual precipitation and the experimental LULC. LULC was defined as the land use from the year 2015 published by the New Jersey Department of Environmental Protection (NJDEP) and is the most up to date LULC dataset in New Jersey at time of writing (New Jersey Department of Environmental Protection (NJDEP) et al., 2019). The initial LULC dataset is at a 30m distribution, which is too fine scale to match up with the other datasets. To make sure all the data was aligned and in the same reference frame, the LULC data was resampled and reprojected to the study area at 100 meters square resolution. To minimize error, the resampling was based on the majority fill of each raster cell, which is the LULC that comprised the largest portion of the new raster cell was selected. Watershed designations were sourced from the New Jersey Geological Survey (NJGS) and were based on the hydrologic unit code 12 (HUC-12) for local watersheds (New Jersey Department of Environmental Protection (NJDEP) & New Jersey

Geological Survey (NJGS), 2009). These data were reprojected and clipped to the study area extent. Precipitation values were sourced from the USGS 1981-2010 Annual Average precipitation raster for the conterminous USA and compiled by Oregon State University (Oregon Climate Service at Oregon State University, 2012). The precipitation map was resampled to the study resolution using a bilinear interpolation and transformed to mm from inches. Bilinear interpolation is recommended for continuous data types and results in a smooth surface after interpolation (ESRI, 2021).

For scenario analysis, the future LULC was defined as the 2015 LULC with reduced forest cover for each LULC. The LULC shift incorporated here did not include any developments in LULC over time to isolate the effect of forest loss on expected ecosystem service outcomes. The change in ecosystem services ($S_r$) was instead assumed to be commensurate with the ratio of *Fraxinus* basal area mortality from the initial state ($A_1$) over the total forest ($TF_1$) basal area estimated from published raster data by Wilson et al. (2012), the expected tree species composition and canopy cover (Alerich et al., n.d.; *Eastern Region Tree Species*, n.d.; U.S. Geological Survey, 2019; Wilson et al., 2012),

$$S_r = \frac{A_1}{TF_1} \cdot F_c. \tag{19}$$

The change in forest cover was defined by the four quartiles of the forest loss because discreet boundaries are necessary to define new LULC classes. Quartiles were used to separate the data due to most losses being less than ten percent of recorded forest cover, with some noted outliers (Table 9). Most InVEST studies focus on LULC shifts over time; however shifts in function within land uses have been acknowledged as a valid method for assessing ecosystem service changes (Ma et al., 2016).

*Table 9: Quartile Decline in Forest Cover Due to the Loss of Fraxinus Defined by the Ratio to Overall Basal Area*

| QUARTILE PERCENT DECLINE | AVERAGE OF QUARTILE |
|---|---|
| **0.1-1.5%** | 0.75% |
| **1.6-3.6%** | 2.6% |
| **3.7-6.0%** | 4.9% |
| **6.1-43.6%** | 24.85% |

LULC values change based on the loss between Forest and either barren or shrubby LULC. Combined with the 4 quartiles, it results in 8 new LULC classifications from each original LULC defined in Appendix 3, Tables 18-25. This change from the base LULC values is defined as,

$$S_a = S + \left((C_s - F_s) \cdot S_{r_{(Qn)}}\right) \quad (20)$$

where the altered biophysical component, $S_a$, is equivalent to the original biophysical factor, $S$, plus the deforestation proportion, $S_{r_{(Qn)}}$, times the difference of the biophysical parameter for the change state (barren or shrubland), $C_s$, and forest (>50%), $F_s$. The alteration of all biophysical parameters is based on the hypothesis that each location that is defined as one LULC is actually a mix of LULC categories that has been defined to fit into a single category. By implementing change across all LULC classes the impacts of *Fraxinus* mortality are spread throughout the landscape depending on the degree of forest mortality (Figure 22).

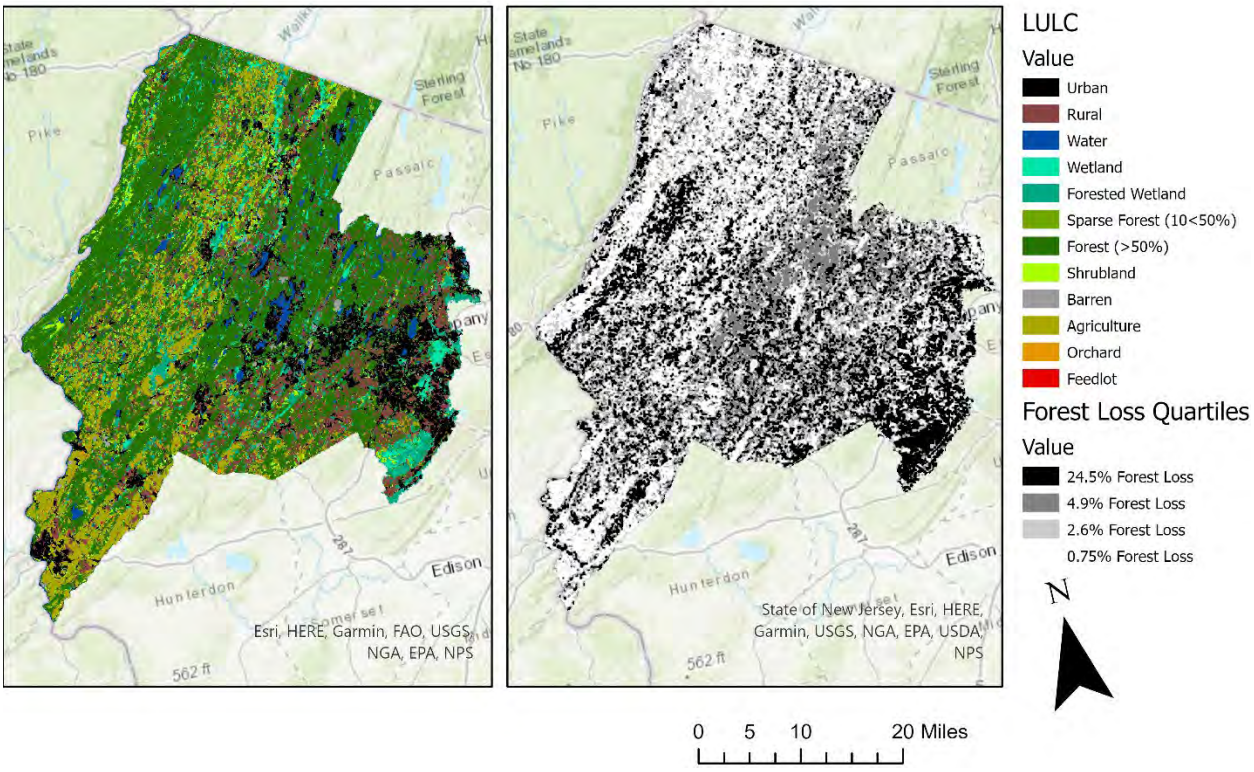


*Figure 22: LULC classes for the study area and the associated forest decline as a function of area. Greater forest losses due to* Fraxinus *decline are seen along the eastern and western edges of the study area with relatively less decline in areas under more intensive land uses. With greater forest loss, greater changes to the biophysical tables for each LULC are employed (Tables 18-25).*

To summarize, new LULC classes were defined by the degree of potential forest loss displayed above (Figure 22). This change was based on the percent forest loss for each land cover based on the sum of all Northeastern species minus *Fraxinus*. Losses of forest were estimated as the ranges in Table 9 and combined with the LULC, which resulted in 48 new land cover classes defined as either being minimally impacted (0.75% Forest Loss), slightly impacted (2.6% Forest Loss), moderately impacted (4.9% Forest Loss), or heavily impacted (24.5% Forest Loss). To quantify the impact in the biophysical tables, it was assumed due to the habit of *Fraxinus* in mixed forests, that post-infestation the service provided by that percent of forest would be similar to shrubland, either due to epicormic sprouting from the *Fraxinus* itself or

because of remaining understory shrub species in closed forests (Kashian, 2016; Kashian et al., 2018). The relationship between these two points was assumed linear and this has some support in the literature as a developing method for assessing the relative change in ES (Brantley et al., 2015; Lavorel et al., 2017; Millennium Ecosystem Assessment (Program), 2005). This scenario was contrasted with a barren site condition where the understory condition and epicormic sprouting are both poor because of an ongoing overgrazing issue in New Jersey by white-tailed deer and poor epicormic sprouting noted in closed forests (Bates, 2019; Kashian et al., 2018; "New Jersey Farm Bureau: Recognized Ecologists and Land Professionals Agree Deer Overpopulation in New Jersey Is an Emergency," 2021).

Factors that were required only for the Annual Water Yield model included the root restricting layer in the soil column, the plant available water content (PAWC) in the soil column, estimated evapotranspiration coefficient, and seasonality, known as the Z-Parameter. The root restricting layer was defined as the soil thickness from the SSURGO database field which referred to the cm of soil present 'tka_0-999' and was transformed from cm of depth to mm and then reprojected to the same reference as the LULC data. The plant available water content (PAWC) was similarly sourced from the SSURGO database as the available water content in the 'AWC 0-999' layer and transformed from cm to mm (Soil Survey Staff, 2020). Evapotranspiration was compiled by the USGS using their Operational Simplified Surface Energy Balance (SSEBop) model and was transformed into appropriate units using the InVEST transformation for sources in Imperial units (Natural Capital Project, 2022; U.S. Geological Survey, 2021). Finally, the Z-Parameter was computed according to

$$Z = \frac{(\omega - 1.25)P}{AWC}$$

*(21)*

where ω is a regional water-energy partitioning term for determining the amount of precipitation that evaporates. The Z-parameter captures the local precipitation pattern and hydrogeological characteristics of the study area and is calculated from three terms, ω, *P* and *AWC*. The term, ω, is estimated as 3.0 from a global data set from Xu et al. (2013), *P* is the precipitation in mm, and *AWC* is the available water content, which in our case is simplified as the PAWC. The result of this calculation gives a variable factor over the whole study area, but the InVEST input is taken as the average of the whole study area, which in this case comes to a seasonality factor (*Z*) of 2.25.

Finally, the factors for the SDR and NDR models included a DEM, erosivity, erodibility and the threshold flow accumulation value. Other inputs to the SDR and NDR models were kept as the InVEST default without sufficient local research to justify altering them (Natural Capital Project, 2022). The DEM was sourced from the USGS 30-m resolution raster and resampled using the bilinear method to the same reference as the LULC data (ESRI, 2021; U.S. Geological Survey, 2000). The erosivity, without an available USA counterpart, was sourced from the European Commission, Joint Research Centre Global Rainfall Erosivity Index, which was already in the proper units for InVEST (Panagos & Ballabio, 2017). The erodibility was taken from a derivative study of gSSURGO data by the Natural Resource Conservation Service and transformed according to the method recommended in the InVEST users guide (Natural Capital Project, 2022; Natural Resources Conservation Service, 2021a).We set the flow accumulation boundary as 1000 cells, as this is the recommended value in the literature and similar to the average connectivity found in the data for the study region (Natural Capital Project, 2022). Flow

accumulation refers to the number of connected cells required to consider overland flow into the waterbodies.

## 3. RESULTS AND DISCUSION

Results from the InVEST model showed the trends appropriate for each of the representative models, with increased export near water bodies decreasing with distance (Figure 23). From Figure 23 we can see that in the current LULC, nutrient and sediment exports are modest. Sediment exports are especially low with most values hovering near zero or acting as sinks for sediments.

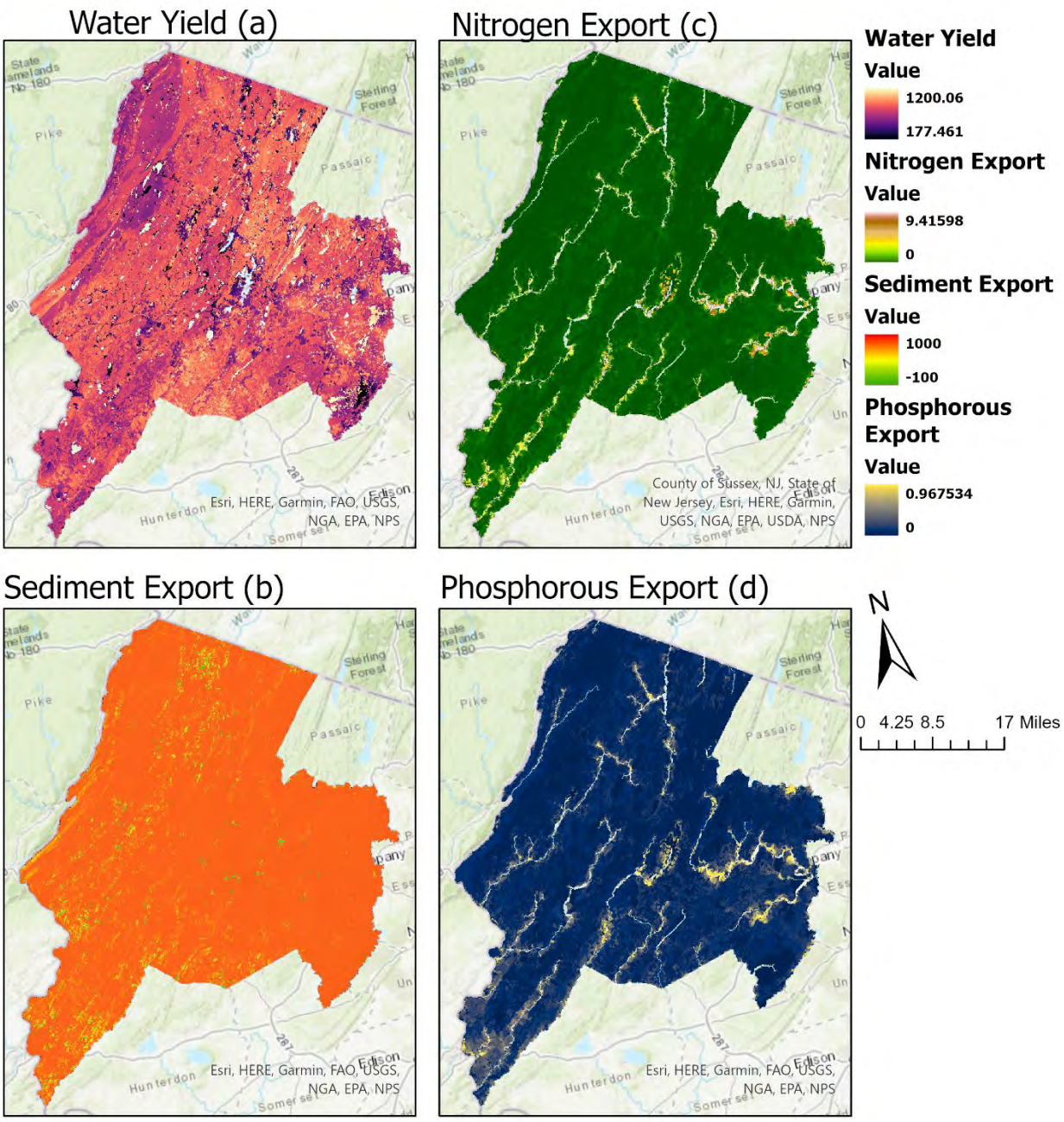


*Figure 23: Baseline Ecosystem Service Maps. Services show a typical distribution with water yield depending on landcover, but all export models being associated with distance to major waterways. Water Yield (a)is measured in cubic meters per year. Sediment Export (b) is measured in metric tons. Nitrogen Export (c) is measured in kilograms per year. Phosphorous Export (d) is measured in kilograms per year.*

When we compare results, we see a pattern that is close to what is expected from a forest disturbance associated with overstory losses, with water yields increasing (Figure 24 (a.1-2)),

leading to increased sediment export (Figure 24 (b.1-2)). The NDR model result was much more variable, and the model seemed sensitive to the simulated nutrient load over other LULC inputs. Precise numbers for New Jersey nitrogen and phosphorous loads from different LULC would aid in defining this result more clearly (Figure 25). Water yield climbs as expected from previous literature review. This trend only seems to be defied in some tree species (Brantley et al., 2015); with greater forest loss, we see an increase in water yield due to the decreased absorption of water from both the canopy and the slowing action of the soil. Sediment export is increased under both new cover regimes, but extremely so under barren conditions (Table 10). This result indicates that undergrowth is vitally important to prevent the worst outcomes. However, in much of the study area it is known that understory grazing pressure from native animals is at unsustainable levels (Bates, 2019). This pressure could be a barrier to retaining the ecosystem services compromised by *Fraxinus* loss. Nutrient export is inconclusive. However, this result would need to be verified with field measurement in future studies. Phosphorous export is lower in shrubby conditions, though nitrogen export slightly increases, as shrubs quickly grow in the gaps (Figure 25). While the inverse is true in barren site conditions. Shifting toward a barren effluent style results in greater phosphorous export, but lower nitrogen export. It is possible that with lower primary productivity from a barren site condition that there is lower nitrogen fixation, which leads to lower export. From testing, this is due to the nitrogen and phosphorous loading variables. The loading variables refer to the expected initial quantity of phosphorous and nitrogen released by the LULC type over a period. If these loading variables are kept constant in the barren scenario, we see increases in both phosphorous and nitrogen export, but without justification to do so, we maintain the loading variables as our calculations indicated the change in LULC class would indicate.

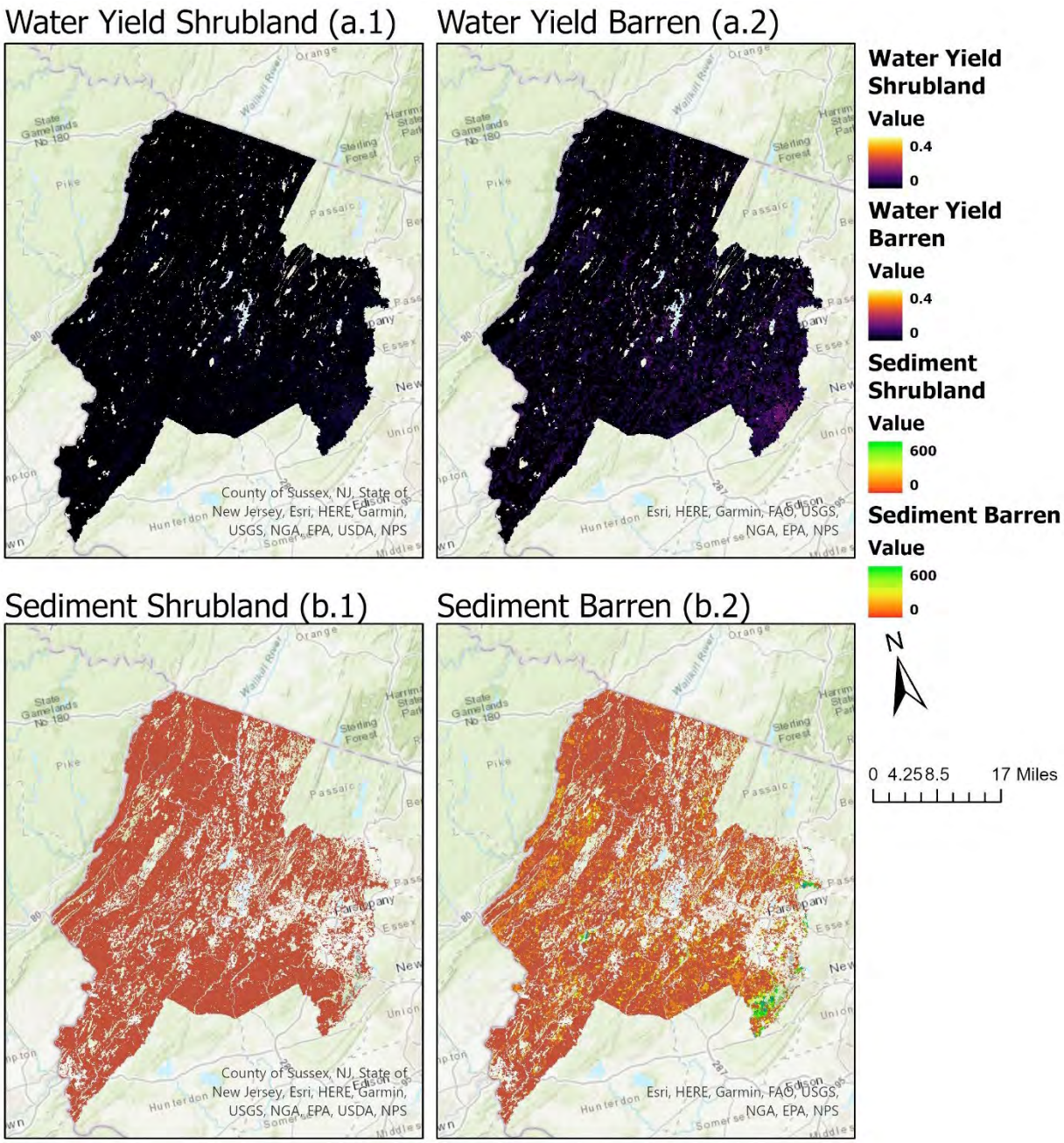


*Figure 24: Proportion Change for Water Yield and Sediment Export. Where (a.1) is the proportional change in water yield in a shrubby condition and (a.2) is the change in a barren site condition. When sites are barren water yields rise due to increased runoff. Additionally, (b.1) is the proportional sedimentation increase in a shrubby condition with slight change and (b.2) is the proportional sedimentation change in a barren condition.*

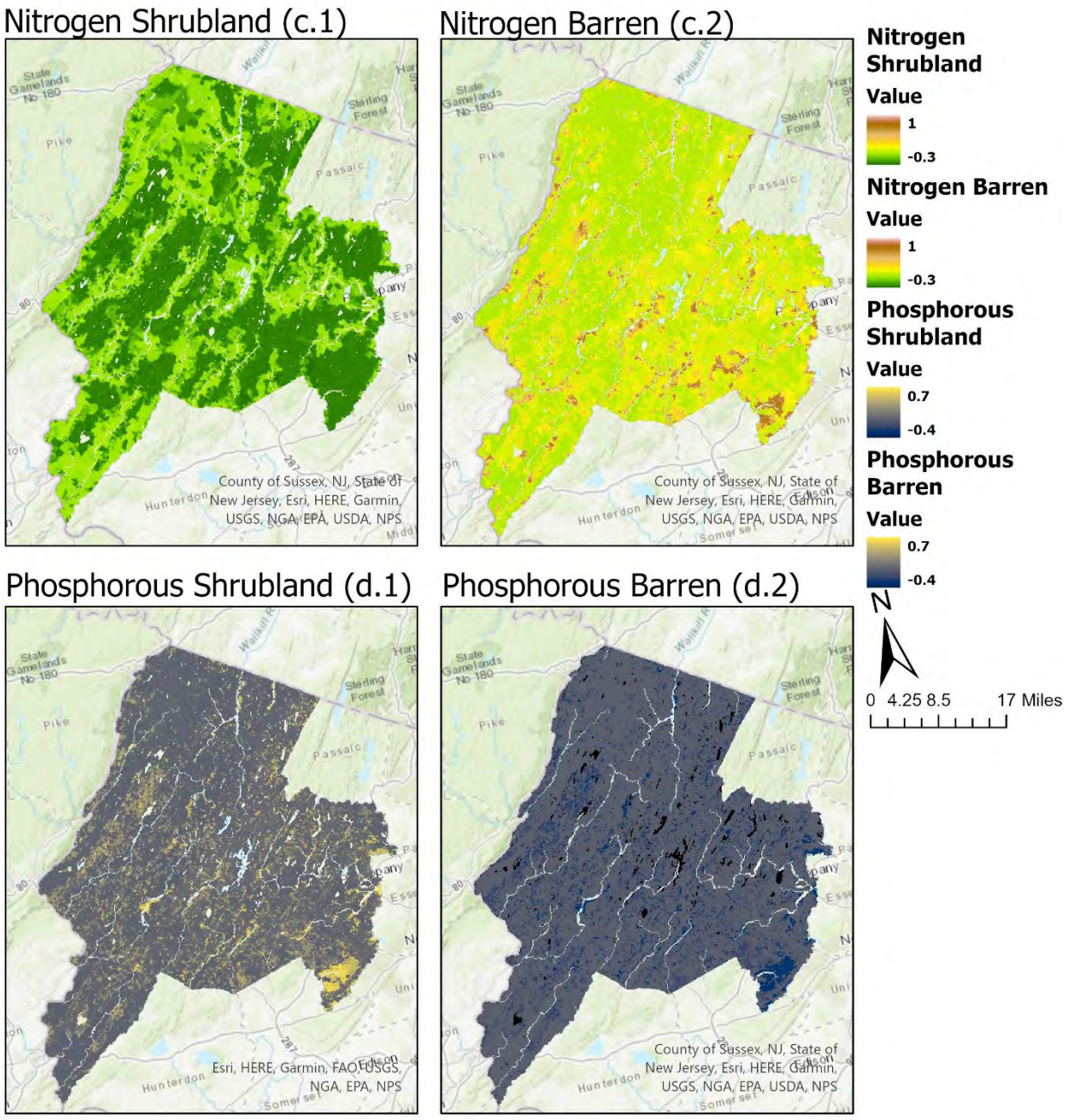


*Figure 25: Phosphorous and Nitrogen Export Change Compared to Baseline. Where (c.1) is the proportional change in nitrogen runoff in a shrubby condition and (c.2) is the change in a barren site condition. When sites are barren nitrogen export rises but decreases in a shrubby condition. Additionally, (d.1) is the proportional change in phosphorous runoff in a shrubby condition that results in no to moderate increases and (d.2) is the change in phosphorous runoff in a barren condition which results in less phosphorous export.*

Overall, the trends in the change in service are less extreme than proportional trends (Figures 24 and 25) indicate, with the notable exception of sedimentation with a barren understory condition, which results in excessive sedimentation compared to baseline. Other services are in line with expectations, with a slight increase in water yield with declining vegetative cover as runoff to the waterways increases (Figure 24) and a moderate increase in overall nutrient loads depending on the LULC shift whether it is toward a barren or shrubby condition (Figure 25 and Table 10).

*Table 10: Overall Ecosystem Service Change under Different Land Use Capacity Changes*

| SERVICE CATEGORY | BASELINE SERVICES | SHRUBLAND TRANSITION | BARREN TRANSITION |
|---|---|---|---|
| **WATER YIELD** | 3,132,633,933 $m^3$ | 3,151,457,056 $m^3$ | 3,183,938,883 $m^3$ |
| **SEDIMENT EXPORT** | 10,253,326.8 ton | 9,948,686.6 ton | 86,138,554.3 ton |
| **NITROGEN EXPORT** | 239,290.3 kg | 212,856 kg | 262,088.8 kg |
| **PHOSPHOROUS EXPORT** | 26,118.1 kg | 27,366.5 kg | 25,631.3 kg |

## 4. CONCLUSIONS AND FUTURE STUDY

Accounting for decreased ecosystem function during and after the mortality of *Fraxinus* will continue to be an active field of research, but more focused on the smaller services, as the disturbance to these larger services are likely temporary, lasting on the order of a decade or less as the forest regrows and fills back in the gaps. However, temporary as this shift may be, we can see severe consequences in provisioning services if the forest itself is not healthy enough to

respond to this disturbance. Additionally, depending on the eventual species composition we may see slightly lower overall performance from native forests due to the increased presence of less productive species, but how far this factor will influence ES provisioning is yet to be fully studied. In the case of *Fraxinus* mortality and ES provisioning there is still opportunity for extensive field work as the situation unfolds. The additional field work could allow the use of LULC change modeling with defined forest loss categories that can spread in time with EAB, rather than the biophysical table shifts employed here.

Given the scenarios evaluated, additional sensitivity analysis is necessary to increase the robustness of the results, but this is not tenable without increased field work, as InVEST model's parameterization has been noted to be site-specific in the literature (Hamel & Bryant, 2017). This site specific nature likely does not invalidate the trends from the results, but rather the overall numbers, as other ES datasets studied are somewhat similar in their relationship between LULC types, but not degree and intensity for the same LULC type (Bai et al., 2019; Berg et al., 2016; Brown & Quinn, 2018; Hamel et al., 2015; Walston et al., 2021). A more specific parameterization of LULC conditions in relation to InVEST model parameters would help with the applicability of the model to the study area. Depending on the region studied, this may prove to be less of a barrier if there has been previous ES research. The results still showcased the importance of maintaining the understory of impacted forests to prevent the worst outcomes.

# CHAPTER 5. SUMMARY AND CONCLUSIONS

## 5.1 Parasitoid Deployment and the Preservation of *Fraxinus*

*Fraxinus* will be extirpated from the forest system if measures are not taken. The losses from the ecosystem and the risk to critical infrastructure mean that this is not a problem that can be ignored. Parasitism is a delicate balance to control EAB too soon and the parasitoids will not be sufficiently established. However, preserving any portion of the extant canopy requires introduction when local concentrations are low. While much of the USA *Fraxinus* have already been infested, there are still untouched regions both here and abroad that will have to deal with EAB infestation in the future and may be able to be preserved through focused introductions of parasitoid vectors.

Our dispersal model results in chapter 2 showed that unless mitigating parasitoids are released when EAB are constrained on a regional level, they are unlikely to be successful at reducing or eliminating the risk of *Fraxinus* extirpation. The inflection points for this result showed at 7-years post EAB infestation, beyond which *Fraxinus* were unable to persist to a substantial extent, even with high rates of parasitism. With other research showing low rates of *Fraxinus* regrowth and recruitment under open-grown conditions, it is unlikely that there will be any appreciable recovery in the closed forest canopy Northeastern *Fraxinus* exist within.

Given that EAB are often undetected until later in the infestation cycle where infestations could be more than 7 years old, it is imperative that tracking be given priority for EAB even as the federal quarantine is removed. Without effective monitoring to catch EAB infestations early

on, parasitoid releases are unlikely to preserve the wider population of *Fraxinus* in the forest structure.

### 5.2 Costs of Avoiding Mitigation Measures

Preserving *Fraxinus* will require significant outlays of public funds beyond timber values and other use values. To justify expenditures on monitoring and parasitoid release, there are other costs aside from those usually discussed. First, the wide-scale mortality of *Fraxinus* presents an extant threat to existing buildings and infrastructure. This threat could impact the electrical distribution grid with incident *Fraxinus* costing upwards of $100 million due to removal and management of mature trees. This cost does not include potential costs to other infrastructure, such as homes, businesses and other buildings that will also be threatened with damage by the decaying timbers dotting the forested landscape. This inclusion would increase costs associated with snag fall in losses to privately held assets.

### 5.3 The Necessity of Forest Health in Minimizing the Ecosystem Services Impact of EAB

Additional costs from widespread *Fraxinus* mortality will be felt in the form of ecosystem service losses. These losses are especially pronounced if the forest condition is otherwise impaired from existing damage. With the existing damage from the overpopulation of large herbivores in New Jersey forests, there is substantial risk from the loss of existing canopy species. When the loss of canopy species is expanded to the landscape, there is the potential for substantial impacts to ecosystem services if the forest understory is not healthy enough to take over.

### 5.4 Research Gaps and Evaluating the Future Forest Structure

*Fraxinus* mortality due to EAB is still an ongoing and growing threat, with EAB continuing to spread through North America. To control these impacts, it will be important to continue monitoring and release control measures where they can be effective. With the massive external liability represented by mortally damaged *Fraxinus* there is plentiful reason to continue management activities.

Future research will need to focus on two key areas: the first is the continued development of more accurate tracking methods to identify EAB before they become uncontrollable, the second is the recovery and effectiveness of parasitoids. These issues are especially important to municipalities, as they decide whether to remove their *Fraxinus*, opt to treat high-value trees with systemic insecticides, or attempt to preserve them in place.

## WORKS CITED

Abell, K. J., Bauer, L. S., Duan, J. J., & Van Driesche, R. (2014). Long-Term Monitoring of the Introduced Emerald Ash Borer (Coleoptera: Buprestidae) Egg Parasitoid, *Oobius agrili* (Hymenoptera: Encyrtidae), in Michigan, USA and Evaluation of a Newly Developed Monitoring Technique. *Biological Control, 79*, 36–42. https://doi.org/10.1016/j.biocontrol.2014.08.002

Abell, K. J., Bauer, L. S., Miller, D. L., Duan, J. J., & Driesche, R. G. V. (2016). Monitoring the Establishment and Flight Phenology of Parasitoids of Emerald Ash Borer (Coleoptera: Buprestidae) in Michigan by using Sentinel Eggs and Larvae. *Florida Entomologist, 99*(4), 667–672. https://doi.org/10.1653/024.099.0413

Alerich, C. L., Klevgard, L., Liff, C., & Miles, P. D. (n.d.). *The Forest Inventory and Analysis Database: Database Description and Users Guide Version 1.7*. Forest Inventory Analysis.

Ali, Q., Bauch, C. T., & Anand, M. (2015). Coupled Human-Environment Dynamics of Forest Pest Spread and Control in a Multi-Patch, Stochastic Setting. *PLOS ONE, 10*(10), e0139353. https://doi.org/10.1371/journal.pone.0139353

Allen, R. G., & Food and Agriculture Organization of the United Nations (Eds.). (1998). *Crop evapotranspiration: Guidelines for computing crop water requirements*. Food and Agriculture Organization of the United Nations.

Amazing Tree Services. (2017). Tree Removal Cost in NJ. *Amazing Tree Services*. https://atreeservicenj.com/tree-removal-cost.asp

Anderson, T., & Dragicevic, S. (2016). A Geosimulation Approach for Data Scarce Environments: Modeling Dynamics of Forest Insect Infestation across Different Landscapes. *ISPRS International Journal of Geo-Information*, *5*(2). https://doi.org/doi:10.3390/ijgi5020009

Animal and Plant Health Inspection Service, U. (2018). Proposed Rules: Removal of Emerald Ash Borer Domestic Quarantine Regulations. *Federal Register*, *83*(182), 47310–47312.

Animal and Plant Health Inspection Service, U. (2020). Removal of Emerald Ash Borer Domestic Quarantine Regulations. *Federal Register*, *85*(241), 81085–81095.

Arbab, N., Grabosky, J., & Leopold, R. (2022). Economic Assessment of Urban Ash Tree Management Options in New Jersey. *Sustainability*, *14*(4), 2172. https://doi.org/10.3390/su14042172

Audley, J. P., Fettig, C. J., Steven Munson, A., Runyon, J. B., Mortenson, L. A., Steed, B. E., Gibson, K. E., Jørgensen, C. L., McKelvey, S. R., McMillin, J. D., & Negrón, J. F. (2021). Dynamics of beetle-killed snags following mountain pine beetle outbreaks in lodgepole pine forests. *Forest Ecology and Management*, *482*, 118870. https://doi.org/10.1016/j.foreco.2020.118870

Bai, Y., Ochuodho, T. O., & Yang, J. (2019). Impact of Land Use and Climate Change on Water-Related Ecosystem Services in Kentucky, USA. *Ecological Indicators*, *102*, 51–64. https://doi.org/10.1016/j.ecolind.2019.01.079

Balderas Torres, A., & Lovett, J. C. (2013). Using Basal Area to Estimate Aboveground Carbon Stocks in Forests: La Primavera Biosphere's Reserve, Mexico. *Forestry*, *86*(2), 267–281. https://doi.org/10.1093/forestry/cps084

Balducci, P. J., Schienbein, L. A., Nguyen, T. B., Brown, D. R., & Fathelrahman, E. M. (2006). An Examination of the Costs and Critical Characteristics of Electric Utility Distribution System Capacity Enhancement Projects. *2005/2006 PES TD*, 78–86. https://doi.org/10.1109/TDC.2006.1668461

Barlow, L.-A., Cecile, J., Bauch, C. T., & Anand, M. (2014). Modelling Interactions between Forest Pest Invasions and Human Decisions Regarding Firewood Transport Restrictions. *PLoS ONE*, *9*(4), e90511. https://doi.org/10.1371/journal.pone.0090511

Baron, J. N., & Rubin, B. D. (2021). Secondary Invasion? Emerald Ash Borer ( *Agrilus planipennis* ) Induced Ash ( *Fraxinus* spp.) Mortality Interacts with Ecological Integrity to Facilitate European Buckthorn ( *Rhamnus cathartica* ). *Canadian Journal of Forest Research*, *51*(3), 455–464. https://doi.org/10.1139/cjfr-2020-0134

Bates, T. (2019, February 19). Protecting Small Forests Fails to Protect Bird Biodiversity. *Rutgers Today*. https://www.rutgers.edu/news/protecting-small-forests-fails-protect-bird-biodiversity

Bauer, L. S., Duan, J. J., Gould, J. R., & Van Driesche, R. (2015). Progress in the Classical Biological Control of *Agrilus planipennis* Fairmaire (Coleoptera: Buprestidae) in North America. *The Canadian Entomologist*, *147*(3), 300–317. https://doi.org/10.4039/tce.2015.18

BenDor, T. K., & Metcalf, S. S. (2006). The Spatial Dynamics of Invasive Species Spread. *System Dynamics Review*, *22*(1), 27–50. https://doi.org/10.1002/sdr.328

BenDor, T. K., Metcalf, S. S., Fontenot, L. E., Sangunett, B., & Hannon, B. (2006). Modeling the spread of the Emerald Ash Borer. *Ecological*, *197*(1–2), 221–236. https://doi.org/doi:10.1016/j.ecolmodel.2006.03.003

Berg, C. E., Mineau, M. M., & Rogers, S. H. (2016). Reprint:Examining the Ecosystem Service of Nutrient Removal in a Coastal Watershed. *Ecosystem Services*, *22*, 309–317. https://doi.org/10.1016/j.ecoser.2016.12.001

Berry, K., Finnoff, D. C., Horan, R. D., & McDermott, S. M. (2017). The Role of Restoration in the Prevention of a Large-Scale Native Species Loss: Case Study of the Invasive Emerald Ash Borer. *Journal of Forest Economics*, *27*, 91–98. https://doi.org/10.1016/j.jfe.2017.03.002

Bíl, M., Andrášik, R., Nezval, V., & Bílová, M. (2017). Identifying locations along railway networks with the highest tree fall hazard. *Applied Geography*, *87*, 45–53. https://doi.org/10.1016/j.apgeog.2017.07.012

Brantley, S. T., Miniat, C. F., Elliott, K. J., Laseter, S. H., & Vose, J. M. (2015). Changes to Southern Appalachian Water Yield and Stormflow after Loss of a Foundation Species: LOSS OF FOUNDATION SPECIES AFFECTS WATER YIELD. *Ecohydrology*, *8*(3), 518–528. https://doi.org/10.1002/eco.1521

Brown, M. G., & Quinn, J. E. (2018). Zoning Does not Improve the Availability of Ecosystem Services in Urban Watersheds. A Case Study from Upstate South Carolina, USA. *Ecosystem Services*, *34*, 254–265. https://doi.org/10.1016/j.ecoser.2018.04.009

Buck, J. H., Parra, G., Lance, D., Reardon, R., & Binion, D. (2014). *2014 Emerald Ash Borer National Research and Technology Development Meeting*. United States Department of Agriculture.

Bureau of Climate Change and Clean Energy. (2021). *NJ Community Solar PV Siting Tool User Guide*. New Jersey Department of Environmental Protection. https://www.state.nj.us/dep/aqes/docs/sstguide.pdf

Bureau of Transportation Statistics, U.S. Department of Commerce, & U.S. Census Bureau, Geography Division. (2016). *TIGER/line Roads County-based (National)-National Geospatial Data Asset (NGDA) TIGER/line Roads County-based* [Vector digital data]. U.S. Department of Transportation. https://tigerweb.geo.census.gov/arcgis/rest/services/TIGERweb/Transportation/MapServer

Burr, S. J., McCullough, D. G., & Poland, T. M. (2018). Density of Emerald Ash Borer (Coleoptera: Buprestidae) Adults and Larvae at Three Stages of the Invasion Wave. *Environmental Entomology*, *47*(1), 121–132. https://doi.org/10.1093/ee/nvx200

Bushaj, S., Büyüktahtakın, İ. E., Yemshanov, D., & Haight, R. G. (2021). Optimizing Surveillance and Management of Emerald Ash Borer in Urban Environments. *Natural Resource Modeling*, *34*(1). https://doi.org/10.1111/nrm.12267

Crocker, S. J., Barnett, C. J., Butler, B. J., Hatfield, M. A., Kurtz, C. M., Lister, T. W., Meneguzzo, D. M., Miles, P. D., Morin, R. S., Nelson, M. D., Piva, R. J., Reimann, R., Smith, J. E., Woodall, C. W., & Zipse, W. (2017). *New Jersey Forests 2013* (NRS-RB-

109; p. NRS-RB-109). U.S. Department of Agriculture, Forest Service, Northern Research Station. https://doi.org/10.2737/NRS-RB-109

Cuddington, K., Sobek-Swant, S., Crosthwaite, J. C., Lyons, D. B., & Sinclair, B. J. (2018). Probability of emerald ash borer impact for Canadian cities and North America: A mechanistic model. *Biological, 20*(9), 2661–2677. https://doi.org/doi:10.1007/s10530-018-1725-0

Depaoli, S., Clifton, J. P., & Cobb, P. R. (2016). Just Another Gibbs Sampler (JAGS): Flexible Software for MCMC Implementation. *Journal of Educational and Behavioral Statistics*, *41*(6), 628–649. https://doi.org/10.3102/1076998616664876

DeSantis, R. D., Moser, W. K., Huggett, R. J., Li, R., Wear, D. N., & Miles, P. D. (2013). *Modeling the Effects of Emerald Ash Borer on Forest Composition in the Midwest and Northeast United States* (NRS-GTR-112; p. NRS-GTR-112). U.S. Department of Agriculture, Forest Service, Northern Research Station. https://doi.org/10.2737/NRS-GTR-112

Diss-Torrance, A., Peterson, K., & Robinson, C. (2018). Reducing Firewood Movement by the Public: Use of Survey Data to Assess and Improve Efficacy of a Regulatory and Educational Program, 2006–2015. *Forests*, *9*(2), 90. https://doi.org/10.3390/f9020090

Dixon, G., & Keyser, C. (2016). Northeast (NE) Variant Overview. *United States Department of Agriculture*, 60.

Dolan, B., & Kilgore, J. (2018). Forest Regeneration Following Emerald Ash Borer (Agrilus planipennis Fairemaire) Enhances Mesophication in Eastern Hardwood Forests. *Forests,9(6), 353*. https://doi.org/doi:10.3390/f9060353

Duan, J., Bauer, L. S., & Van Driesche, R. G. (2017). Emerald Ash Borer Biocontrol in Ash Saplings: The Potential for Early Stage Recovery of North American Ash Trees. *Forest Ecology and Management*, *394*, 64–72. https://doi.org/10.1016/j.foreco.2017.03.024

Duan, J., Bauer, L., van Driesche, R., & Gould, J. (2018). Progress and Challenges of Protecting North American Ash Trees from the Emerald Ash Borer Using Biological Control. *Forests*, *9*(3), 142. https://doi.org/10.3390/f9030142

Duan, J. J., Larson, K., Watt, T., Gould, J., & Lelito, J. P. (2013). Effects of Host Plant and Larval Density on Intraspecific Competition in Larvae of the Emerald Ash Borer (Coleoptera: Buprestidae). *Environmental Entomology*, *42*(6), 1193–1200. https://doi.org/10.1603/EN13209

Duan, J., Oppel, C. B., Ulyshen, M. D., Bauer, L. S., & LeLito, J. (2011). Biology and Life History of *Tetrastichus planipennisi* (Hymenoptera: Eulophidae), a Larval Endoparasitoid of the Emerald Ash Borer (Coleoptera: Buprestidae). *Florida Entomologist*, *94*(4), 933–940. https://doi.org/10.1653/024.094.0430

Duan, J., Van Driesche, R. G., Crandall, R. S., Schmude, J. M., Rutledge, C. E., Slager, B. H., Gould, J. R., & Elkinton, J. S. (2019). Establishment and Early Impact of Spathius galinae (Hymenoptera: Braconidae) on Emerald Ash Borer (Coleoptera: Buprestidae) in the Northeastern United States. *Journal of Economic Entomology*, *112*(5), 2121–2130. https://doi.org/10.1093/jee/toz159

*Eastern Region Tree Species*. (n.d.). U.S. Forest Service. https://www.fs.usda.gov/Internet/FSE_DOCUMENTS/stelprdb5428009.pdf

ESRI. (2021). *Cell size and resampling in analysis*. ESRI. https://desktop.arcgis.com/en/arcmap/latest/extensions/spatial-analyst/performing-analysis/cell-size-and-resampling-in-analysis.htm

Evans, A. (2016). The Speed of Invasion: Rates of Spread for Thirteen Exotic Forest Insects and Diseases. *Forests*, *7*(12), 99. https://doi.org/10.3390/f7050099

Fissore, C., McFadden, J. P., Nelson, K. C., Peters, E. B., Hobbie, S. E., King, J. Y., Baker, L. A., & Jakobsdottir, I. (2012). Potential Impacts of Emerald Ash Borer Invasion on Biogeochemical and Water Cycling in Residential Landscapes Across a Metropolitan Region. *Urban Ecosystems*, *15*(4), 1015–1030. https://doi.org/10.1007/s11252-012-0239-2

Flower, C. E., Fant, J., Hoban, S., Knight, K., Steger, L., Aubihl, E., Gonzalez-Meler, M., Forry, S., Hille, A., & Royo, A. (2018). Optimizing Conservation Strategies for a Threatened Tree Species: In Situ Conservation of White Ash (Fraxinus americana L.) Genetic Diversity through Insecticide Treatment. *Forests*, *9*(4), 202. https://doi.org/10.3390/f9040202

Flower, C. E., Knight, K. S., & Gonzalez-Meler, M. A. (2013). Impacts of the Emerald Ash Borer (*Agrilus planipennis* Fairmaire) Induced Ash (*Fraxinus spp.*) Mortality on Forest Carbon Cycling and Successional Dynamics in the Eastern United States. *Biological Invasions*, *15*(4), 931–944. https://doi.org/10.1007/s10530-012-0341-7

Flower, C. E., Knight, K. S., Rebbeck, J., & Gonzalez-Meler, M. A. (2013). The Relationship Between the Emerald Ash Borer (*Agrilus planipennis*) and ash (*Fraxinus spp.*) Tree Decline: Using Visual Canopy Condition Assessments and Leaf Isotope Measurements to

Assess Pest Damage. *Forest Ecology and Management*, *303*, 143–147. https://doi.org/10.1016/j.foreco.2013.04.017

Forest Inventory and Analysis. (2022). *Design and Analysis Toolkit for Inventory and Monitoring web application.* St. Paul, MN: U.S. Department of Agriculture, Forest Service, Northern Research Station. https://www.fs.fed.us/emc/rig/DATIM/index.shtml.

Gaudon, J. M., Allison, J. D., & Smith, S. M. (2018). Factors Influencing the Dispersal of a Native Parasitoid, *Phasgonophora sulcata*, Attacking the Emerald Ash Borer: Implications for Biological Control. *BioControl*, *63*(6), 751–761. https://doi.org/10.1007/s10526-018-9900-x

Gilbert, M., Gregoire, J.-C., Freise, J. F., & Heitland, W. (2004). Long-Distance Dispersal and Human Population Density Allow the Prediction of Invasive Patterns in the Horse Chestnut Leafminer *Cameraria ohridella*. *Journal of Animal Ecology*, *73*(3), 459–468. https://doi.org/10.1111/j.0021-8790.2004.00820.x

Goins, S. M., Chapman, J. I., & McEwan, R. W. (2013). Composition Shifts, Disturbance, and Canopy-Accession Strategy in an Oldgrowth Forest of Southwestern Ohio, USA. *Natural Areas Journal*, *33*(4), 384–394. https://doi.org/10.3375/043.033.0401

Gould, J. S., Murphy, T., Slager, B., Bauer, L. S., Duan, J., & Petrice, T. (2020). Emerald Ash Borer, Agrilus planipennis (Fairmaire), Biological Control Release and Recovery Guidelines 2020. *United States Department of Agriculture*, 75.

Granger, J. J., Zobel, J. M., & Buckley, D. S. (2019). Differential Impacts of Emerald Ash Borer (Agrilus planipennis Fairmaire) on Forest Communities Containing Native Ash (Fraxinus

spp.) Species in Eastern North America. *Forest Science*, fxz063. https://doi.org/10.1093/forsci/fxz063

Hamel, P., & Bryant, B. P. (2017). Uncertainty Assessment in Ecosystem Services Analyses: Seven Challenges and Practical Responses. *Ecosystem Services*, *24*, 1–15. https://doi.org/10.1016/j.ecoser.2016.12.008

Hamel, P., Chaplin-Kramer, R., Sim, S., & Mueller, C. (2015). A New Approach to Modeling the Sediment Retention Service (InVEST 3.0): Case Study of the Cape Fear Catchment, North Carolina, USA. *Science of The Total Environment*, *524–525*, 166–177. https://doi.org/10.1016/j.scitotenv.2015.04.027

Harmon, M. E., & Bell, D. M. (2020). Mortality in Forested Ecosystems: Suggested Conceptual Advances. *Forests*, *11*(5), 572. https://doi.org/10.3390/f11050572

Hauer, R. J., & Peterson, W. D. (2017). Effects of Emerald Ash Borer on Municipal Forestry Budgets. *Landscape and Urban Planning*, *157*, 98–105. https://doi.org/10.1016/j.landurbplan.2016.05.023

Hughes, W., Zhang, W., Bagtzoglou, A. C., Wanik, D., Pensado, O., Yuan, H., & Zhang, J. (2021). Damage modeling framework for resilience hardening strategy for overhead power distribution systems. *Reliability Engineering & System Safety*, *207*, 107367. https://doi.org/10.1016/j.ress.2020.107367

Jennings, D. E., Duan, J. J., Bauer, L. S., Schmude, J. M., Wetherington, M. T., & Shrewsbury, P. M. (2016). Temporal Dynamics of Woodpecker Predation on Emerald Ash Borer ( *Agrilus planipennis* ) in the Northeastern U.S.A.: Woodpecker Predation on EAB. *Agricultural and Forest Entomology*, *18*(2), 174–181. https://doi.org/10.1111/afe.12142

Jennings, D. E., Duan, J. J., Bean, D., Gould, J. R., Rice, K. A., & Shrewsbury, P. M. (2016). Monitoring the establishment and abundance of introduced parasitoids of emerald ash borer larvae in Maryland, U.S.A. *Biological Control*, *101*, 138–144. https://doi.org/10.1016/j.biocontrol.2016.07.006

Jennings, D. E., Duan, J. J., & Shrewsbury, P. M. (2015). Biotic Mortality Factors Affecting Emerald Ash Borer ( *Agrilus planipennis* ) are Highly Dependent on Life Stage and Host Tree Crown Condition. *Bulletin of Entomological Research*, *105*(5), 598–606. https://doi.org/10.1017/S0007485315000498

Jennings, D. E., Duan, J., & Shrewsbury, P. (2018). Comparing Methods for Monitoring Establishment of the Emerald Ash Borer (Agrilus planipennis, Coleoptera: Buprestidae) Egg Parasitoid Oobius agrili (Hymenoptera: Encyrtidae) in Maryland, USA. *Forests*, *9*(10), 659. https://doi.org/10.3390/f9100659

Jones, B. A. (2018). Forest-attacking Invasive Species and Infant Health: Evidence From the Invasive Emerald Ash Borer. *Ecological Economics*, *154*, 282–293. https://doi.org/10.1016/j.ecolecon.2018.08.010

Jones, B. A., & McDermott, S. M. (2015). Linking Environmental Management to Health Outcomes: A Case Study of the Emerald Ash Borer. *Applied Economics Letters*, 1–6. https://doi.org/10.1080/13504851.2015.1034836

Jones, M. I., Gould, J. R., Warden, M. L., & Fierke, M. K. (2019). Dispersal of Emerald Ash Borer (Coleoptera: Buprestidae) Parasitoids Along an Ash Corridor in Western New York. *Biological Control*, *128*, 94–101. https://doi.org/10.1016/j.biocontrol.2018.09.004

Kashian, D. M. (2016). Sprouting and seed production may promote persistence of green ash in the presence of the emerald ash borer. *Ecosphere, 7*(4), e01332. https://doi.org/10.1002/ecs2.1332

Kashian, D. M., Bauer, L., Spei, B., Duan, J., & Gould, J. (2018). Potential Impacts of Emerald Ash Borer Biocontrol on Ash Health and Recovery in Southern Michigan. *Forests*, *9*(6), 296. https://doi.org/10.3390/f9060296

Knight, K. S., Brown, J. P., & Long, R. P. (2013). Factors Affecting the Survival of Ash (*Fraxinus spp.*) Trees Infested by Emerald Ash Borer (*Agrilus planipennis*). *Biological Invasions, 15*(2), 371–383. https://doi.org/10.1007/s10530-012-0292-z

Kovacs, K. F., Mercader, R. J., Haight, R. G., Siegert, N. W., McCullough, D. G., & Liebhold, A. M. (2011). The influence of satellite populations of emerald ash borer on projected economic costs in U.S. communities, 2010–2020. *Journal of Environmental Management, 92*(9), 2170–2181. https://doi.org/10.1016/j.jenvman.2011.03.043

Kutta, E., & Hubbart, J. (2018). Changing Climatic Averages and Variance: Implications for Mesophication at the Eastern Edge of North America's Eastern Deciduous Forest. *Forests*, *9*(10), 605. https://doi.org/10.3390/f9100605

Larsen, P. H., Boehlert, B., Eto, J., Hamachi-LaCommare, K., Martinich, J., & Rennels, L. (2018). Projecting Future Costs to U.S. Electric Utility Customers from Power Interruptions. *Energy, 147*, 1256–1277. https://doi.org/10.1016/j.energy.2017.12.081

Lavorel, S., Bayer, A., Bondeau, A., Lautenbach, S., Ruiz-Frau, A., Schulp, N., Seppelt, R., Verburg, P., Teeffelen, A. V., Vannier, C., Arneth, A., Cramer, W., & Marba, N. (2017). Pathways to bridge the biophysical realism gap in ecosystem services mapping

approaches. *Ecological Indicators*, *74*, 241–260. https://doi.org/10.1016/j.ecolind.2016.11.015

Liu, H., Bauer, L. S., Gao, R., Zhao, T., Petrice, T. R., & Haack, R. A. (2003). *Exploratory Survey for the Emerald Ash Borer*, Agrilus Planipennis *(Coleoptera: Buprestidae), and Its Natural Enemies in China*. 16.

Liu, H., Bauer, L. S., Miller, D. L., Zhao, T., Gao, R., Song, L., Luan, Q., Jin, R., & Gao, C. (2007). Seasonal Abundance of *Agrilus planipennis* (Coleoptera: Buprestidae) and its Natural Enemies *Oobius agrili* (Hymenoptera: Encyrtidae) and *Tetrastichus planipennisi* (Hymenoptera: Eulophidae) in China. *Biological Control*, *42*(1), 61–71. https://doi.org/10.1016/j.biocontrol.2007.03.011

Lustig, A., Worner, S. P., Pitt, J. P. W., Doscher, C., Stouffer, D. B., & Senay, S. D. (2017). A Modeling Framework for the Establishment and Spread of Invasive Species in Heterogeneous Environments. *Ecology and Evolution*, *7*(20), 8338–8348. https://doi.org/10.1002/ece3.2915

Lyons, D. B. (2015). What's killing the green menace: Mortality factors affecting the emerald ash borer (Coleoptera: Buprestidae) in North America? *The Canadian Entomologist, 147*(03), 263–276. https://doi.org/10.4039/tce.2014.62

Lyttek, E., Lal, P., Nieddu, G., Forgoston, E., & Wieczerak, T. (2019). Modeling *Agrilus planipennis* F. (Coleoptera: Buprestidae) Spread in New Jersey. *Journal of Economic Entomology*, *112*(5), 2482–2488. https://doi.org/10.1093/jee/toz122

Ma, S., Duggan, J. M., Eichelberger, B. A., McNally, B. W., Foster, J. R., Pepi, E., Conte, M. N., Daily, G. C., & Ziv, G. (2016). Valuation of Ecosystem Services to Inform Management

of Multiple-Use Landscapes. *Ecosystem Services*, *19*, 6–18. https://doi.org/10.1016/j.ecoser.2016.03.005

Margulies, E., Bauer, L., & Ibáñez, I. (2017). Buying Time: Preliminary Assessment of Biocontrol in the Recovery of Native Forest Vegetation in the Aftermath of the Invasive Emerald Ash Borer. *Forests*, *8*(10), 369. https://doi.org/10.3390/f8100369

Matthes, J., Lang, A., Jevon, F., & Russell, S. (2018). Tree Stress and Mortality from Emerald Ash Borer Does Not Systematically Alter Short-Term Soil Carbon Flux in a Mixed Northeastern U.S. Forest. *Forests*, *9*(1), 37. https://doi.org/10.3390/f9010037

McCullough, D. G., Mercader, R. J., & Siegert, N. W. (2015). Developing and integrating tactics to slow ash (Oleaceae) mortality caused by emerald ash borer (Coleoptera: Buprestidae). *The Canadian Entomologist*, *147*(03), 349–358. https://doi.org/10.4039/tce.2015.3

McCullough, D. G., & Siegert, N. W. (2007). Estimating Potential Emerald Ash Borer (Coleoptera: Buprestidae) Populations Using Ash Inventory Data. *Journal of Economic Entomology*, *100*(5), 1577–1586. https://doi.org/10.1603/0022-0493(2007)100[1577:EPEABC]2.0.CO;2

McRoberts, R. E., Bechtold, W. A., Patterson, P. L., Scott, C. T., & Reams, G. A. (2005). The Enhanced Forest Inventory and Analysis Program of the USDA Forest Service: Historical Perspective and Announcement of Statistical Documentation. *Journal of Forestry*, 5.

Mercader, R. J., McCullough, D. G., Storer, A. J., Bedford, J. M., Heyd, R., Siegert, N. W., Katovich, S., & Poland, T. M. (2016). Estimating local spread of recently established emerald ash borer, Agrilus planipennis , infestations and the potential to influence it with

a systemic insecticide and girdled ash trees. *Forest Ecology and Management*, *366*, 87–97. https://doi.org/10.1016/j.foreco.2016.02.005

Mercader, R. J., Siegert, N. W., Liebhold, A. M., & McCullough, D. G. (2009). Dispersal of the emerald ash borer, *Agrilus planipennis* , in newly-colonized sites. *Agricultural and Forest Entomology*, *11*(4), 421–424. https://doi.org/10.1111/j.1461-9563.2009.00451.x

Mercader, R. J., Siegert, N. W., Liebhold, A. M., & McCullough, D. G. (2011). Influence of foraging behavior and host spatial distribution on the localized spread of the emerald ash borer, Agrilus planipennis. *Population Ecology*, *53*(2), 271–285. https://doi.org/10.1007/s10144-010-0233-6

Millennium Ecosystem Assessment (Program) (Ed.). (2005). *Ecosystems and human well-being: Synthesis*. Island Press.

Moosewood Tree Service. (2017, March). *The Average Cost of Tree Removal*. https://www.moosewoodtreeservice.com/single-post/2017/03/05/the-average-cost-of-tree-removal

Morin, R. S., Liebhold, A. M., Pugh, S. A., & Crocker, S. J. (2017). Regional Assessment of Emerald Ash Borer, *Agrilus planipennis*, Impacts in Forests of the Eastern United States. *Biological Invasions*, *19*(2), 703–711. https://doi.org/10.1007/s10530-016-1296-x

Muirhead, J. R., Leung, B., Overdijk, C., Kelly, D. W., Nandakumar, K., Marchant, K. R., & MacIsaac, H. J. (2006). Modelling Local and Long-Distance Dispersal of Invasive Emerald Ash Borer *Agrilus planipennis* (Coleoptera) in North America. *Diversity <html_ent Glyph="@amp;" Ascii="&"/> Distributions*, *12*(1), 71–79. https://doi.org/10.1111/j.1366-9516.2006.00218.x

Murphy, T. C., Gould, J. R., Van Driesche, R. G., & Elkinton, J. S. (2018). Interactions Between Woodpecker Attack and Parasitism by Introduced Parasitoids of the Emerald Ash Borer. *Biological Control*, *122*, 109–117. https://doi.org/10.1016/j.biocontrol.2018.04.011

Murphy, T. C., Van Driesche, R. G., Gould, J. R., & Elkinton, J. S. (2017). Can Spathius galinae attack emerald ash borer larvae feeding in large ash trees? *Biological Control, 114*, 8–13. https://doi.org/10.1016/j.biocontrol.2017.07.004

National Centers for Environmental Information. (2021). *U.S. Climate Normals 2020: U.S. Monthly Climate Normals (1991-2020)*. National Oceanic and Atmospheric Administration(NOAA). https://www.ncei.noaa.gov/access/search/data-search/normals-monthly-1991-2020

Natural Capital Project. (2022). *InVEST 3.12.0.post26+ug.g230fb3d User's Guide*. https://storage.googleapis.com/releases.naturalcapitalproject.org/invest-userguide/latest/index.html#

Natural Resources Conservation Service. (1986). *Urban Hydrology for Small Watersheds, Technical Release 55 (TR-55)*. United State Department of Agriculture. https://www.nrc.gov/docs/ML1421/ML14219A437.pdf

Natural Resources Conservation Service. (2021a). *USA SSURGO - Erodibility Factor*. Natural Resources Conservation Service. https://landscape11.arcgis.com/arcgis/

Natural Resources Conservation Service. (2021b). *USA SSURGO - Soil Hydrologic Group*. ESRI. https://landscape11.arcgis.com/arcgis/

New Jersey Board of Public Utilities (NJBPU), New Jersey Department of Environmental Protection (NJDEP), New Jersey Department of Transportation (NJDOT), New Jersey

Department of Community Affairs (NJDCA), New Jersey Department of Labor and Workforce Development (NJDOL), New Jersey Economic Development Authority (NJEDA), & NJ TRANSIT. (2019). *2019 New Jersey Energy Master Plan Pathway to 2050*. State of New Jersey. https://www.nj.gov/emp/docs/pdf/2020_NJBPU_EMP.pdf

New Jersey Department of Environmental Protection (NJDEP), Division of Information Technology (DOIT), & Bureau of Geographic Information System (BGIS). (2019). *Land Use/Land Cover of New Jersey 2015 (Download)*. NJDEP Bureau of GIS. https://www.arcgis.com/home/item.html?id=6f76b90deda34cc98aec255e2defdb45

New Jersey Department of Environmental Protection (NJDEP), & New Jersey Geological Survey (NJGS). (2009). *12 Digit Hydrologic Unit Code Delineations for New Jersey, Clipped at New Jersey State Boundary*. NJ Department of Environmental Protection (NJDEP).

New Jersey Farm Bureau: Recognized Ecologists and Land Professionals Agree Deer Overpopulation in New Jersey is an Emergency. (2021, April 26). *Insider NJ*, 1.

Nowack, D., Crane, D., Stevens, J., & Walton, J. (2003). Potential Damage from Emerald Ash Borer. *USDA Forest Service, Northern Research Station*.

Nowacki, G. J., & Abrams, M. D. (2008). The Demise of Fire and "Mesopication" of Forests in the Eastern United States. *BioScience*, *58*(2), 123–138.

Oberle, B., Covey, K. R., Dunham, K. M., Hernandez, E. J., Walton, M. L., Young, D. F., & Zanne, A. E. (2018). Dissecting the Effects of Diameter on Wood Decay Emphasizes the Importance of Cross-Stem Conductivity in Fraxinus americana. *Ecosystems*, *21*(1), 85–97. https://doi.org/10.1007/s10021-017-0136-x

Oberle, B., Ogle, K., Zanne, A. E., & Woodall, C. W. (2018). When a Tree Falls: Controls on Wood Decay Predict Standing Dead Tree Fall and New Risks in Changing Forests. *PLOS ONE*, *13*(5), e0196712. https://doi.org/10.1371/journal.pone.0196712

Oregon Climate Service at Oregon State University. (2012). *1981-2010 Annual Average Precipitation by State*. USDA/NRCS - National Geospatial Center of Excellence.

Orlova-Bienkowskaja, M. J., & Bieńkowski, A. O. (2018). Modeling Long-Distance Dispersal of Emerald Ash Borer in European Russia and Prognosis of Spread of this Pest to Neighboring Countries within next 5 Years. *Ecology and Evolution*, *8*(18), 9295–9304. https://doi.org/10.1002/ece3.4437

Orlova-Bienkowskaja, M. J., & Bieńkowski, A. O. (2020). Minimum Winter Temperature as a Limiting Factor of the Potential Spread of Agrilus planipennis, an Alien Pest of Ash Trees, in Europe. *Insects*, *11*(4), 258. https://doi.org/10.3390/insects11040258

Panagos, P., & Ballabio, C. (2017). *Global Rainfall Erosivity*. European Commission, Joint research Centre. https://esdac.jrc.ec.europa.eu/content/global-rainfall-erosivity

Parisio, M. S., Gould, J. R., Vandenberg, J. D., Bauer, L. S., & Fierke, M. K. (2017). Evaluation of Recovery and Monitoring Methods for Parasitoids Released Against Emerald Ash Borer. *Biological Control*, *106*, 45–53. https://doi.org/10.1016/j.biocontrol.2016.12.009

Perry, K., Herms, D., Klooster, W., Smith, A., Hartzler, D., Coyle, D., & Gandhi, K. (2018). Downed Coarse Woody Debris Dynamics in Ash (Fraxinus spp.) Stands Invaded by Emerald Ash Borer (Agrilus planipennis Fairmaire). *Forests*, *9*(4), 191. https://doi.org/10.3390/f9040191

Peterson, K., & Diss-Torrance, A. (2012). Motivation for Compliance with Environmental Regulations Related to Forest Health. *Journal of Environmental Management*, *112*, 104–119. https://doi.org/10.1016/j.jenvman.2012.06.023

Pimentel, D., Zuniga, R., & Morrison, D. (2005). Update on the environmental and economic costs associated with alien-invasive species in the United States. *Ecological Economics*, *52*(3), 273–288. https://doi.org/10.1016/j.ecolecon.2004.10.002

Pitt, J. P., Worner, S. P., & Suarez, A. V. (2009). Predicting Argentine ant spread over the heterogeneous landscape using a spatially explicit stochastic model. *Ecological*, *19*(5), 1176–1186. https://doi.org/doi:10.1890/08-1777.1

Plummer, M. (2003, March 20). JAGS: A Program for Analysis of Bayesian Graphical Models Using Gibbs Sampling. *Proceedings of the 3rd International Workshop on Distributed Statistical Computing (DSC 2003)*. A Meeting on the Future of Statistical Computing, Vienna, Austria. http://www.ci.tuwien.ac.at/Conferences/DSC-2003/

Poland, T. M., Chen, Y., Koch, J., & Pureswaran, D. (2015). Review of the emerald ash borer (Coleoptera: Buprestidae), life history, mating behaviours, host plant selection, and host resistance. *The Canadian Entomologist*, *147*(03), 252–262. https://doi.org/10.4039/tce.2015.4

Poland, T. M., & McCullough, D. G. (2006). Emerald Ash Borer: Invasion of the Urban Forest and the Threat to North America's Ash Resource. *Journal of Forestry*, 7.

Polasky, S., Nelson, E., Pennington, D., & Johnson, K. A. (2011). The Impact of Land-Use Change on Ecosystem Services, Biodiversity and Returns to Landowners: A Case Study

in the State of Minnesota. *Environmental and Resource Economics*, *48*(2), 219–242. https://doi.org/10.1007/s10640-010-9407-0

Poulos, H. M., & Camp, A. E. (2010). Decision Support for Mitigating the Risk of Tree Induced Transmission Line Failure in Utility Rights-of-Way. *Environmental Management*, *45*(2), 217–226. https://doi.org/10.1007/s00267-009-9422-5

Powell, J. A., Garlick, M. J., Bentz, B. J., & Friedenberg, N. (2018). Differential Dispersal and the Allee Effect Create Power-Law Behaviour: Distribution of Spot Infestations During Mountain Pine Beetle Outbreaks. *Journal of Animal Ecology*, *87*(1), 73–86. https://doi.org/10.1111/1365-2656.12700

Prasad, A. M., Iverson, L. R., Peters, M. P., Bossenbroek, J. M., Matthews, S. N., Davis Sydnor, T., & Schwartz, M. W. (2010). Modeling the invasive emerald ash borer risk of spread using a spatially explicit cellular model. *Landscape Ecology*, *25*(3), 353–369. https://doi.org/10.1007/s10980-009-9434-9

PRISM Climate Group at Oregon State University. (2022). *United States Average Monthly Total Precipitation, 1991-2020 (4km; BIL)*. PRISM Climate Group at Oregon State University. prism.oregonstate.edu

Public Service Electric & Gas Co. (PSE&G). (2007). *69 kV Statewide Initiative*. PSE&G. https://www.psegtransmission.com/reliability-projects/69kv#:~:text=Since%202007%2C%20PSE%26G%20has%20installed,miles%20will%20have%20been%20upgraded.

Pugh, S. A., Liebhold, A. M., & Morin, R. S. (2011). Changes in ash tree demography associated with emerald ash borer invasion, indicated by regional forest inventory data from the

Great Lakes States. *Canadian Journal of Forest Research*, *41*(11), 2165–2175. https://doi.org/10.1139/x11-138

Quinn, N. F., Gould, J. S., Rutledge, C. E., Fassler, A., Elkinton, J. S., & Duan, J. J. (2022). Spread and Phenology of *Spathius galinae* and *Tetrastichus planipennisi*, Recently Introduced for Biocontrol of Emerald Ash Borer (Coleoptera: Buprestidae) in the Northeastern United States. *Biological Control*, *165*, 104794. https://doi.org/10.1016/j.biocontrol.2021.104794

Rastetter, E. B., Ohman, M. D., Elliott, K. J., Rehage, J. S., Rivera-Monroy, V. H., Boucek, R. E., Castañeda-Moya, E., Danielson, T. M., Gough, L., Groffman, P. M., Jackson, C. R., Miniat, C. F., & Shaver, G. R. (2021). Time Lags: Insights from the U.S. Long Term Ecological Research Network. *Ecosphere*, *12*(5). https://doi.org/10.1002/ecs2.3431

Ren, J., Adam, J. C., Hicke, J. A., Hanan, E. J., Tague, C. L., Liu, M., Kolden, C. A., & Abatzoglou, J. T. (2021). How Does Water Yield Respond to Mountain Pine Beetle Infestation in a Semiarid Forest? *Hydrology and Earth System Sciences*, *25*(9), 4681–4699. https://doi.org/10.5194/hess-25-4681-2021

Ricketts, M., Flower, C., Knight, K., & Gonzalez-Meler, M. (2018). Evidence of Ash Tree (*Fraxinus spp.*) Specific Associations with Soil Bacterial Community Structure and Functional Capacity. *Forests*, *9*(4), 187. https://doi.org/10.3390/f9040187

Robinett, M. A., & McCullough, D. G. (2019). White Ash ( *Fraxinus americana* ) Survival in the Core of the Emerald Ash Borer ( *Agrilus planipennis* ) Invasion. *Canadian Journal of Forest Research*, *49*(5), 510–520. https://doi.org/10.1139/cjfr-2018-0320

Roscoe, L. E., Barry Lyons, D., & Smith, S. M. (2016). Observations on the Life-History Traits of the North American Parasitoid *Phasgonophora sulcata* Westwood (Hymenoptera: Chalcididae) Attacking *Agrilus planipennis* (Coleoptera: Buprestidae) in Ontario, Canada. *The Canadian Entomologist*, *148*(3), 294–306. https://doi.org/10.4039/tce.2015.72

Schlesinger, R. (1990). Fraxinus Americana *L. White Ash*. North Central Forest Experiment Station.

Selbig, W. R., Loheide, S. P., Shuster, W., Scharenbroch, B. C., Coville, R. C., Kruegler, J., Avery, W., Haefner, R., & Nowak, D. (2022). Quantifying the Stormwater Runoff Volume Reduction Benefits of Urban Street Tree Canopy. *Science of The Total Environment*, *806*, 151296. https://doi.org/10.1016/j.scitotenv.2021.151296

Siegert, N. W., Engelken, P. J., & McCullough, D. G. (2021). Changes in Demography and Carrying Capacity of Green Ash and Black Ash Ten Years after Emerald Ash Borer Invasion of Two Ash-Dominant Forests. *Forest Ecology and Management*, *494*, 119335. https://doi.org/10.1016/j.foreco.2021.119335

Siegert, N. W., McCullough, D. G., Liebhold, A. M., & Telewski, F. W. (2014). Dendrochronological Reconstruction of the Epicentre and Early Spread of Emerald Ash Borer in North America. *Diversity and Distributions*, *20*(7), 847–858. https://doi.org/10.1111/ddi.12212

Siegert, N. W., McCullough, D. G., Williams, D. W., Fraser, I., Poland, T. M., & Pierce, S. J. (2010). Dispersal of *Agrilus planipennis* (Coleoptera: Buprestidae) From Discrete

Epicenters in Two Outlier Sites. *Environmental Entomology*, *39*(2), 253–265. https://doi.org/10.1603/EN09029

Siegert, N. W., Mercader, R. J., & McCullough, D. G. (2015). Spread and dispersal of emerald ash borer (Coleoptera: Buprestidae): estimating the spatial dynamics of a difficult-to-detect invasive forest pest. *The Canadian Entomologist*, *147*(03), 338–348. https://doi.org/10.4039/tce.2015.11

Sims, C., Aadland, D., Finnoff, D., & Powell, J. (2013). How Ecosystem Service Provision Can Increase Forest Mortality from Insect Outbreaks. *Land Economics*, *89*(1), 154–176. https://doi.org/10.3368/le.89.1.154

Soil Survey Staff. (2020). *The Gridded Soil Survey Geographic (SSURGO) Database for New Jersey*. United States Department of Agriculture, Natural Resources Conservation Service. https://gdg.sc.egov.usda.gov/

Steiner, K. C., Graboski, L. E., Knight, K. S., Koch, J. L., & Mason, M. E. (2019). Genetic, Spatial, and Temporal Aspects of Decline and Mortality in a *Fraxinus* Provenance Test Following Invasion by the Emerald Ash Borer. *Biological Invasions*, *21*(11), 3439–3450. https://doi.org/10.1007/s10530-019-02059-w

Stępniak, M., & Jacobs-Crisioni, C. (2017). Reducing the Uncertainty Induced by Spatial Aggregation in Accessibility and Spatial Interaction Applications. *Journal of Transport Geography*, *61*, 17–29. https://doi.org/10.1016/j.jtrangeo.2017.04.001

Tluczek, A. R., Mccullough, D. G., & Poland, T. M. (2011). Influence of Host Stress on Emerald Ash Borer (Coleoptera: Buprestidae) Adult Density, Development, and Distribution in

<I>Fraxinus pennsylvanica</I> Trees. *Environmental Entomology*, *40*(2), 357–366. https://doi.org/10.1603/EN10219

U.S. Geological Survey. (2000). *National Elevation Data 30 meter*. USDA/NRCS - National Geospatial Center of Excellence.

U.S. Geological Survey. (2019). *NLCD 2016 USFS Tree Canopy Cover (CONUS)*. U.S. Geological Survey. https://www.mrlc.gov/downloads/sciweb1/shared/mrlc/metadata/nlcd_2016_treecanopy_2019_08_31.img.xml

U.S. Geological Survey. (2021). *SSEBop Actual Evapotranspiration Products (Version 5.0, February 2021)*. U.S. Geological Survey.

Vanatta, A., Hauer, H., & Schuettpelz, N. (2012). Economic Analysis of Emerald Ash Borer (Coleoptera Buprestidae) Management Options. *Journal of Economic Entomology*, *1*(196–206).

Walston, L. J., Li, Y., Hartmann, H. M., Macknick, J., Hanson, A., Nootenboom, C., Lonsdorf, E., & Hellmann, J. (2021). Modeling the Ecosystem Services of Native Vegetation Management Practices at Solar Energy Facilities in the Midwestern United States. *Ecosystem Services*, *47*, 101227. https://doi.org/10.1016/j.ecoser.2020.101227

Wang, H., Seaborn, T., Wang, Z., Caudill, C. C., & Link, T. E. (2021). Modeling Tree Canopy Height using Machine Learning over Mixed Vegetation Landscapes. *International Journal of Applied Earth Observation and Geoinformation*, *101*, 102353. https://doi.org/10.1016/j.jag.2021.102353

Warwick, W., Hardy, T., Hoffman, M., & Homer, J. (2016). Electricity Distribution System Baseline Report. *U.S. Department of Energy*, 120.

Wilson, B. T., Lister, A. J., & Riemann, R. I. (2012). A nearest-neighbor imputation approach to mapping tree species over large areas using forest inventory plots and moderate resolution raster data. *Forest Ecology and Management*, *271*, 182–198. https://doi.org/10.1016/j.foreco.2012.02.002

Wolfe, J., Jin, X., Bahr, T., & Holzer, N. (2017). Application of Softmax Regression and its Validation for Spectral-Based Land Cover Mapping. *The International Archives of the Photogrammetry, Remote Sensing and Spatial Information Sciences*, *XLII-1/W1*, 455–459. https://doi.org/10.5194/isprs-archives-XLII-1-W1-455-2017

Woudenberg, S. W., Conkling, B. L., O'Connell, B. M., LaPoint, E. B., Turner, J. A., & Waddell, K. L. (2010). *The Forest Inventory and Analysis Database: Database description and users manual version 4.0 for Phase 2* (RMRS-GTR-245; p. RMRS-GTR-245). U.S. Department of Agriculture, Forest Service, Rocky Mountain Research Station. https://doi.org/10.2737/RMRS-GTR-245

Xu, X., Liu, W., Scanlon, B. R., Zhang, L., & Pan, M. (2013). Local and Global Factors Controlling Water-Energy Balances within the Budyko Framework. *Geophysical Research Letters*, *40*(23), 6123–6129. https://doi.org/10.1002/2013GL058324

Yemshanov, D., Koch, F. H., Barry Lyons, D., Ducey, M., & Koehler, K. (2012). A Dominance-Based Approach to Map Risks of Ecological Invasions in the Presence of Severe Uncertainty: A Dominance-Based Approach to Map Ecological Invasions. *Diversity and Distributions*, *18*(1), 33–46. https://doi.org/10.1111/j.1472-4642.2011.00848.x

Yemshanov, D., Koch, F. H., Mckenney, D. W., Downing, M. C., & Sapio, F. (2009). Mapping Invasive Species Risks with Stochastic Models: A Cross-Border United States-Canada Application for Sirex noctilio Fabricius. *Risk*, *29*(6), 868–884. https://doi.org/doi:10.1111/j.1539-6924.2009.01203

Zarandian, A., Baral, H., Stork, N. E., Ling, M. A., Yavari, A. R., Jafari, H. R., & Amirnejad, H. (2017). Modeling of Ecosystem Services Informs Spatial Planning in Lands Adjacent to the Sarvelat and Javaherdasht Protected Area in Northern Iran. *Land Use Policy*, *61*, 487–500. https://doi.org/10.1016/j.landusepol.2016.12.003

Zomer, R. J., & Trabucco, A. (2022). Version 3 of the “Global Aridity Index and Potential Evapotranspiration (ET0) Database”: Estimation of Penman-Monteith Reference Evapotranspiration. (In Press). *CGIAR-CSI GeoPortal*, 6.

# Appendix 1: Chapter 2 Supplementary Information

## A1 Derivation of Parameters

In this Appendix, we detail the derivation for all variables involved in the system of equations for EAB spread presented in Chapter 2. We simulate EAB for a period of 20 years (*T*), where each year has 12 constituent months (*t*). The study period was set as 20 years, to account for the historical spread of EAB within a region once it has been infested before it enters an endemic state (Poland et al., 2015; Siegert et al., 2014). Meters were the unit of distance, where locations are defined as 100-meter squares ($hs = 100m$). Each of these locations (*hs*) represents a square hectare (*ha*) and are organized in a grid structure covering the study area. The study area is bounded by a band of null locations to create a regular rectangular grid and to prevent EAB diffusion through the boundary of the study area. Hectares were chosen as the spatial unit based on Wilson et al. (2012), where BA was tracked in terms of per *ha.* EAB are tracked in the x and y dimensions as they diffuse between locations and cause damage to *Fraxinus*.

### A1.1 Converting Surface Area to Basal Area

A fundamental problem arose when deriving the variables involved in the life cycle of EAB: translating the inventory term basal area (BA) into the experimentally recorded unit of surface area (SA). EAB feeds on the inner layer of bark, so consumption and other observations are recorded in terms of SA, but most forest records are in terms of the cross-sectional area of the local trees, BA. BA is the unit type in the data and is a common unit in forest management. To cross the divide between the biology of EAB and forest inventories, it is vitally important to start by transforming SA to BA. To transform SA to BA, we used the data in McCullough et al.

(2007), where measured *Fraxinus* were measured for both their diameter at breast height (DBH) and the entire SA was measured. This takes the form of the polynomial equation

$$SA = 0.024DBH^2 - 0.307DBH + 2.63,$$

*( 22 )*

where SA is measured in square meters and DBH is measured in centimeters. From here, we relate BA to SA using the relationship between BA and DBH known as the Forester's constant (*FC*) and the quadratic mean diameter function, used to calculate basal area (Balderas Torres & Lovett, 2013),

$$DBH = \sqrt{\frac{BA}{tphFC}}.$$

*( 23 )*

Equation (23) is used to estimate the average diameter of trees in a stand, where *FC* is a rate constant between the DBH and the BA comprised of pi and the unit shift between centimeters and square meters, ($FC = 0.00007854$), finally *tph* indicates the number of trees per hectare. The result is the average DBH of a tree in the stand, but because we are not solving for the individual tree DBH, but entire hectares, we cancel the trees per hectare (*tph*) term which gives a result that is measured in $\frac{cm}{ha}$ as the population terms in the original formula cancel out,

$$DBH = \sqrt{\frac{BA}{FC}}.$$

*( 24 )*

We then substituted the solution for DBH from eq. (24) into eq. (22).

$$SA = 0.024\frac{BA}{FC} - 0.307\sqrt{\frac{BA}{FC}} + 2.63.$$

*( 25 )*

Finally, we substitute in the value for FC from eq. (25) resulting in eq. (26),

$$SA = 305.577BA - 34.641\sqrt{BA} + 2.63.$$

*( 26 )*

For most of our future derivations from here we need to assume full growth of *Fraxinus*, such as for the logistic growth of *Fraxinus*. The carrying capacity of *Fraxinus* is $34.44\,\frac{m^2}{ha}$ of basal area in the Northeast, which using eq. (26) is equivalent to $10323.59\,\frac{m^2}{ha}$ surface area (Dixon & Keyser, 2016). This constant establishes our foundational understanding between the SA of *Fraxinus* and the recorded BA.

**A1.2 Consumption of Fraxinus by EAB**

EAB were tracked for both adult ($E_a$) and larval ($E_l$) stages as the number of individuals per hectare,

$$E_a = \frac{in}{ha},$$

$$E_l = \frac{in}{ha}.$$

EAB adults are not responsible for considerable damage to *Fraxinus*, like EAB larva and so do not cause damage, but for EAB larva do and consume *Fraxinus* at a rate, *C*. The consumption rate is derived from an experiment that determined that an average of 88.9 EAB per square meter SA could successfully emerge from *Fraxinus* phloem before that area could no longer support EAB (McCullough & Siegert, 2007). It is assumed that the EAB consume the

total mass of available food even though this is not the case. We then define *C* by the number of EAB that can successfully reproduce per unit area,

$$C = \frac{1m^2SA}{88.9E_l \cdot T}.$$

*( 27 )*

To reflect the on-season monthly timescale instead of the reported annual rate we divide by 4:

$$C = \frac{1m^2SA}{88.9E_l \cdot 4t}.$$

*( 28 )*

The next step is to change $m^2SA$ into *ha* to balance with *A* which is measured in $\frac{m^2BA}{ha}$. We divide *C* by the absolute amount of *Fraxinus* surface area (SA) that could exist in a cell from eq. (26). This transformation shifts the units in the numerator of *C* from $m^2(SA)$ into *ha*,

$$\frac{1m^2SA}{88.9E_l \cdot 4t} \cdot \frac{1ha}{10323.59m^2SA} = 0.0000002724 \frac{ha}{E_l t}.$$

*( 29 )*

The consumption term (*C*) when combined with the population of EAB larva ($E_l$) and the density of *Fraxinus* (*A*) results in units of $\frac{ha}{\frac{in}{ha}t} \cdot \frac{in}{ha} \cdot \frac{m^2BA}{ha} = \frac{m^2BA}{t}$ which is the same as both terms in the equations for the growth of *Fraxinus*.

### A1.3 Growth and Adaptation of Fraxinus

The growth of *Fraxinus* is derived from even-aged stands where the size of the tree is dependent on the number of years it has been present (Table 11) (Schlesinger, 1990). Other site conditions could slow the growth of *Fraxinus*, but absent information on those conditions we use the numbers in Table 11 for growth, as by using these numbers we do not require other inputs for

site conditions that are often difficult or impossible to map given the limited spatial data available.

*Table 11: Age and Approximate Basal Area (BA). From Schlesinger et al. (1990) transformed from DBH to basal area (BA).*

| *Age* | *Basal Area ($m^2$)* |
|---|---|
| *20* | 0.007854 |
| *30* | 0.02545 |
| *40* | 0.04909 |
| *50* | 0.07069 |
| *60* | 0.1018 |
| *70* | 0.1452 |

Starting from the data in Table 11, we assume exponential growth and solve for the rate constant for the growth of *Fraxinus*. Where we define growth by the formula $P_T = P_i e^{rT}$, where $P_T$ is the population at time $T$, $P_i$ is the population at the initial time step, and $r$ is the rate constant. We alternatively set $T$ as 50, for the time between year 20 and year 70, or 7 for growth from sprouting to juvenile size. We define juvenile growth time as 7 rather than 20 because younger specimens exhibit a much higher rate of growth than Table 11 indicates, but it is measured as 20 due to a noted lag period where the saplings pause in the mid-story and are looking for a break in the canopy, which can last anywhere from 5-15 years. When this constraint is removed the growth time for the first period is only 7 years (Schlesinger, 1990). We then solve for the growth rate where

$$P_T = \begin{cases} 0.007854 & T = 7 \\ 0.1452 & T = 50 \end{cases},$$

and

$$P_i = \begin{cases} 0.0005067 & T = 7 \\ 0.007854 & T = 50 \end{cases}.$$

For $P_i$ we assume that the sapling has a radius of 1 mm at year zero when T=7. We use T=7 to define damaged *Fraxinus* defined by saplings and sprout stumps that grow quickly and T=50 is used to define the normal growth of Fraxinus in a more mature setting.

The final rates, *r,* for undamaged and damaged *Fraxinus* are $r$=0.00483 and, $r$=0.0383 per month, *t*. These two variations on the rate of growth create a dynamic system where understory saplings grow 7 times faster than overstory trees, but then transfer to a slower growth once the stand has begun to mature. These two growth rates allow *Fraxinus* to maintain a slight presence in the study area, even under intense EAB infestation, rather than being completely extirpated. This increased growth rate is triggered when *Fraxinus* populations fall below 0.10 of their initial density (Kashian, 2016). While this process could not continue indefinitely, it is currently uncertain how long a background of quick growing *Fraxinus* sprouts and saplings could persist in the forest system and under what conditions they simply fail (Robinett & McCullough, 2019).

Next, we evaluate the crowding coefficient for *Fraxinus,* $\hat{C}$. The crowding coefficient is based on the total crowding of *Fraxinus* from the Forest Vegetation Simulator, FVS, system (Dixon & Keyser, 2016). In a fully stocked forest in the Northeastern USA, $34.44m^2$ of BA could potentially grow per *ha* of land ($BA_{max}$).

We use Verhulst logistic growth with respect to time to define instantaneous growth to define the *Fraxinus* system such that

$$\frac{dA}{dt} = rA - \frac{rA^2}{BA},$$

where *r* is the growth rate when *T* equals 50, *t* is the time in months, *A* is the population of *Fraxinus* and *BA* is the carrying capacity of *Fraxinus*. This defines our crowding coefficient, $\hat{C}$,as the ratio of the growth rate, *r,* and the maximum basal area, $BA_{max}$, which equals 0.0001403. To check the veracity of the terms, the solution to Verhulst logistic growth was utilized to verify growth in the model environment continued as expected

$$A(t) = \frac{BA}{1+\frac{BA-A_0}{A_0}(e^{-rt})}. \quad (31)$$

We integrate local forest cover ($F_c$) as a proportion into the crowding variable ($\hat{\mathrm{C}}\mathrm{A}^2$) to change the carrying capacity of *Fraxinus* across the landscape due to varying landcover. This variable is assumed constant over the simulation period. We utilized the forest cover of the 2016 national map as the source for this factor (U.S. Geological Survey, 2019). And while this is canopy cover, it does indicate which areas are under forest cover, which is an improvement in detail over land use and land cover maps where level of cover is not tracked. The data in this file is stored as a percentage of forest cover with values between 0 and 100 percent, with undefined data having values of up to 255, this indicates water bodies and other landcovers that are not covered in this set. We multiply our crowding coefficient, $\hat{C}$, by the unitless proportion of forest cover $\frac{1}{F} = F_c$, where $F_c$ refers to the proportion of forest cover and *F* refers to the percentage stored in the original dataset, with all undefined values set as 0. The equation takes the final form of eq. (4)

$$\frac{dA}{dt} = \begin{cases} \hat{G}_1 \mathrm{A} - \hat{\mathrm{C}} \mathrm{F_c} \mathrm{A}^2 - \mathrm{CE_l A} & \frac{\mathrm{A}}{\mathrm{A}_{(1)}} \geq 0.1 \mathrm{F_c} \\ \hat{G}_2 \mathrm{A} - \hat{\mathrm{C}} \mathrm{F_c} \mathrm{A}^2 - \mathrm{CE_l A} & \frac{\mathrm{A}}{\mathrm{A}_{(1)}} < 0.1 \mathrm{F_c} \end{cases}.$$

### A1.4 Diffusion Coefficient of EAB

Mercader et al. (2009) showed that in a forest with abundant *Fraxinus*, the vast majority of individual EAB are found within 800 meters of the infestation. Their experimental results followed a decaying exponential of the form:

$$f(D) = 27.08e^{-(0.037D)},$$

*( 32 )*

where *D* is the distance from the origin. *f(D)* is the probability density function (PDF) for EAB and describes the distribution of EAB at the end of a single year. To normalize *f(D)*, the area under the PDF must be equal to one. It was stated in the experiment that after 800 meters distance from the origin that the vast majority of tracked EAB were discovered, which we used as our upper limit for the PDF. To find the area we integrate over the domain

$$\int_0^{800} 27.08e^{-(0.037D)} dD = \left(\frac{0.2708}{-0.037}\right) e^{(-0.037D)}.$$

*( 33 )*

Once we evaluate the curve our to 800 meters, the area under the curve defined in eq. (32) is far higher than 1. We solve for the area under the curve from the origin up to a distance of 800 meters

$$\left(\frac{0.2708}{-0.037}\right) \cdot \left[e^{(-0.037(800))} - 1\right] = \frac{0.2708}{0.037} = 7.3189,$$

*( 34 )*

which results in a normalization factor of 7.3189. We integrate this normalization factor into our diffusion distances according to eq. (35).

$$F(D) = \left(\frac{0.2708}{7.3189}\right) e^{(-0.037D)}.$$

*( 35 )*

For each year, *T*, the diffusion rate is varied between the bounds of 5m and 805m to capture most spread events defined under the curve. For each distance, a different model run is realized. The runs are compiled, $D_z$, and reduced to the proportion that would be expected under eq. (35) and the result is used as the input for the next *T*, eq. (36).

$$D_z = \sum F(D).$$

*( 36 )*

After experimentation we noted slightly more EAB than should be expected after compiling all diffusion coefficients using eq. (35) and eq. (36). After eliminating other possibilities, we attribute to our 800-meter integration limit. We included the rate at which additional EAB appeared as a normalization factor in addition to eq. (35) to prevent leakage due to the bounds of the integral. This term equals 1.011260648225738, which only compensated for a 1 percent error after compiling diffusion coefficients.

In eq. (1), $D_u$ is the diffusion coefficient which is the diffusion in the *x* and *y* directions and is calculated from *D* which is the experimentally determined distance. We calculate $D_u$ according to eq. (37) to transform the linear distance into circular diffusion and change the unit of time from a yearly rate to a monthly rate by dividing by 4,

$$D_u = \pi \cdot \left(\frac{D}{4}\right)^2.$$

*( 37 )*

For future terms, it is useful to know the average of the PDF for EAB diffusion in eq. (35). To solve for the average, we integrate eq. (38) with respect to *D*, to determine the average *D* value observed by Mercader et al. (2009).

$$< D >= \int_0^{800} \left(\frac{0.2708}{7.3189}\right) De^{(-0.037D)}\, dD, \tag{38}$$

$$< D >= 27.027. \tag{39}$$

Determining the average of the PDF is necessary, eq. (39), because EAB diffusion is not strictly predicted by distance and EAB adults are known to be attracted to areas with dense *Fraxinus* and areas with stressed *Fraxinus*. Mercader et al. (2016)'s observed that their data collected in 2009 was collected in an area where *Fraxinus* was abundant and evenly distributed. In a follow up experiment by Siegert et al. (2010), the effects of low density and stress were observed in an area with much lower densities of host trees and a few stressed trees. Data collected here showed an increased propensity for EAB to colonize sites with more available phloem $\left(> 1000 \frac{m^2}{ha}\right)$ and stressed individual trees. Stressed trees offer lower resistance to EAB and so are more attractive to EAB. We identify areas that have abundant *Fraxinus* and areas that have already been damaged by EAB in previous years, *T*, to estimate the influence of site factors on the dispersal of EAB.

The site factors are assumed to cause the diffusion of EAB to shift either positively or negatively. For instance, low abundance of *Fraxinus*, $A_b$, has been observed to have a positive effect on the rate of EAB spread, with a maximum factor of 10.0909 over baseline spread when

no *Fraxinus* are present, which could lead to spread events of over 8km (Siegert et al., 2010; Tluczek et al., 2011).

The second factor was related to the impact of stress on EAB diffusion, $A_{sf}$. This was sourced from Mercader et al. (2011) and Mercader et al. (2016), where experiments regarding the spread impacts of both damaged trees and purposefully girdled specimens were tracked and sampled for EAB density. Through their experiments they found the limit for stress as a factor was 7, which was dependent on the quantity of damaged *Fraxinus* compared to the *Fraxinus* present in the first timestep (Table 12).

*Table 12:* Fraxinus *Stress and Density Influence on EAB Diffusion*

| ***Condition*** | ***Outcome*** | ***Reference*** |
|---|---|---|
| ***Full Density (34.44 $m^2$ BA) Average Diffusion*** | $27.074\frac{m}{T}$ | (Mercader et al., 2009) |
| ***Low Density Average Diffusion*** | $322.3\frac{m}{T}$ | (Siegert et al., 2010) |
| ***No Stressed Fraxinus*** | Normal rate of spread | (Mercader et al., 2009) |
| ***Stressed Fraxinus*** | 7 times normal rate | (Mercader et al., 2011, 2016) |

Overall, the influence of site factors, $A_s$ is set as the ratio between the relative abundance of *Fraxinus,* $A_b$, and the stress caused by EAB, $A_{sf}$,

$$A_s = \frac{A_b}{A_{sf}} \quad (40)$$

$A_b$ represents the ratio between the local density of *Fraxinus, A,* scaled according to the maximum noted additional spread of EAB when *Fraxinus* is sparse (Table 12). With the

available experimental data, when *Fraxinus* is at carrying capacity, the $A_b$ is considered to be 1, and when *Fraxinus* is less than 1 percent of carrying capacity, $A_b$ is considered 10. We make a linear assumption between our two data points and solve to give us eq. (41),

$$A_b = 10.0909 - 0.2639A.$$

*( 41 )*

We simplify the numbers to a factor of 10 due to the noted imperfections of the data and so drop the influence of density slightly to compensate.

The second factor, $A_{sf}$ is dependent on the separate ratio value $A_L$, which is the ratio of *Fraxinus* at the initial time minus the current *Fraxinus* all over the *Fraxinus* at the initial time. This gives us a ratio for the decline of *Fraxinus* compared to the initial time step.

$$A_L = \frac{A_{(0)} - A_{(i)}}{A_{(0)}}.$$

*( 42 )*

We then take the resulting ratio and apply it to three thresholds for stress-induced spread from Mercader et al. (2016) and again use a linear interpretation between the two points.

$$A_{sf} = \begin{cases} 1 & A_L < 0.0016 \\ 18.27A_L + 0.97 & 0.0016 > A_L > 0.33. \\ 7 & A_L > 0.33 \end{cases}$$

*( 43 )*

This constrains the limits of this effect as either negligible, or maximum effect with the highest observed impact on spread (lower by a factor of 7) (Mercader et al., 2011, 2016) and the third case bridges the two extremes.

The first case in eq. (43) states that there was no influence from stress if less than 1.6 percent of the *Fraxinus* had been consumed by EAB. Then between that point and the tested

point of 33 percent of the *Fraxinus* consumption, the relationship for stress was assumed to stretch linearly based on the percentage reduction of *Fraxinus* from 1 to 7, and then the relationship stopped increasing.

### A1.5 EAB Reproduction and Crowding

EAB reproduces at a rate of 12 ± 4.74 percent per year (Mercader et al., 2016). Mercader et al. (2016)'s results indicate that the population of EAB increases twelvefold every year in low density populations.

The units of EAB growth are $\frac{ha}{m^2 t}$ because it is a ratio regarding time with respect both to space and available basal area. For our initial numbers we can say that EAB grow with both respect to time and area. This value does not need additional transformation to be used, as results from previous iteration of this model showed limited sensitivity to EAB growth rate within known bounds (Lyttek et al., 2019). EAB growth then equals to the maximal growth rate of EAB over the number of months ($t$) in the active season of the year ($T$)

$$\bar{G} = \frac{12\frac{E_l}{E_a T}}{4\frac{t}{T}}.$$

*( 44 )*

Data regarding the crowding of EAB proved to be rare, with the exception of one study (J. Duan et al., 2013), which mapped EAB survivorship rates with their density per unit of surface area, *SA*. To solve for our crowding rate in eq. (2), $\bar{C}$,we used data from the survivorship curve to determine an appropriate crowding term. We used data from their lowest density test as there was still significant mortality, which was conducted at a rate of 200 EAB per square meter

of *SA*. We take the second half of eq. (2) and when the units are evaluated, we need $\bar{C}\ to\ have$ units of individuals per hectare over basal area,

$$\bar{C}A(t_i) - E_l(t_i) = \frac{inE_l ha}{m^2 BA} \cdot \frac{m^2 BA}{ha} - inE_l.$$

*( 45 )*

To solve for $\bar{C}$ we use J. Duan et al., (2013)'s experimental results per square meter of *SA* and the conversion of a fully grown stand of *Fraxinus* from *SA* to *BA*,

$$\bar{C} = 119\frac{inE_l}{m^2 SA} \cdot 10323.59\frac{m^2 SAha}{m^2 BA},$$

*( 46 )*

which results in a crowding coefficient of $\bar{C} = 1228507.21$.

Future generations of $E_a$ in future *T* are equal to the previous *T's* final $E_l$ population. This is further discussed in section 1.6.3 in eq. (49).

### A1.6 Parasitism of EAB

The addition of parasitoids has become the primary focus of EAB management, yet at this point, there is no known threshold analysis regarding the success of these introductions with the primary goal of preserving *Fraxinus*. There are 4 species of concern—three exotic and one native—which we will be exploring (Tables 1 and 13).

*Table 13: Primary Sources of and Rates of the Four Simulated Parasitoids. Rate refers to the assessed annual mortality caused by this parasitoid to EAB.*

| PARASITOID | ORIGIN | TARGET | RATE | REFERENCE |
|---|---|---|---|---|
| *OOBIUS AGRILI* | Exotic | EAB Eggs | 0-0.68 | (J. Duan et al., 2018) |
| *TETRASTICHUS PLANIPENNISI* | Exotic | EAB Larvae | 0-0.44 | (J. Duan et al., 2018) |
| *SPATHIUS GALINAE* | Exotic | EAB Larvae | 0-0.78 | (J. Duan et al., 2019) |
| *PHASGONOPHORA SULCATA* | Native | Mature EAB Larvae | 0-0.343 | (Roscoe et al., 2016) |

### *A1.6.1 Oobius agrili*

*Oobius agrili* is an egg parasitoid that directly affects fecundity over the active period of EAB by targeting and eliminating EAB before they cause damage. The timing between the parasitoid and EAB laying eggs can be affected by asynchronous tendencies between EAB and *Oobius agrili's* emergence in the spring, leading to lower effectiveness outside of *Oobius agrili's* native conditions. Variable climactic conditions lead to extremely variable impact on EAB, but continuous prevention of EAB growth is possible. To simulate the effect of *Oobius agrili*, we alter the growth rate of $E_l$ by the rate $P_{oa}$. Given that *Oobius agrili* has been measured in isolation, this rate can be defined as a strict proportion and used directly with only a transformation to a to a monthly rate from the published annual survey data.

The transformation between annual and monthly rates is necessary because parasitoids are usually observed on an annual time frame, which does not work in a continuous model. In this case, we borrow from interest formulas from finance regarding interest and future value calculations for annuities. In annuity calculations, the known annual rates are used to calculate the initial and ending populations that would be expected. Rates are adjusted, so they better fit the expected decline noted in annual rates (Table 1),

$$E_l(T) = E_l(t) \cdot \left(\frac{P_{oa}^4 - 1}{P_{oa}}\right),$$

*( 47 )*

where the $E_l(T)$ is the expected population at the end of a year when some number of $E_l$ eggs are laid, $E_l(t)$ is the monthly rate of population increase that results in the population $E_l(T)$, and $\left(\frac{P_{oa}^4 - 1}{P_{oa}}\right)$ is the rate of decline, which is defined as the annual rate raised to the 4th power, for the number of active periods, minus 1 over the annual rate. We solve for the monthly rate and integrate into eq. (2) to reduce growth of EAB.

$$E_l(t_i) = E_l(t_i) + \min\left(\bar{G}E_a(t_i)(1 - P_{oa}), \bar{C}A(t_i) - E_l(t_i)\right)$$

### *A1.6.2 Tetrastichus planipennisi and Spathius galinae*

Both *Tetrastichus planipennisi* and *Spathius galinae* parasitoids attack 3rd and 4th instar EAB larva, are usually released together and so a combined factor is appropriate. To approximate the continuous parasitism by these species, the mortality rate is based on an exponential function linked to the growth rate of EAB and the time step. The ceiling is capped at the absolute value discovered for *Spathius galinae*, $P_{Sg}$, and the floor defined as the minimum for *Tetrastichus planipennisi*, $P_{Tp}$, as they prey on EAB larva that are in different diameter classes of *Fraxinus* and so are only fully effective when deployed together (Table 13)

$$P_{Tp} + P_{Sg} = P_{mp}.$$

*( 48 )*

A timestep adjustment like *Oobius agrili* was applied to $P_{mp}$ as well (Table 1), eq. (47). Which is then used as a continuous mortality rate across the active season.

### *A1.6.3 Phasgonophora sulcate and EAB Emergence*

The final parasitoid is a native that normally parasitizes other members of the *Agrilus* genus besides EAB but has been observed aggressively parasitizing EAB in some areas of the Northeast USA and Canada. This species has an annual life cycle and overwinters like EAB, so parasitized EAB continue to consume *Fraxinus* throughout their larval stage. However, no new adult emerges in the spring and instead, a new parasitoid emerges.

This makes the parasitoid a vector that effectively limits the new emerging adult EAB population. Additionally, similar rates have been observed around woodpeckers in heavily infested stands and trees developing resistance (D. E. Jennings et al., 2016; D. Kashian et al., 2018; D. Kashian, 2016). Additionally, no transformation of the annual rate is needed, as the rate is applied once yearly as a failure rate according to eq. (8) below

$$E_{a\left(\frac{t_0}{T_1}\right)} = E_{l\left(\frac{t_{12}}{T_0}\right)}(1 - P_{Ps}),$$

*( 49 )*

$$E_{l\left(\frac{t_0}{T_1}\right)} = 0$$

*( 50 )*

where the population of $E_a$ at the initial timestep, $t_0$, in year $T_1$ equals the population of $E_l$ in the last timestep, $t_{12}$, of the previous year, $T_0$, eq. (49). The population of $E_l$ in the first timestep of the following year, $T_1$, is then set to zero as larva graduate into adults, eq. (50).

### *A1.6.4 Application and Integration of Parasitism*

There is significant variability in rates of parasitism especially when we are looking at introduction and sometimes establishment fails and can lead to exceptionally low effectiveness. To integrate this randomness, each parasitoid has variable effectiveness across the landscape

within bounds. This rate changes with each new year, *T*, of the simulation, which is appropriate as surveys of parasitoids invariably show variability year-to-year, even in established sites. Distributions for *Oobius agrili*, *Tetrastichus planipennisi*, and *Spathius galinae* are based on quintiles of their expected distributions from experimental evidence (Table 13), while *Phasgonophora sulcata* is shifted by one standard deviation, 0.02, of its mean (Table 1).

### A1.7 Random Introduction of EAB

The introduction of EAB, given the rest of the model system, was assumed to be random across the study area, but fixed by a random number seed to allow for repeatability. These introductions caused variance, but all scenarios followed a similar trajectory. New infestation points were chosen as the intersection between two random number streams. The first vector was set at a positive rate of 0.1 and the second was set at a rate of 0.0027 set by a different seed to place new infestations at rate similar to dendrochronological studies for EAB (Siegert et al., 2014). This methodology was used to place a varied, but low number of introduced events for the study area (Table 14) and is an assumption on the rate of new introductions consistent with other papers (Ali et al., 2015; Mercader et al., 2016).

Siegert et al. (2014) found on average 7.4 new infestations per year, with an average dispersal distance of 24.5 km, which is in line with the size of our smaller study area, if slightly larger, but this study was done over a much larger area. In our model, new infestation sizes were kept small at 4 new individuals per year. Through parameterization testing we found early on that the existence of a disjointed population is more of a deciding factor rather than the size, as tests with larger introductions showed insignificant difference.

*Table 14: New Infestation Points in Sampled Seeds. This is listed here to show that the number of infestation points is consistent with literature that showed a rate of 7.4 new infestations a year on average for an area the size of our study area (Siegert et al., 2014).*

| | *Introduction Points by Seed* |
|---|---|
| *Seed 1* | 3 |
| *Seed 2* | 5 |
| *Seed 3* | 6 |
| *Seed 4* | 10 |
| *Seed 5* | 10 |
| *Seed 6* | 7 |
| *Seed 7* | 6 |
| *Seed 8* | 8 |
| *Seed 9* | 3 |
| *Seed 10* | 5 |
| *Seed 11* | 6 |
| *Seed 12* | 8 |
| *Seed 13* | 11 |
| *Seed 14* | 7 |
| *Seed 15* | 5 |
| *Seed 16* | 5 |

*Table 15: Full Parameter List and Primary Sources for the Derivation of the EAB Spread Model*

| PARAMETER | NAME | UNITS | SOURCE | SECTION |
|---|---|---|---|---|
| $T$ | Years | $Year$ | (Poland et al , 2015) | *A1* |
| $T$ | Months | $\frac{Month}{Year}$ | (Poland et al , 2015) | *A1* |
| $H_S$ | Point Distance | $m$ | (Wilson et al , 2012) | *A1* |
| $X$ | x-axis distance | $m$ | ---------- | *A1* |
| $Y$ | y-axis distance | $m$ | ---------- | *A1* |
| $C$ | EAB Consumption | $-$ | (McCullough & Siegert, 2007) | *A1.2* |
| $\widehat{G_{1-2}}$ | *Fraxinus* Growth | $\frac{1}{t}$ | (Schlesinger, 1990) | *A1.3* |
| $\widehat{C}$ | *Fraxinus* Crowding | $\frac{ha}{m^2 \cdot t}$ | (Dixon & Keyser, 2016; Gould et al , 2020) | *A1.3* |
| $F_C$ | Forest Cover | $\frac{1}{\%}$ | (U S Geological Survey, 2019) | *A1.3* |
| $A$ | *Fraxinus* Density | $\frac{BA}{ha}$ | (Wilson et al , 2012) | *A1.3* |
| $D$ | Diffusion Rate | $\frac{m}{T}$ | (Mercader et al , 2009; Siegert et al , 2010) | *A1.4* |
| $D_U$ | Diffusion Coefficient | $\frac{m^2}{t}$ | (Mercader et al , 2009; Siegert et al , 2010) | *A1.4* |
| $A_B$ | *Fraxinus* Abundance | $\frac{A_i}{A_{max}}$ | (Mercader et al , 2009; Siegert et al , 2010) | *A1.4* |
| $A_{SF}$ | *Fraxinus* Stress | $unitless$ | (Mercader et al , 2009, 2011) | *A1.4* |
| $A_S$ | Combined Stress Factor | $\frac{A_b}{A_{st}}$ | (Mercader et al , 2009, 2011; Siegert et al , 2010) | *A1.4* |
| $E_A$ | EAB Adults Density | $\frac{in}{ha}$ | (Poland et al , 2015) | *A1.4* |
| $E_L$ | EAB Larva Density | $\frac{in}{ha}$ | (Poland et al , 2015) | *A1.4* |
| $\bar{G}$ | EAB Growth | $\frac{E_i}{E_a \cdot t}$ | (McCullough & Siegert, 2007; Mercader et al , 2016) | *A1.5* |
| $\bar{C}$ | EAB Crowding | $\frac{E_i}{m^2 BA}$ | (J Duan et al , 2013; McCullough & Siegert, 2007) | *A1.5* |
| $P_{OA}$ | Egg Parasitism | $\frac{1}{t}$ | (J Duan et al , 2018) | *A1.6.1* |
| $P_{MP}$ | Mid-season Parasitism | $\frac{1}{t}$ | (J Duan et al , 2018; J Duan et al , 2019) | *A1.6.2* |
| $P_{SP}$ | End-season Parasitism | $\frac{1}{12t}$ | (Roscoe et al , 2016) | *A1.6.3* |
| $R$ | Risk | $Binary$ | (Ali et al , 2015; Mercader et al , 2016; Siegert et al , 2014) | *A1.7* |
| $L$ | Introduction Rate | $\frac{E_a}{t}$ | (Siegert et al , 2014) | *A1.7* |
| $RL$ | New Infestation Risk | $Percent$ | (Siegert et al , 2014, 2015) | *A1.7* |
| $\omega$ | EAB Test Mortality | $\frac{1}{t}$ | Testing Variable | *A1.7* |

## Appendix 2: Chapter 3 Supplementary Information

### A3.1 Altered Derivation for EAB Consumption and *Fraxinus* Growth

We utilize an alternative parameterization for the EAB-*Fraxinus* PDE model when we are evaluating *Fraxinus* decline over EAB population dynamics. This alternative parameterization is focused on eq. (4) where we relate EAB consumption, *C*, to the populations of both EAB larva, $E_l$, and *Fraxinus* density, *A*. In this model we remove the relation to *A*, and instead focus squarely on EAB biology for the consumption term, as detailed in eq. (10). We start with the same data found in Appendix 1.2 for this variant but discount the data about *Fraxinus*. We start with the consumption noted in McCullough & Siegert, (2007) and derive for the same units without the inclusion of *A* as a variable,

$$\frac{1m^2SA}{88.9EAB_l \cdot 4t}.$$

To balance the combined term $CE_l$ needs units of $\frac{BA}{ha \cdot t}$, and the term *C* needs units of $\frac{BA}{in \cdot t}$ to balance with the units of $\mathrm{E}\left(\frac{in}{ha}\right)$. Currently, *C* is in terms of $\frac{m^2(SA)}{in \cdot t}$. To transform this, we transform the *ha* term in *E* into $m^2(SA)$. To do this, we calculate the maximum surface area per *ha*, which according to the equation is $10323.59\frac{SA}{ha}$. We solve for SA in 1 BA, which is $299.8\frac{SA}{BA}$

Thus, the consumption term in this version is defined in eq. (10) by eq. (51),

$$0.002812\frac{m^2(SA)}{in \cdot t} \cdot \frac{1BA}{299.8m^2(SA)} = 0.000009381\frac{BA}{in \cdot t}. \quad (51)$$

## Appendix 3: Chapter 4 Supplementary Information

*Table 16: Summary of Spatial and Single Factor Inputs for InVEST*

| INPUTS: | DEFINITION | SOURCE |
|---|---|---|
| GENERAL PARAMETERS: | ---------- | ---------- |
| **LAND USE LAND COVER RASTER (LULC)** | Land use of the study area as it exists now with estimated carbon pools | (New Jersey Department of Environmental Protection (NJDEP) et al , 2019) |
| **EXPERIMENTAL LULC RASTER** | Same LULC Base, but with Decreased Forest defined by Quantiles | (New Jersey Department of Environmental Protection (NJDEP) et al , 2019; Wilson et al , 2012) |
| **PRECIPITATION RASTER** | Average Millimeters of annual precipitation | (Oregon Climate Service at Oregon State University, 2012) |
| **WATERSHEDS AND SUBWATERSHEDS SHAPEFILE** | Shapefile of the huc-12 watershed designations from the USGS | (New Jersey Department of Environmental Protection (NJDEP) & New Jersey Geological Survey (NJGS), 2009) |
| WATER YIELD SPECIFIC: | ---------- | ---------- |
| **SEASONALITY VALUE (Z PARAMETER)** | Z is Defined as 2 25, the average of the study area | Product of Available water capacity (AWC), Average Precipitation and 1 25 times the ω factor (Xu et al , 2013) |
| **EVAPOTRANSPIRATION RASTER** | Operational Simplified Surface Energy Balance (SSEBop) results | (U S Geological Survey, 2021) |
| **ROOT RESTRICTING LAYER RASTER** | The thickness of soil components at the sample point Sourced from the 'tka_0-999' layer | (Soil Survey Staff, 2020) |
| **PLANT AVAILABLE WATER CONTENT RASTER (PAWC)** | Sourced from the 'AWC 0-999' layer | (Soil Survey Staff, 2020) |
| SDR AND NDR SPECIFIC: | ---------- | ---------- |
| **DIGITAL ELEVATION MODEL RASTER (DEM)** | 6-30m DEMs for New Jersey Resampled to the study area and stitched together | (U S Geological Survey, 2000) |
| **EROSIVITY RASTER** | Global Erosivity index | (Panagos & Ballabio, 2017) |
| **SOIL ERODIBILITY RASTER** | Erodibility of the conterminous United States | (Natural Resources Conservation Service, 2021a) |
| **THRESHOLD FLOW ACCUMULATION VALUE** | 1000 Default Value and like that calculated using GIS software | Number of connected pixels to define a stream |
| **BORSELLI K PARAMETER** | 2 | InVEST Default |
| **BORSELLI IC0 PARAMETER** | 200m | InVEST Default |
| **MAXIMUM SDR VALUE** | 0 8 | InVEST Default |
| **SUBSURFACE CRITICAL LENGTH (NITROGEN)** | 100 (Pixel Size) | InVEST Default |
| **SUBSURFACE MAXIMUM RETENTION EFFICIENCY (NITROGEN)** | 100 (Pixel Size) | InVEST Default |

*Table 17: Biophysical Table Values for InVEST Parameterization Before* Fraxinus *Mortality*

| Code | Nutrient Retention Model (NDR) | | | | | | | Sediment Retention Model (SDR) | | Annual Water Yield | | |
|---|---|---|---|---|---|---|---|---|---|---|---|---|
| **Land Use** | **Nitrogen Load (kg)** | **Nitrogen Effluence** | **Critical Nitrogen Length (m)** | **Subsurface Proportion of Nitrogen** | **Phosphorous Load (kg)** | **Phosphorous Effluence** | **Critical Phosphorous Length (m)** | **USLE Cover Factor (*C*)** | **USLE Practice Factor (*P*)** | **Vegetative State** | **Root Depth (mm)** | **$K_c$** |
| **Null** | 0 | 0 | 0 | 0 | 0 | 0 | 0 | 0 | 0 | 0 | 0 | 0 |
| **Urban** | 13 | 0.1 | 100 | 0 | 1.5 | 0.2 | 100 | 0 | 0.001 | 0 | 0 | 0.84 |
| **Rural** | 6.5 | 0.2 | 100 | 0 | 1 | 0.4 | 100 | 0.04 | 0.001 | 1 | 2000 | 0.9 |
| **Water** | 0 | 0 | 100 | 0 | 0 | 0 | 100 | 0 | 1 | 0 | 0 | 1.25 |
| **Wetland** | 9.73 | 0.8 | 100 | 0 | 0.14 | 0.8 | 100 | 0.004 | 1 | 1 | 1500 | 0.3 |
| **Forested Wetland** | 9.73 | 0.8 | 100 | 0 | 0.14 | 0.8 | 100 | 0.003 | 1 | 1 | 2500 | 1 |
| **Sparse Forest (10<50%)** | 1.54 | 0.8 | 100 | 0 | 0.275 | 0.6 | 100 | 0.007 | 1 | 1 | 2500 | 0.9 |
| **Forest (>50%)** | 2 | 0.6 | 100 | 0 | 0.25 | 0.6 | 100 | 0.009 | 1 | 1 | 3000 | 1 |
| **Shrubland** | 1.5 | 0.8 | 100 | 0 | 0.5 | 0.5 | 100 | 0.004 | 1 | 1 | 2000 | 0.8 |
| **Barren** | 3.4 | 0.1 | 100 | 0 | 0.1 | 0.6 | 100 | 1 | 1 | 0 | 0 | 0.5 |
| **Agriculture** | 10 | 0.3 | 100 | 0 | 0.99 | 0.4 | 100 | 0 24 | 0.5 | 1 | 1000 | 0.8 |
| **Orchard** | 10 | 0.8 | 100 | 0 | 0.99 | 0.5 | 100 | 0.004 | 0.5 | 1 | 2000 | 0.9 |
| **Feedlot** | 13 | 0.1 | 100 | 0 | 1.5 | 0.2 | 100 | 0 | 0.001 | 1 | 2000 | 0.8 |

*Table 18: Biophysical Table Values for InVEST Parameterization After* Fraxinus *Mortality when The Understory Condition is Shrubby and 24.85% of the Site lost Forest Cover*

| Code | Nutrient Retention Model (NDR) | | | | | | | Sediment Retention Model (SDR) | | Annual Water Yield | | |
|---|---|---|---|---|---|---|---|---|---|---|---|---|
| **Land Use** | **Nitrogen Load (kg)** | **Nitrogen Effluence** | **Critical Nitrogen Length (m)** | **Subsurface Proportion of Nitrogen** | **Phosphorous Load (kg)** | **Phosphorous Effluence** | **Critical Phosphorous Length (m)** | **USLE Cover Factor (*C*)** | **USLE Practice Factor (*P*)** | **Vegetative State** | **Root Depth (mm)** | **$K_c$** |
| **Null** | 0 | 0 | 0 | 0 | 0 | 0 | 0 | 0 | 0 | 0 | 0 | 0 |
| **Urban** | 12.876 | 0.150 | 100 | 0 | 1.562 | 0.175 | 100 | 0 | 0.001 | 0 | 0 | 0.790 |
| **Rural** | 6.376 | 0.250 | 100 | 0 | 1.062 | 0.375 | 100 | 0.039 | 0.001 | 1 | 1752 | 0.850 |
| **Water** | 0 | 0.050 | 100 | 0 | 0.062 | 0 | 100 | 0 | 1 | 0 | 0 | 1.200 |
| **Wetland** | 9.606 | 0.850 | 100 | 0 | 0.202 | 0.775 | 100 | 0.003 | 1 | 1 | 1252 | 0.250 |
| **Forested Wetland** | 9.606 | 0.850 | 100 | 0 | 0.202 | 0.775 | 100 | 0.002 | 1 | 1 | 2252 | 0.950 |
| **Sparse Forest (10<50%)** | 1.416 | 0.850 | 100 | 0 | 0.337 | 0.575 | 100 | 0.006 | 1 | 1 | 2252 | 0.850 |
| **Forest (>50%)** | 1.876 | 0.650 | 100 | 0 | 0.312 | 0.575 | 100 | 0.008 | 1 | 1 | 2752 | 0.950 |
| **Shrubland** | 1.376 | 0.850 | 100 | 0 | 0.562 | 0.475 | 100 | 0.003 | 1 | 1 | 1752 | 0.750 |
| **Barren** | 3.276 | 0.150 | 100 | 0 | 0.162 | 0.575 | 100 | 1.000 | 1 | 0 | 0 | 0.450 |
| **Agriculture** | 9.876 | 0.350 | 100 | 0 | 1.052 | 0.375 | 100 | 0.239 | 0.5 | 1 | 752 | 0.750 |
| **Orchard** | 9.876 | 0.850 | 100 | 0 | 1.052 | 0.475 | 100 | 0.003 | 0.5 | 1 | 1752 | 0.850 |
| **Feedlot** | 12.876 | 0.150 | 100 | 0 | 1.562 | 0.175 | 100 | 0 | 0.001 | 1 | 1752 | 0.750 |

*Table 19: Biophysical Table Values for InVEST Parameterization After* Fraxinus *Mortality when The Understory Condition is Shrubby and 4.9% of the Site lost Forest Cover*

| Code | Nutrient Retention Model (NDR) | | | | | | | Sediment Retention Model (SDR) | | Annual Water Yield | | |
|---|---|---|---|---|---|---|---|---|---|---|---|---|
| **Land Use** | **Nitrogen Load (kg)** | **Nitrogen Effluence** | **Critical Nitrogen Length (m)** | **Subsurface Proportion of Nitrogen** | **Phosphorous Load (kg)** | **Phosphorous Effluence** | **Critical Phosphorous Length (m)** | **USLE Cover Factor (*C*)** | **USLE Practice Factor (*P*)** | **Vegetative State** | **Root Depth (mm)** | **$K_c$** |
| **Null** | 0 | 0 | 0 | 0 | 0 | 0 | 0 | 0 | 0 | 0 | 0 | 0 |
| **Urban** | 12.976 | 0.110 | 100 | 0 | 1.512 | 0.195 | 100 | 0 | 0.001 | 0 | 0 | 0.830 |
| **Rural** | 6.476 | 0.210 | 100 | 0 | 1.012 | 0.395 | 100 | 0.040 | 0.001 | 1 | 1951 | 0.890 |
| **Water** | 0 | 0.010 | 100 | 0 | 0.012 | 0 | 100 | 0 | 1 | 0 | 0 | 1.240 |
| **Wetland** | 9.706 | 0.810 | 100 | 0 | 0.152 | 0.795 | 100 | 0.004 | 1 | 1 | 1451 | 0.290 |
| **Forested Wetland** | 9.706 | 0.810 | 100 | 0 | 0.152 | 0.795 | 100 | 0.003 | 1 | 1 | 2451 | 0.990 |
| **Sparse Forest (10<50%)** | 1.516 | 0.810 | 100 | 0 | 0.287 | 0.595 | 100 | 0.007 | 1 | 1 | 2451 | 0.890 |
| **Forest (>50%)** | 1.976 | 0.610 | 100 | 0 | 0.262 | 0.595 | 100 | 0.009 | 1 | 1 | 2951 | 0.990 |
| **Shrubland** | 1.476 | 0.810 | 100 | 0 | 0.512 | 0.495 | 100 | 0.004 | 1 | 1 | 1951 | 0.790 |
| **Barren** | 3.376 | 0.110 | 100 | 0 | 0.112 | 0.595 | 100 | 1.000 | 1 | 0 | 0 | 0.490 |
| **Agriculture** | 9.976 | 0.310 | 100 | 0 | 1.002 | 0.395 | 100 | 0.240 | 0.5 | 1 | 951 | 0.790 |
| **Orchard** | 9.976 | 0.810 | 100 | 0 | 1.002 | 0.495 | 100 | 0.004 | 0.5 | 1 | 1951 | 0.890 |
| **Feedlot** | 12.976 | 0.110 | 100 | 0 | 1.512 | 0.195 | 100 | 0 | 0.001 | 1 | 1951 | 0.790 |

*Table 20: Biophysical Table Values for InVEST Parameterization After* Fraxinus *Mortality when The Understory Condition is Shrubby and 2.6% of the Site lost Forest Cover*

| Code | Nutrient Retention Model (NDR) | | | | | | | Sediment Retention Model (SDR) | | Annual Water Yield | | |
|---|---|---|---|---|---|---|---|---|---|---|---|---|
| **Land Use** | **Nitrogen Load (kg)** | **Nitrogen Effluence** | **Critical Nitrogen Length (m)** | **Subsurface Proportion of Nitrogen** | **Phosphorous Load (kg)** | **Phosphorous Effluence** | **Critical Phosphorous Length (m)** | **USLE Cover Factor (*C*)** | **USLE Practice Factor (*P*)** | **Vegetative State** | **Root Depth (mm)** | **$K_c$** |
| **Null** | 0 | 0 | 0 | 0 | 0 | 0 | 0 | 0 | 0 | 0 | 0 | 0 |
| **Urban** | 12.987 | 0.105 | 100 | 0 | 1.507 | 0.197 | 100 | 0 | 0.001 | 0 | 0 | 0.835 |
| **Rural** | 6.487 | 0.205 | 100 | 0 | 1.007 | 0.397 | 100 | 0.040 | 0.001 | 1 | 1974 | 0.895 |
| **Water** | 0 | 0.005 | 100 | 0 | 0.007 | 0 | 100 | 0 | 1 | 0 | 0 | 1.245 |
| **Wetland** | 9.717 | 0.805 | 100 | 0 | 0.147 | 0.797 | 100 | 0.004 | 1 | 1 | 1474 | 0.295 |
| **Forested Wetland** | 9.717 | 0.805 | 100 | 0 | 0.147 | 0.797 | 100 | 0.003 | 1 | 1 | 2474 | 0.995 |
| **Sparse Forest (10<50%)** | 1.527 | 0.805 | 100 | 0 | 0.282 | 0.597 | 100 | 0.007 | 1 | 1 | 2474 | 0.895 |
| **Forest (>50%)** | 1.987 | 0.605 | 100 | 0 | 0.257 | 0.597 | 100 | 0.009 | 1 | 1 | 2974 | 0.995 |
| **Shrubland** | 1.487 | 0.805 | 100 | 0 | 0.507 | 0.497 | 100 | 0.004 | 1 | 1 | 1974 | 0.795 |
| **Barren** | 3.387 | 0.105 | 100 | 0 | 0.107 | 0.597 | 100 | 1.000 | 1 | 0 | 0 | 0.495 |
| **Agriculture** | 9.987 | 0.305 | 100 | 0 | 0.997 | 0.397 | 100 | 0.240 | 0.5 | 1 | 974 | 0.795 |
| **Orchard** | 9.987 | 0.805 | 100 | 0 | 0.997 | 0.497 | 100 | 0.004 | 0.5 | 1 | 1974 | 0.895 |
| **Feedlot** | 12.987 | 0.105 | 100 | 0 | 1.507 | 0.197 | 100 | 0 | 0.001 | 1 | 1974 | 0.795 |

*Table 21: Biophysical Table Values for InVEST Parameterization After* Fraxinus *Mortality when The Understory Condition is Shrubby and 0.75% of the Site lost Forest Cover*

| Code | Nutrient Retention Model (NDR) | | | | | | | Sediment Retention Model (SDR) | | Annual Water Yield | | |
|---|---|---|---|---|---|---|---|---|---|---|---|---|
| **Land Use** | **Nitrogen Load (kg)** | **Nitrogen Effluence** | **Critical Nitrogen Length (m)** | **Subsurface Proportion of Nitrogen** | **Phosphorous Load (kg)** | **Phosphorous Effluence** | **Critical Phosphorous Length (m)** | **USLE Cover Factor (*C*)** | **USLE Practice Factor (*P*)** | **Vegetative State** | **Root Depth (mm)** | **$K_c$** |
| **Null** | 0 | 0 | 0 | 0 | 0 | 0 | 0 | 0 | 0 | 0 | 0 | 0 |
| **Urban** | 12.996 | 0.102 | 100 | 0 | 1.502 | 0.199 | 100 | 0 | 0.001 | 0 | 0 | 0.839 |
| **Rural** | 6.496 | 0.202 | 100 | 0 | 1.002 | 0.399 | 100 | 0.040 | 0.001 | 1 | 1993 | 0.899 |
| **Water** | 0 | 0.002 | 100 | 0 | 0.002 | 0 | 100 | 0 | 1 | 0 | 0 | 1.249 |
| **Wetland** | 9.726 | 0.802 | 100 | 0 | 0.142 | 0.799 | 100 | 0.004 | 1 | 1 | 1493 | 0.299 |
| **Forested Wetland** | 9.726 | 0.802 | 100 | 0 | 0.142 | 0.799 | 100 | 0.003 | 1 | 1 | 2493 | 0.999 |
| **Sparse Forest (10<50%)** | 1.536 | 0.802 | 100 | 0 | 0.277 | 0.599 | 100 | 0.007 | 1 | 1 | 2493 | 0.899 |
| **Forest (>50%)** | 1.996 | 0.602 | 100 | 0 | 0.252 | 0.599 | 100 | 0.009 | 1 | 1 | 2993 | 0.999 |
| **Shrubland** | 1.496 | 0.802 | 100 | 0 | 0.502 | 0.499 | 100 | 0.004 | 1 | 1 | 1993 | 0.799 |
| **Barren** | 3.396 | 0.102 | 100 | 0 | 0.102 | 0.599 | 100 | 1.000 | 1 | 0 | 0 | 0.499 |
| **Agriculture** | 9.996 | 0.302 | 100 | 0 | 0.992 | 0.399 | 100 | 0.240 | 0.5 | 1 | 993 | 0.799 |
| **Orchard** | 9.996 | 0.802 | 100 | 0 | 0.992 | 0.499 | 100 | 0.004 | 0.5 | 1 | 1993 | 0.899 |
| **Feedlot** | 12.996 | 0.102 | 100 | 0 | 1.502 | 0.199 | 100 | 0 | 0.001 | 1 | 1993 | 0.799 |

*Table 22: Biophysical Table Values for InVEST Parameterization After* Fraxinus *Mortality when The Understory Condition is Barren and 24.85% of the Site lost Forest Cover*

| Code | Nutrient Retention Model (NDR) | | | | | | | Sediment Retention Model (SDR) | | Annual Water Yield | | |
|---|---|---|---|---|---|---|---|---|---|---|---|---|
| **Land Use** | **Nitrogen Load (kg)** | **Nitrogen Effluence** | **Critical Nitrogen Length (m)** | **Subsurface Proportion of Nitrogen** | **Phosphorous Load (kg)** | **Phosphorous Effluence** | **Critical Phosphorous Length (m)** | **USLE Cover Factor (*C*)** | **USLE Practice Factor (*P*)** | **Vegetative State** | **Root Depth (mm)** | **$K_c$** |
| **Null** | 0 | 0 | 0 | 0 | 0 | 0 | 0 | 0 | 0 | 0 | 0 | 0 |
| **Urban** | 13.348 | 0 | 100 | 0 | 1.463 | 0.2 | 100 | 0.246 | 0.001 | 0 | 0 | 0.716 |
| **Rural** | 6.848 | 0.076 | 100 | 0 | 0.963 | 0.4 | 100 | 0.286 | 0.001 | 1 | 1255 | 0.776 |
| **Water** | 0.348 | 0 | 100 | 0 | 0 | 0 | 100 | 0.246 | 1 | 0 | 0 | 1.126 |
| **Wetland** | 10.078 | 0.676 | 100 | 0 | 0.103 | 0.8 | 100 | 0.250 | 1 | 1 | 755 | 0.176 |
| **Forested Wetland** | 10.078 | 0.676 | 100 | 0 | 0.103 | 0.8 | 100 | 0.249 | 1 | 1 | 1755 | 0.876 |
| **Sparse Forest (10<50%)** | 1.888 | 0.676 | 100 | 0 | 0.233 | 0.6 | 100 | 0.253 | 1 | 1 | 1755 | 0.776 |
| **Forest (>50%)** | 2.348 | 0.476 | 100 | 0 | 0.213 | 0.6 | 100 | 0.255 | 1 | 1 | 2255 | 0.876 |
| **Shrubland** | 1.848 | 0.676 | 100 | 0 | 0.463 | 0.5 | 100 | 0.250 | 1 | 1 | 1255 | 0.676 |
| **Barren** | 3.748 | 0 | 100 | 0 | 0.063 | 0.6 | 100 | 1 | 1 | 0 | 0 | 0.376 |
| **Agriculture** | 10.348 | 0.176 | 100 | 0 | 0.953 | 0.4 | 100 | 0.486 | 0.5 | 1 | 255 | 0.676 |
| **Orchard** | 10.348 | 0.676 | 100 | 0 | 0.953 | 0.5 | 100 | 0.250 | 0.5 | 1 | 1255 | 0.776 |
| **Feedlot** | 13.348 | 0 | 100 | 0 | 1.463 | 0.2 | 100 | 0.246 | 0.001 | 1 | 1255 | 0.676 |

*Table 23: Biophysical Table Values for InVEST Parameterization After* Fraxinus *Mortality when The Understory Condition is Barren and 4.9% of the Site lost Forest Cover*

| Code | Nutrient Retention Model (NDR) | | | | | | | Sediment Retention Model (SDR) | | Annual Water Yield | | |
|---|---|---|---|---|---|---|---|---|---|---|---|---|
| **Land Use** | **Nitrogen Load (kg)** | **Nitrogen Effluence** | **Critical Nitrogen Length (m)** | **Subsurface Proportion of Nitrogen** | **Phosphorous Load (kg)** | **Phosphorous Effluence** | **Critical Phosphorous Length (m)** | **USLE Cover Factor (*C*)** | **USLE Practice Factor (*P*)** | **Vegetative State** | **Root Depth (mm)** | **$K_c$** |
| **Null** | 0 | 0 | 0 | 0 | 0 | 0 | 0 | 0 | 0 | 0 | 0 | 0 |
| **Urban** | 13.067 | 0.076 | 100 | 0 | 1.493 | 0.2 | 100 | 0.049 | 0.001 | 0 | 0 | 0.812 |
| **Rural** | 6.567 | 0.176 | 100 | 0 | 0.993 | 0.4 | 100 | 0.089 | 0.001 | 1 | 1853 | 0.876 |
| **Water** | 0.067 | 0 | 100 | 0 | 0 | 0 | 100 | 0.049 | 1 | 0 | 0 | 1.226 |
| **Wetland** | 9.797 | 0.776 | 100 | 0 | 0.133 | 0.8 | 100 | 0.053 | 1 | 1 | 1353 | 0.276 |
| **Forested Wetland** | 9.797 | 0.776 | 100 | 0 | 0.133 | 0.8 | 100 | 0.052 | 1 | 1 | 2353 | 0.976 |
| **Sparse Forest (10<50%)** | 1.607 | 0.776 | 100 | 0 | 0.268 | 0.6 | 100 | 0.056 | 1 | 1 | 2353 | 0.876 |
| **Forest (>50%)** | 2.067 | 0.576 | 100 | 0 | 0.243 | 0.6 | 100 | 0.058 | 1 | 1 | 2853 | 0.976 |
| **Shrubland** | 1.567 | 0.776 | 100 | 0 | 0.493 | 0.5 | 100 | 0.053 | 1 | 1 | 1853 | 0.776 |
| **Barren** | 3.467 | 0.076 | 100 | 0 | 0.093 | 0.6 | 100 | 1 | 1 | 0 | 0 | 0.476 |
| **Agriculture** | 10.067 | 0.276 | 100 | 0 | 0.983 | 0.4 | 100 | 0.289 | 0.5 | 1 | 853 | 0.776 |
| **Orchard** | 10.067 | 0.776 | 100 | 0 | 0.983 | 0.5 | 100 | 0.053 | 0.5 | 1 | 1853 | 0.876 |
| **Feedlot** | 13.067 | 0.076 | 100 | 0 | 1.493 | 0.2 | 100 | 0.049 | 0.001 | 1 | 1853 | 0.776 |

*Table 24: Biophysical Table Values for InVEST Parameterization After* Fraxinus *Mortality when The Understory Condition is Barren and 2.6% of the Site lost Forest Cover*

| Code | Nutrient Retention Model (NDR) | | | | | | | Sediment Retention Model (SDR) | | Annual Water Yield | | |
|---|---|---|---|---|---|---|---|---|---|---|---|---|
| **Land Use** | **Nitrogen Load (kg)** | **Nitrogen Effluence** | **Critical Nitrogen Length (m)** | **Subsurface Proportion of Nitrogen** | **Phosphorous Load (kg)** | **Phosphorous Effluence** | **Critical Phosphorous Length (m)** | **USLE Cover Factor (*C*)** | **USLE Practice Factor (*P*)** | **Vegetative State** | **Root Depth (mm)** | **$K_c$** |
| **Null** | 0 | 0 | 0 | 0 | 0 | 0 | 0 | 0 | 0 | 0 | 0 | 0 |
| **Urban** | 13.036 | 0.087 | 100 | 0 | 1.496 | 0.2 | 100 | 0.026 | 0.001 | 0 | 0 | 0.827 |
| **Rural** | 6.536 | 0.187 | 100 | 0 | 0.996 | 0.4 | 100 | 0.066 | 0.001 | 1 | 1922 | 0.887 |
| **Water** | 0.036 | 0 | 100 | 0 | 0 | 0 | 100 | 0.026 | 1 | 0 | 0 | 1.237 |
| **Wetland** | 9.766 | 0.787 | 100 | 0 | 0.136 | 0.8 | 100 | 0.030 | 1 | 1 | 1422 | 0.287 |
| **Forested Wetland** | 9.766 | 0.787 | 100 | 0 | 0.136 | 0.8 | 100 | 0.029 | 1 | 1 | 2422 | 0.987 |
| **Sparse Forest (10<50%)** | 1.576 | 0.787 | 100 | 0 | 0.271 | 0.6 | 100 | 0.033 | 1 | 1 | 2422 | 0.887 |
| **Forest (>50%)** | 2.036 | 0.587 | 100 | 0 | 0.246 | 0.6 | 100 | 0.035 | 1 | 1 | 2922 | 0.987 |
| **Shrubland** | 1.536 | 0.787 | 100 | 0 | 0.496 | 0.5 | 100 | 0.030 | 1 | 1 | 1922 | 0.787 |
| **Barren** | 3.436 | 0.087 | 100 | 0 | 0.096 | 0.6 | 100 | 1 | 1 | 0 | 0 | 0.487 |
| **Agriculture** | 10.036 | 0.287 | 100 | 0 | 0.986 | 0.4 | 100 | 0.266 | 0.5 | 1 | 922 | 0.787 |
| **Orchard** | 10.036 | 0.787 | 100 | 0 | 0.986 | 0.5 | 100 | 0.030 | 0.5 | 1 | 1922 | 0.887 |
| **Feedlot** | 13.036 | 0.087 | 100 | 0 | 1.496 | 0.2 | 100 | 0.026 | 0.001 | 1 | 1922 | 0.787 |

*Table 25: Biophysical Table Values for InVEST Parameterization After* Fraxinus *Mortality when The Understory Condition is Barren and 0.75% of the Site lost Forest Cover*

| Code | Nutrient Retention Model (NDR) | | | | | | | Sediment Retention Model (SDR) | | Annual Water Yield | | |
|---|---|---|---|---|---|---|---|---|---|---|---|---|
| **Land Use** | **Nitrogen Load (kg)** | **Nitrogen Effluence** | **Critical Nitrogen Length (m)** | **Subsurface Proportion of Nitrogen** | **Phosphorous Load (kg)** | **Phosphorous Effluence** | **Critical Phosphorous Length (m)** | **USLE Cover Factor (*C*)** | **USLE Practice Factor (*P*)** | **Vegetative State** | **Root Depth (mm)** | **$K_c$** |
| **Null** | 0 | 0 | 0 | 0 | 0 | 0 | 0 | 0 | 0 | 0 | 0 | 0 |
| **Urban** | 13.011 | 0.096 | 100 | 0 | 1.499 | 0.2 | 100 | 0.007 | 0.001 | 0 | 0 | 0.836 |
| **Rural** | 6.511 | 0.196 | 100 | 0 | 0.999 | 0.4 | 100 | 0.047 | 0.001 | 1 | 1978 | 0.896 |
| **Water** | 0.011 | 0 | 100 | 0 | 0 | 0 | 100 | 0.007 | 1 | 0 | 0 | 1.246 |
| **Wetland** | 9.741 | 0.796 | 100 | 0 | 0.139 | 0.8 | 100 | 0.011 | 1 | 1 | 1478 | 0.296 |
| **Forested Wetland** | 9.741 | 0.796 | 100 | 0 | 0.139 | 0.8 | 100 | 0.010 | 1 | 1 | 2478 | 0.996 |
| **Sparse Forest (10<50%)** | 1.551 | 0.796 | 100 | 0 | 0.274 | 0.6 | 100 | 0.014 | 1 | 1 | 2478 | 0.896 |
| **Forest (>50%)** | 2.011 | 0.596 | 100 | 0 | 0.249 | 0.6 | 100 | 0.016 | 1 | 1 | 2978 | 0.996 |
| **Shrubland** | 1.511 | 0.796 | 100 | 0 | 0.499 | 0.5 | 100 | 0.011 | 1 | 1 | 1978 | 0.796 |
| **Barren** | 3.411 | 0.096 | 100 | 0 | 0.099 | 0.6 | 100 | 1 | 1 | 0 | 0 | 0.496 |
| **Agriculture** | 10.011 | 0.296 | 100 | 0 | 0.989 | 0.4 | 100 | 0.247 | 0.5 | 1 | 978 | 0.796 |
| **Orchard** | 10.011 | 0.796 | 100 | 0 | 0.989 | 0.5 | 100 | 0.011 | 0.5 | 1 | 1978 | 0.896 |
| **Feedlot** | 13.011 | 0.096 | 100 | 0 | 1.499 | 0.2 | 100 | 0.007 | 0.001 | 1 | 1978 | 0.796 |

### 3.1 Seasonal Water Yield Figures and Tables

Seasonal Water Yield was also completed in the course of the study to check on the impacts to watershed recharge rates and quickflow (QF) during storm events. We found that the results backed up the results found for sedimentation discussed in Chapter 4. QF dramatically increased under barren site conditions and only moderately so under shrubby conditions, which would likely lead to increased storm surge and sedimentation. Recharge rates were similar with stable conditions when the understory was shrubby but increased dramatically in the Eastern section of the study area under barren site conditions. Input sources for the seasonal water yield model (Table 26) are included after the figures showing the results from the Seasonal Water Yield model (Figures 26-28), as well as the biophysical value tables for the three model runs (Tables 27-35).

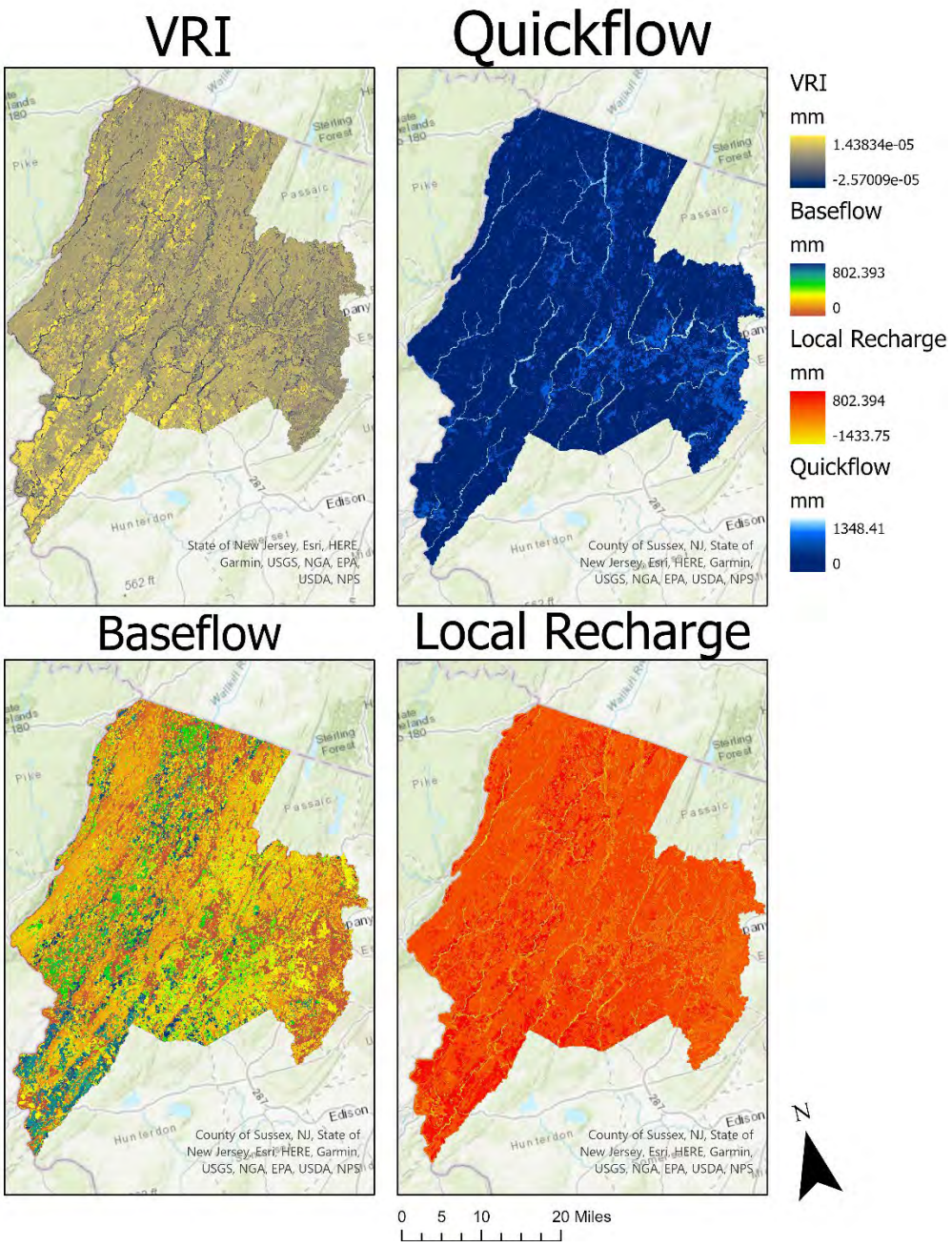


*Figure 26: Seasonal Water Yield Results with Base parameterizations. VRI is a measure of impact on recharge that can either be positive or negative, which is contrasted with Local Recharge, which is calculated on a pixel by pixel basis. Quickflow (QF) indicates the amount of rain water that will run off the surface quickly in the event of a normal rain event in the space, while baseflow indicates the amount of water from each pixel that reaches a stream or other waterbody.*

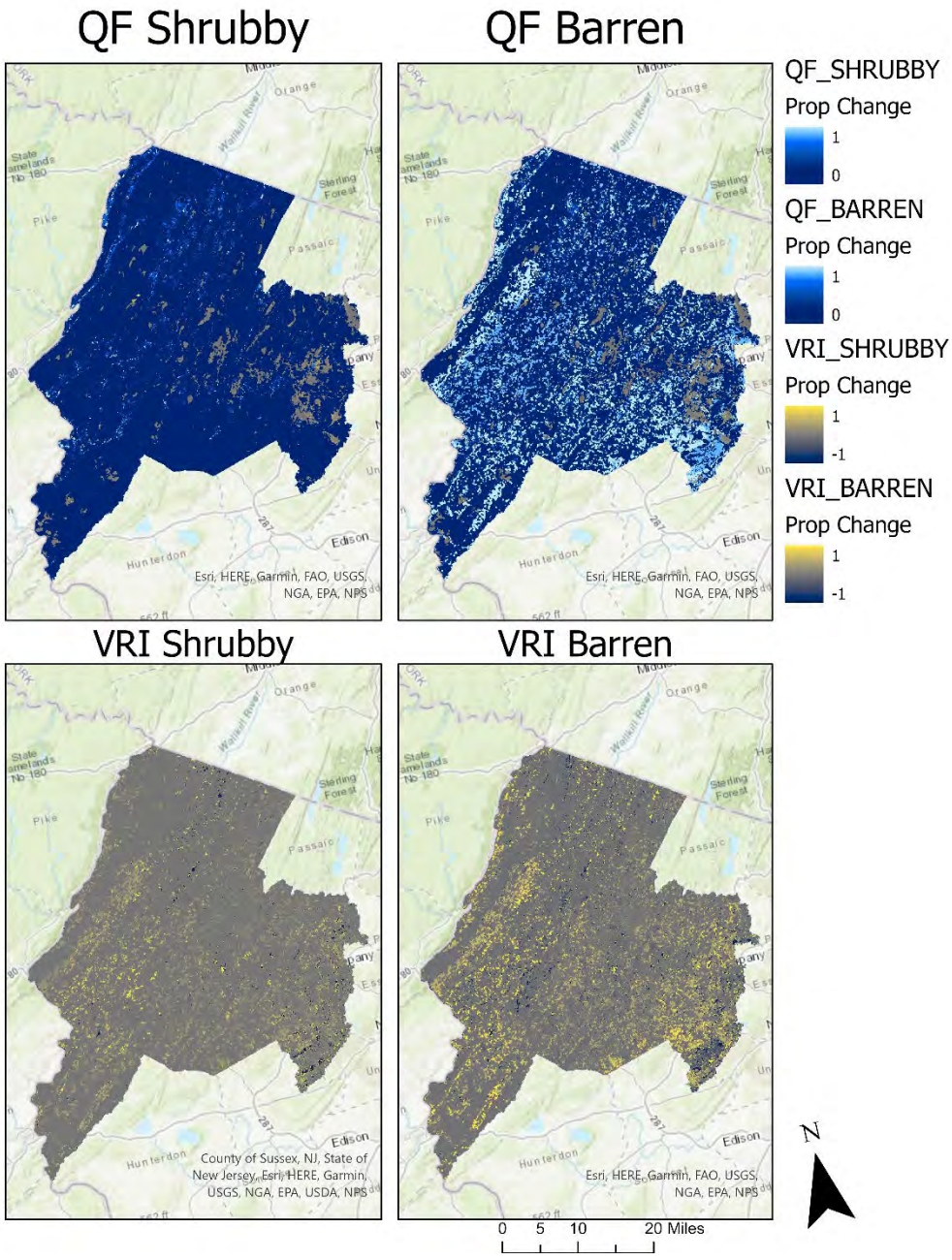


*Figure 27: Proportional Change to Quickflow (QF) and VRI, Map of the values of recharge contribution, positive or negative, to the total recharge. Quickflow is significantly greater under barren site conditions. However, the contribution to recharge rate is more difficult to see in this map, as there are both significant positive and negative changes across the landscape.*

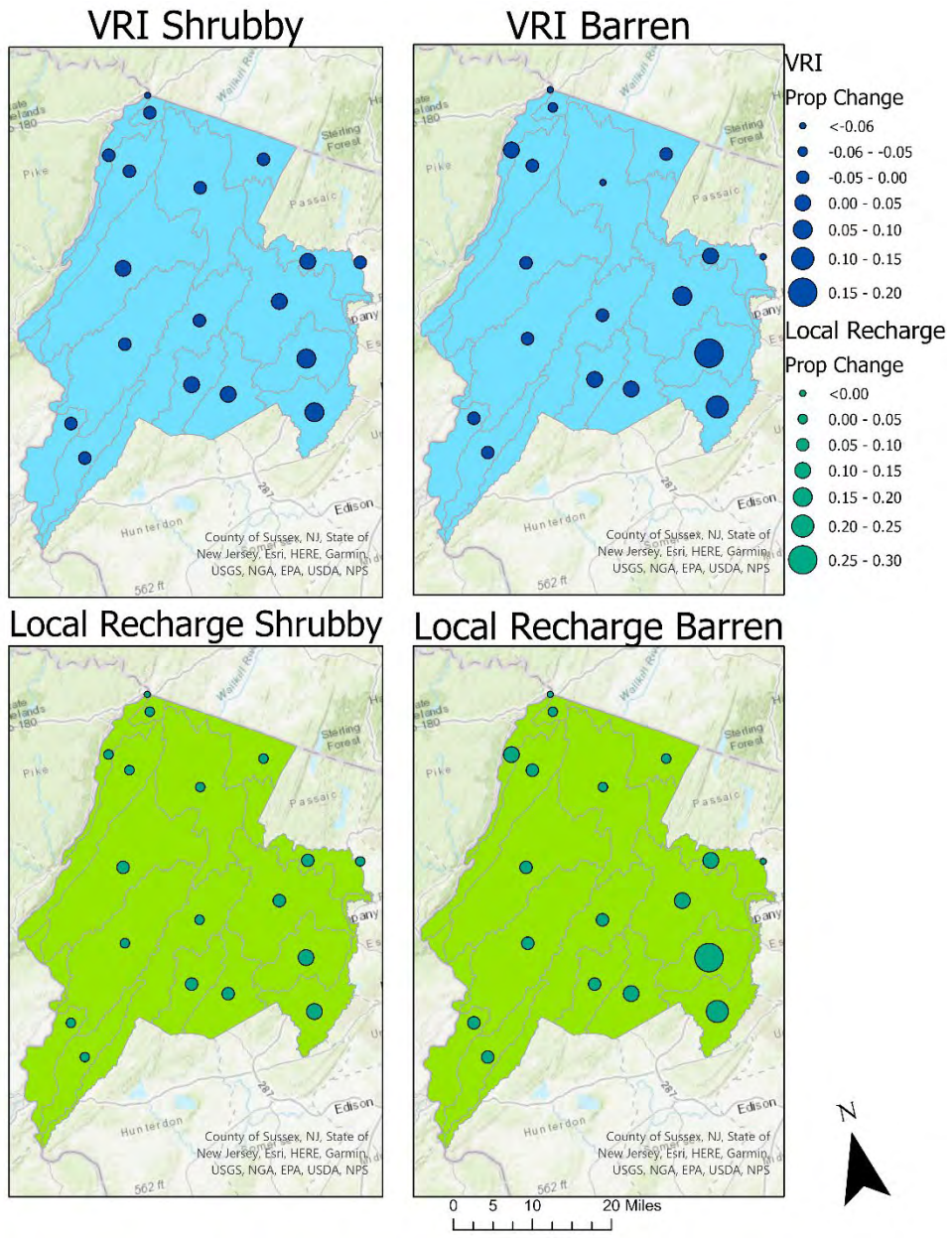


*Figure 28: Proportional change to VRI and Local recharge displayed by sub-watershed. Using the summed polygons of the VRI and Local Recharge rates we can see that the impact to recharge rates is outsized in the Eastern section of the study area. This is pronounced especially for the barren site values, but there is a small increase under shrubby conditions as well.*

*Table 26: Summary of Spatial and Single Factor Inputs for InVEST Seasonal Water Yield Model*

| INPUTS: | DEFINITION | SOURCE |
|---|---|---|
| **LAND USE LAND COVER RASTER (LULC)** | Land use of the study area as it exists now with estimated carbon pools | (New Jersey Department of Environmental Protection (NJDEP) et al , 2019) |
| **EXPERIMENTAL LULC RASTER** | Same LULC Base, but with Decreased Forest defined by Quantiles | (New Jersey Department of Environmental Protection (NJDEP) et al , 2019; Wilson et al , 2012) |
| **PRECIPITATION RASTER** | Average Millimeters of monthly precipitation | (PRISM Climate Group at Oregon State University, 2022) |
| **WATERSHEDS AND SUBWATERSHEDS SHAPEFILE** | Shapefile of the huc-12 watershed designations from the USGS | (New Jersey Department of Environmental Protection (NJDEP) & New Jersey Geological Survey (NJGS), 2009) |
| **EVAPOTRANSPORTATION ($ET_0$)** | Measure of evaporation due to LULC | (Zomer & Trabucco, 2022) |
| **SOIL HYDROLOGIC GROUP** | Level of compaction and general make up of local soils from SSURGO soils database | (Natural Resources Conservation Service, 2021b) |
| **CURVE NUMBER FOR SOIL GROUPS** | Measure of soil response to water under each different LULC | (Natural Resources Conservation Service, 1986) |
| **KC VALUES FOR EACH MONTH** | Cover factors for the study area Dependent on LULC and time of year from FAO tables | (Allen & Food and Agriculture Organization of the United Nations, 1998) |
| **RAIN EVENTS TABLE** | Number of Rain Events by Month Average for the Study Area | (National Centers for Environmental Information, 2021) |
| **THRESHOLD FLOW ACCUMULATION VALUE** | 1000 Default Value and like that calculated using GIS software | Number of connected pixels to define a stream |
| **ALPHA M PARAMETER** | 1/12 | InVEST Default |
| **BETA I PARAMETER** | 1 | InVEST Default |
| **GAMMA PARAMETER** | 1 | InVEST Default |

*Table 27: Biophysical Table Values for InVEST Parameterization for Seasonal Water Yield. Curve Numbers A-D refer to soil types and Kc 1-12 refers to the monthly cover factors for each site.*

| Land Use | Curve Number A | Curve Number B | Curve Number C | Curve Number D | $K_c$_1 | $K_c$_2 | $K_c$_3 | $K_c$_4 | $K_c$_5 | $K_c$_6 | $K_c$_7 | $K_c$_8 | $K_c$_9 | $K_c$_10 | $K_c$_11 | $K_c$_12 |
|---|---|---|---|---|---|---|---|---|---|---|---|---|---|---|---|---|
| **Null** | 0 | 0 | 0 | 0 | 0.000 | 0.000 | 0.000 | 0.000 | 0.000 | 0.000 | 0.000 | 0.000 | 0.000 | 0.000 | 0.000 | 0.000 |
| **Urban** | 98 | 98 | 98 | 98 | 0.000 | 0.000 | 0.000 | 0.000 | 0.000 | 0.000 | 0.000 | 0.000 | 0.000 | 0.000 | 0.000 | 0.000 |
| **Rural** | 46 | 65 | 77 | 82 | 0.840 | 0.840 | 0.840 | 0.840 | 0.840 | 0.840 | 0.840 | 0.840 | 0.840 | 0.840 | 0.840 | 0.840 |
| **Water** | 98 | 98 | 98 | 98 | 0.900 | 0.900 | 0.900 | 0.900 | 0.900 | 0.900 | 0.900 | 0.900 | 0.900 | 0.900 | 0.900 | 0.900 |
| **Wetland** | 98 | 98 | 98 | 98 | 1.250 | 1.250 | 1.250 | 1.250 | 1.250 | 1.250 | 1.250 | 1.250 | 1.250 | 1.250 | 1.250 | 1.250 |
| **Forested Wetland** | 82 | 82 | 82 | 86 | 0.133 | 0.133 | 0.133 | 0.133 | 0.533 | 0.533 | 0.533 | 0.533 | 0.533 | 0.133 | 0.133 | 0.133 |
| **Sparse Forest (10<50%)** | 45 | 66 | 77 | 83 | 0.789 | 0.789 | 0.789 | 0.789 | 1.296 | 1.296 | 1.296 | 1.296 | 1.296 | 0.789 | 0.789 | 0.789 |
| **Forest (>50%)** | 30 | 55 | 70 | 77 | 0.704 | 0.704 | 0.704 | 0.704 | 1.174 | 1.174 | 1.174 | 1.174 | 1.174 | 0.704 | 0.704 | 0.704 |
| **Shrubland** | 35 | 56 | 70 | 77 | 0.846 | 0.846 | 0.846 | 0.846 | 1.216 | 1.216 | 1.216 | 1.216 | 1.216 | 0.846 | 0.846 | 0.846 |
| **Barren** | 77 | 86 | 91 | 94 | 0.677 | 0.677 | 0.677 | 0.677 | 0.973 | 0.973 | 0.973 | 0.973 | 0.973 | 0.677 | 0.677 | 0.677 |
| **Agriculture** | 67 | 78 | 85 | 89 | 0.500 | 0.500 | 0.500 | 0.500 | 0.500 | 0.500 | 0.500 | 0.500 | 0.500 | 0.500 | 0.500 | 0.500 |
| **Orchard** | 32 | 58 | 72 | 79 | 0.440 | 0.440 | 0.440 | 0.440 | 0.440 | 0.879 | 1.670 | 1.811 | 1.723 | 0.440 | 0.440 | 0.440 |
| **Feedlot** | 59 | 74 | 82 | 86 | 0.614 | 0.614 | 0.614 | 0.614 | 0.920 | 1.227 | 1.227 | 1.350 | 1.350 | 1.043 | 0.614 | 0.614 |

*Table 28: Biophysical Table Values for InVEST Parameterization for Seasonal Water Yield when the condition is shrubby and the Forest loss is 24.5%. Curve Numbers A-D refer to soil types and Kc 1-12 refers to the monthly cover factors for each site.*

| Land Use | Curve Number A | Curve Number B | Curve Number C | Curve Number D | $K_c$_1 | $K_c$_2 | $K_c$_3 | $K_c$_4 | $K_c$_5 | $K_c$_6 | $K_c$_7 | $K_c$_8 | $K_c$_9 | $K_c$_10 | $K_c$_11 | $K_c$_12 |
|---|---|---|---|---|---|---|---|---|---|---|---|---|---|---|---|---|
| Null | 98 | 98 | 98 | 98 | 0.800 | 0.800 | 0.800 | 0.800 | 0.800 | 0.800 | 0.800 | 0.800 | 0.800 | 0.800 | 0.800 | 0.800 |
| Urban | 48 | 66 | 77 | 82 | 0.880 | 0.880 | 0.880 | 0.880 | 0.860 | 0.860 | 0.860 | 0.860 | 0.860 | 0.880 | 0.880 | 0.880 |
| Rural | 98 | 98 | 98 | 98 | 0.940 | 0.940 | 0.940 | 0.940 | 0.920 | 0.920 | 0.920 | 0.920 | 0.920 | 0.940 | 0.940 | 0.940 |
| Water | 98 | 98 | 98 | 98 | 1.290 | 1.290 | 1.290 | 1.290 | 1.270 | 1.270 | 1.270 | 1.270 | 1.270 | 1.290 | 1.290 | 1.290 |
| Wetland | 84 | 83 | 82 | 86 | 0.170 | 0.170 | 0.170 | 0.170 | 0.550 | 0.550 | 0.550 | 0.550 | 0.550 | 0.170 | 0.170 | 0.170 |
| Forested Wetland | 47 | 67 | 77 | 83 | 0.830 | 0.830 | 0.830 | 0.830 | 1.310 | 1.310 | 1.310 | 1.310 | 1.310 | 0.830 | 0.830 | 0.830 |
| Sparse Forest (10<50%) | 32 | 56 | 70 | 77 | 0.740 | 0.740 | 0.740 | 0.740 | 1.190 | 1.190 | 1.190 | 1.190 | 1.190 | 0.740 | 0.740 | 0.740 |
| Forest (>50%) | 37 | 57 | 70 | 77 | 0.890 | 0.890 | 0.890 | 0.890 | 1.230 | 1.230 | 1.230 | 1.230 | 1.230 | 0.890 | 0.890 | 0.890 |
| Shrubland | 79 | 87 | 91 | 94 | 0.720 | 0.720 | 0.720 | 0.720 | 0.990 | 0.990 | 0.990 | 0.990 | 0.990 | 0.720 | 0.720 | 0.720 |
| Barren | 69 | 79 | 85 | 89 | 0.540 | 0.540 | 0.540 | 0.540 | 0.520 | 0.520 | 0.520 | 0.520 | 0.520 | 0.540 | 0.540 | 0.540 |
| Agriculture | 34 | 59 | 72 | 79 | 0.480 | 0.480 | 0.480 | 0.480 | 0.450 | 0.890 | 1.690 | 1.830 | 1.740 | 0.480 | 0.480 | 0.480 |
| Orchard | 61 | 75 | 82 | 86 | 0.650 | 0.650 | 0.650 | 0.650 | 0.940 | 1.240 | 1.240 | 1.370 | 1.370 | 1.080 | 0.650 | 0.650 |
| Feedlot | 98 | 98 | 98 | 98 | 0.800 | 0.800 | 0.800 | 0.800 | 0.800 | 0.800 | 0.800 | 0.800 | 0.800 | 0.800 | 0.800 | 0.800 |

*Table 29: Biophysical Table Values for InVEST Parameterization for Seasonal Water Yield when the condition is shrubby and the Forest loss is 4.9%. Curve Numbers A-D refer to soil types and Kc 1-12 refers to the monthly cover factors for each site.*

| Land Use | Curve Number A | Curve Number B | Curve Number C | Curve Number D | $K_c$_1 | $K_c$_2 | $K_c$_3 | $K_c$_4 | $K_c$_5 | $K_c$_6 | $K_c$_7 | $K_c$_8 | $K_c$_9 | $K_c$_10 | $K_c$_11 | $K_c$_12 |
|---|---|---|---|---|---|---|---|---|---|---|---|---|---|---|---|---|
| **Null** | 98 | 98 | 98 | 98 | 0.010 | 0.010 | 0.010 | 0.010 | 0.010 | 0.010 | 0.010 | 0.010 | 0.010 | 0.010 | 0.010 | 0.010 |
| **Urban** | 47 | 66 | 77 | 82 | 0.850 | 0.850 | 0.850 | 0.850 | 0.850 | 0.850 | 0.850 | 0.850 | 0.850 | 0.850 | 0.850 | 0.850 |
| **Rural** | 98 | 98 | 98 | 98 | 0.910 | 0.910 | 0.910 | 0.910 | 0.910 | 0.910 | 0.910 | 0.910 | 0.910 | 0.910 | 0.910 | 0.910 |
| **Water** | 98 | 98 | 98 | 98 | 1.260 | 1.260 | 1.260 | 1.260 | 1.260 | 1.260 | 1.260 | 1.260 | 1.260 | 1.260 | 1.260 | 1.260 |
| **Wetland** | 83 | 83 | 82 | 86 | 0.150 | 0.150 | 0.150 | 0.150 | 0.540 | 0.540 | 0.540 | 0.540 | 0.540 | 0.150 | 0.150 | 0.150 |
| **Forested Wetland** | 46 | 67 | 77 | 83 | 0.800 | 0.800 | 0.800 | 0.800 | 1.300 | 1.300 | 1.300 | 1.300 | 1.300 | 0.800 | 0.800 | 0.800 |
| **Sparse Forest (10<50%)** | 31 | 56 | 70 | 77 | 0.720 | 0.720 | 0.720 | 0.720 | 1.180 | 1.180 | 1.180 | 1.180 | 1.180 | 0.720 | 0.720 | 0.720 |
| **Forest (>50%)** | 36 | 57 | 70 | 77 | 0.860 | 0.860 | 0.860 | 0.860 | 1.220 | 1.220 | 1.220 | 1.220 | 1.220 | 0.860 | 0.860 | 0.860 |
| **Shrubland** | 78 | 87 | 91 | 94 | 0.690 | 0.690 | 0.690 | 0.690 | 0.980 | 0.980 | 0.980 | 0.980 | 0.980 | 0.690 | 0.690 | 0.690 |
| **Barren** | 68 | 79 | 85 | 89 | 0.510 | 0.510 | 0.510 | 0.510 | 0.510 | 0.510 | 0.510 | 0.510 | 0.510 | 0.510 | 0.510 | 0.510 |
| **Agriculture** | 33 | 59 | 72 | 79 | 0.450 | 0.450 | 0.450 | 0.450 | 0.450 | 0.890 | 1.680 | 1.820 | 1.730 | 0.450 | 0.450 | 0.450 |
| **Orchard** | 60 | 75 | 82 | 86 | 0.630 | 0.630 | 0.630 | 0.630 | 0.930 | 1.230 | 1.230 | 1.360 | 1.360 | 1.060 | 0.630 | 0.630 |
| **Feedlot** | 98 | 98 | 98 | 98 | 0.010 | 0.010 | 0.010 | 0.010 | 0.010 | 0.010 | 0.010 | 0.010 | 0.010 | 0.010 | 0.010 | 0.010 |

*Table 30: Biophysical Table Values for InVEST Parameterization for Seasonal Water Yield when the condition is shrubby and the Forest loss is 2.6%. Curve Numbers A-D refer to soil types and Kc 1-12 refers to the monthly cover factors for each site.*

| Land Use | Curve Number A | Curve Number B | Curve Number C | Curve Number D | $K_c$_1 | $K_c$_2 | $K_c$_3 | $K_c$_4 | $K_c$_5 | $K_c$_6 | $K_c$_7 | $K_c$_8 | $K_c$_9 | $K_c$_10 | $K_c$_11 | $K_c$_12 |
|---|---|---|---|---|---|---|---|---|---|---|---|---|---|---|---|---|
| Null | 98 | 98 | 98 | 98 | 0.010 | 0.010 | 0.010 | 0.010 | 0.010 | 0.010 | 0.010 | 0.010 | 0.010 | 0.010 | 0.010 | 0.010 |
| Urban | 47 | 66 | 77 | 82 | 0.850 | 0.850 | 0.850 | 0.850 | 0.850 | 0.850 | 0.850 | 0.850 | 0.850 | 0.850 | 0.850 | 0.850 |
| Rural | 98 | 98 | 98 | 98 | 0.910 | 0.910 | 0.910 | 0.910 | 0.910 | 0.910 | 0.910 | 0.910 | 0.910 | 0.910 | 0.910 | 0.910 |
| Water | 98 | 98 | 98 | 98 | 1.260 | 1.260 | 1.260 | 1.260 | 1.260 | 1.260 | 1.260 | 1.260 | 1.260 | 1.260 | 1.260 | 1.260 |
| Wetland | 83 | 83 | 82 | 86 | 0.140 | 0.140 | 0.140 | 0.140 | 0.540 | 0.540 | 0.540 | 0.540 | 0.540 | 0.140 | 0.140 | 0.140 |
| Forested Wetland | 46 | 67 | 77 | 83 | 0.800 | 0.800 | 0.800 | 0.800 | 1.300 | 1.300 | 1.300 | 1.300 | 1.300 | 0.800 | 0.800 | 0.800 |
| Sparse Forest (10<50%) | 31 | 56 | 70 | 77 | 0.710 | 0.710 | 0.710 | 0.710 | 1.180 | 1.180 | 1.180 | 1.180 | 1.180 | 0.710 | 0.710 | 0.710 |
| Forest (>50%) | 36 | 57 | 70 | 77 | 0.850 | 0.850 | 0.850 | 0.850 | 1.220 | 1.220 | 1.220 | 1.220 | 1.220 | 0.850 | 0.850 | 0.850 |
| Shrubland | 78 | 87 | 91 | 94 | 0.690 | 0.690 | 0.690 | 0.690 | 0.980 | 0.980 | 0.980 | 0.980 | 0.980 | 0.690 | 0.690 | 0.690 |
| Barren | 68 | 79 | 85 | 89 | 0.510 | 0.510 | 0.510 | 0.510 | 0.510 | 0.510 | 0.510 | 0.510 | 0.510 | 0.510 | 0.510 | 0.510 |
| Agriculture | 33 | 59 | 72 | 79 | 0.450 | 0.450 | 0.450 | 0.450 | 0.450 | 0.890 | 1.680 | 1.820 | 1.730 | 0.450 | 0.450 | 0.450 |
| Orchard | 60 | 75 | 82 | 86 | 0.620 | 0.620 | 0.620 | 0.620 | 0.930 | 1.230 | 1.230 | 1.360 | 1.360 | 1.050 | 0.620 | 0.620 |
| Feedlot | 98 | 98 | 98 | 98 | 0.010 | 0.010 | 0.010 | 0.010 | 0.010 | 0.010 | 0.010 | 0.010 | 0.010 | 0.010 | 0.010 | 0.010 |

*Table 31: Biophysical Table Values for InVEST Parameterization for Seasonal Water Yield when the condition is shrubby and the Forest loss is 0.75%. Curve Numbers A-D refer to soil types and Kc 1-12 refers to the monthly cover factors for each site.*

| Land Use | Curve Number A | Curve Number B | Curve Number C | Curve Number D | $K_c$_1 | $K_c$_2 | $K_c$_3 | $K_c$_4 | $K_c$_5 | $K_c$_6 | $K_c$_7 | $K_c$_8 | $K_c$_9 | $K_c$_10 | $K_c$_11 | $K_c$_12 |
|---|---|---|---|---|---|---|---|---|---|---|---|---|---|---|---|---|
| Null | 98 | 98 | 98 | 98 | 0.010 | 0.010 | 0.010 | 0.010 | 0.010 | 0.010 | 0.010 | 0.010 | 0.010 | 0.010 | 0.010 | 0.010 |
| Urban | 47 | 66 | 77 | 82 | 0.850 | 0.850 | 0.850 | 0.850 | 0.850 | 0.850 | 0.850 | 0.850 | 0.850 | 0.850 | 0.850 | 0.850 |
| Rural | 98 | 98 | 98 | 98 | 0.910 | 0.910 | 0.910 | 0.910 | 0.910 | 0.910 | 0.910 | 0.910 | 0.910 | 0.910 | 0.910 | 0.910 |
| Water | 98 | 98 | 98 | 98 | 1.260 | 1.260 | 1.260 | 1.260 | 1.260 | 1.260 | 1.260 | 1.260 | 1.260 | 1.260 | 1.260 | 1.260 |
| Wetland | 83 | 83 | 82 | 86 | 0.140 | 0.140 | 0.140 | 0.140 | 0.540 | 0.540 | 0.540 | 0.540 | 0.540 | 0.140 | 0.140 | 0.140 |
| Forested Wetland | 46 | 67 | 77 | 83 | 0.790 | 0.790 | 0.790 | 0.790 | 1.300 | 1.300 | 1.300 | 1.300 | 1.300 | 0.790 | 0.790 | 0.790 |
| Sparse Forest (10<50%) | 31 | 56 | 70 | 77 | 0.710 | 0.710 | 0.710 | 0.710 | 1.180 | 1.180 | 1.180 | 1.180 | 1.180 | 0.710 | 0.710 | 0.710 |
| Forest (>50%) | 36 | 57 | 70 | 77 | 0.850 | 0.850 | 0.850 | 0.850 | 1.220 | 1.220 | 1.220 | 1.220 | 1.220 | 0.850 | 0.850 | 0.850 |
| Shrubland | 78 | 87 | 91 | 94 | 0.680 | 0.680 | 0.680 | 0.680 | 0.980 | 0.980 | 0.980 | 0.980 | 0.980 | 0.680 | 0.680 | 0.680 |
| Barren | 68 | 79 | 85 | 89 | 0.510 | 0.510 | 0.510 | 0.510 | 0.510 | 0.510 | 0.510 | 0.510 | 0.510 | 0.510 | 0.510 | 0.510 |
| Agriculture | 33 | 59 | 72 | 79 | 0.450 | 0.450 | 0.450 | 0.450 | 0.440 | 0.880 | 1.680 | 1.820 | 1.730 | 0.450 | 0.450 | 0.450 |
| Orchard | 60 | 75 | 82 | 86 | 0.620 | 0.620 | 0.620 | 0.620 | 0.930 | 1.230 | 1.230 | 1.360 | 1.360 | 1.050 | 0.620 | 0.620 |
| Feedlot | 98 | 98 | 98 | 98 | 0.010 | 0.010 | 0.010 | 0.010 | 0.010 | 0.010 | 0.010 | 0.010 | 0.010 | 0.010 | 0.010 | 0.010 |

*Table 32: Biophysical Table Values for InVEST Parameterization for Seasonal Water Yield when the condition is barren and the Forest loss is 24.5%. Curve Numbers A-D refer to soil types and Kc 1-12 refers to the monthly cover factors for each site.*

| Land Use | Curve Number A | Curve Number B | Curve Number C | Curve Number D | $K_c$_1 | $K_c$_2 | $K_c$_3 | $K_c$_4 | $K_c$_5 | $K_c$_6 | $K_c$_7 | $K_c$_8 | $K_c$_9 | $K_c$_10 | $K_c$_11 | $K_c$_12 |
|---|---|---|---|---|---|---|---|---|---|---|---|---|---|---|---|---|
| Null | 98 | 98 | 98 | 98 | 0.760 | 0.760 | 0.760 | 0.760 | 0.670 | 0.670 | 0.670 | 0.670 | 0.670 | 0.840 | 0.760 | 0.760 |
| Urban | 58 | 73 | 83 | 87 | 0.820 | 0.820 | 0.820 | 0.820 | 0.730 | 0.730 | 0.730 | 0.730 | 0.730 | 0.900 | 0.820 | 0.820 |
| Rural | 98 | 98 | 98 | 98 | 1.170 | 1.170 | 1.170 | 1.170 | 1.080 | 1.080 | 1.080 | 1.080 | 1.080 | 1.250 | 1.170 | 1.170 |
| Water | 98 | 98 | 98 | 98 | 0.050 | 0.050 | 0.050 | 0.050 | 0.360 | 0.360 | 0.360 | 0.360 | 0.360 | 0.140 | 0.050 | 0.050 |
| Wetland | 94 | 90 | 88 | 91 | 0.710 | 0.710 | 0.710 | 0.710 | 1.120 | 1.120 | 1.120 | 1.120 | 1.120 | 0.790 | 0.710 | 0.710 |
| Forested Wetland | 57 | 74 | 83 | 88 | 0.620 | 0.620 | 0.620 | 0.620 | 1.000 | 1.000 | 1.000 | 1.000 | 1.000 | 0.710 | 0.620 | 0.620 |
| Sparse Forest (10<50%) | 42 | 63 | 76 | 82 | 0.760 | 0.760 | 0.760 | 0.760 | 1.040 | 1.040 | 1.040 | 1.040 | 1.040 | 0.850 | 0.760 | 0.760 |
| Forest (>50%) | 47 | 64 | 76 | 82 | 0.600 | 0.600 | 0.600 | 0.600 | 0.800 | 0.800 | 0.800 | 0.800 | 0.800 | 0.680 | 0.600 | 0.600 |
| Shrubland | 89 | 94 | 97 | 98 | 0.420 | 0.420 | 0.420 | 0.420 | 0.330 | 0.330 | 0.330 | 0.330 | 0.330 | 0.500 | 0.420 | 0.420 |
| Barren | 79 | 86 | 91 | 94 | 0.360 | 0.360 | 0.360 | 0.360 | 0.270 | 0.710 | 1.500 | 1.640 | 1.550 | 0.440 | 0.360 | 0.360 |
| Agriculture | 44 | 66 | 78 | 84 | 0.530 | 0.530 | 0.530 | 0.530 | 0.750 | 1.050 | 1.050 | 1.180 | 1.180 | 1.050 | 0.530 | 0.530 |
| Orchard | 71 | 82 | 88 | 91 | 0.720 | 0.720 | 0.720 | 0.720 | 0.630 | 0.630 | 0.630 | 0.630 | 0.630 | 0.800 | 0.720 | 0.720 |
| Feedlot | 98 | 98 | 98 | 98 | 0.760 | 0.760 | 0.760 | 0.760 | 0.670 | 0.670 | 0.670 | 0.670 | 0.670 | 0.840 | 0.760 | 0.760 |

*Table 33: Biophysical Table Values for InVEST Parameterization for Seasonal Water Yield when the condition is barren and the Forest loss is 4.9%. Curve Numbers A-D refer to soil types and Kc 1-12 refers to the monthly cover factors for each site.*

| Land Use | Curve Number A | Curve Number B | Curve Number C | Curve Number D | $K_c$_1 | $K_c$_2 | $K_c$_3 | $K_c$_4 | $K_c$_5 | $K_c$_6 | $K_c$_7 | $K_c$_8 | $K_c$_9 | $K_c$_10 | $K_c$_11 | $K_c$_12 |
|---|---|---|---|---|---|---|---|---|---|---|---|---|---|---|---|---|
| Null | 98 | 98 | 98 | 98 | 0.830 | 0.830 | 0.830 | 0.830 | 0.810 | 0.810 | 0.810 | 0.810 | 0.810 | 0.840 | 0.830 | 0.830 |
| Urban | 49 | 67 | 79 | 83 | 0.890 | 0.890 | 0.890 | 0.890 | 0.870 | 0.870 | 0.870 | 0.870 | 0.870 | 0.900 | 0.890 | 0.890 |
| Rural | 98 | 98 | 98 | 98 | 1.240 | 1.240 | 1.240 | 1.240 | 1.220 | 1.220 | 1.220 | 1.220 | 1.220 | 1.250 | 1.240 | 1.240 |
| Water | 98 | 98 | 98 | 98 | 0.120 | 0.120 | 0.120 | 0.120 | 0.500 | 0.500 | 0.500 | 0.500 | 0.500 | 0.140 | 0.120 | 0.120 |
| Wetland | 85 | 84 | 84 | 87 | 0.780 | 0.780 | 0.780 | 0.780 | 1.270 | 1.270 | 1.270 | 1.270 | 1.270 | 0.790 | 0.780 | 0.780 |
| Forested Wetland | 48 | 68 | 79 | 84 | 0.690 | 0.690 | 0.690 | 0.690 | 1.140 | 1.140 | 1.140 | 1.140 | 1.140 | 0.710 | 0.690 | 0.690 |
| Sparse Forest (10<50%) | 33 | 57 | 72 | 78 | 0.830 | 0.830 | 0.830 | 0.830 | 1.190 | 1.190 | 1.190 | 1.190 | 1.190 | 0.850 | 0.830 | 0.830 |
| Forest (>50%) | 38 | 58 | 72 | 78 | 0.660 | 0.660 | 0.660 | 0.660 | 0.940 | 0.940 | 0.940 | 0.940 | 0.940 | 0.680 | 0.660 | 0.660 |
| Shrubland | 80 | 88 | 93 | 95 | 0.490 | 0.490 | 0.490 | 0.490 | 0.470 | 0.470 | 0.470 | 0.470 | 0.470 | 0.500 | 0.490 | 0.490 |
| Barren | 70 | 80 | 87 | 90 | 0.430 | 0.430 | 0.430 | 0.430 | 0.410 | 0.850 | 1.640 | 1.780 | 1.690 | 0.440 | 0.430 | 0.430 |
| Agriculture | 35 | 60 | 74 | 80 | 0.600 | 0.600 | 0.600 | 0.600 | 0.890 | 1.200 | 1.200 | 1.320 | 1.320 | 1.050 | 0.600 | 0.600 |
| Orchard | 62 | 76 | 84 | 87 | 0.790 | 0.790 | 0.790 | 0.790 | 0.770 | 0.770 | 0.770 | 0.770 | 0.770 | 0.800 | 0.790 | 0.790 |
| Feedlot | 98 | 98 | 98 | 98 | 0.830 | 0.830 | 0.830 | 0.830 | 0.810 | 0.810 | 0.810 | 0.810 | 0.810 | 0.840 | 0.830 | 0.830 |

*Table 34: Biophysical Table Values for InVEST Parameterization for Seasonal Water Yield when the condition is shrubby and the Forest loss is 2.6%. Curve Numbers A-D refer to soil types and Kc 1-12 refers to the monthly cover factors for each site.*

| Land Use | Curve Number A | Curve Number B | Curve Number C | Curve Number D | $K_c$_1 | $K_c$_2 | $K_c$_3 | $K_c$_4 | $K_c$_5 | $K_c$_6 | $K_c$_7 | $K_c$_8 | $K_c$_9 | $K_c$_10 | $K_c$_11 | $K_c$_12 |
|---|---|---|---|---|---|---|---|---|---|---|---|---|---|---|---|---|
| **Null** | 98 | 98 | 98 | 98 | 0.840 | 0.840 | 0.840 | 0.840 | 0.830 | 0.830 | 0.830 | 0.830 | 0.830 | 0.840 | 0.840 | 0.840 |
| **Urban** | 48 | 66 | 78 | 83 | 0.900 | 0.900 | 0.900 | 0.900 | 0.890 | 0.890 | 0.890 | 0.890 | 0.890 | 0.900 | 0.900 | 0.900 |
| **Rural** | 98 | 98 | 98 | 98 | 1.250 | 1.250 | 1.250 | 1.250 | 1.240 | 1.240 | 1.240 | 1.240 | 1.240 | 1.250 | 1.250 | 1.250 |
| **Water** | 98 | 98 | 98 | 98 | 0.130 | 0.130 | 0.130 | 0.130 | 0.520 | 0.520 | 0.520 | 0.520 | 0.520 | 0.140 | 0.130 | 0.130 |
| **Wetland** | 84 | 83 | 83 | 87 | 0.780 | 0.780 | 0.780 | 0.780 | 1.280 | 1.280 | 1.280 | 1.280 | 1.280 | 0.790 | 0.780 | 0.780 |
| **Forested Wetland** | 47 | 67 | 78 | 84 | 0.700 | 0.700 | 0.700 | 0.700 | 1.160 | 1.160 | 1.160 | 1.160 | 1.160 | 0.710 | 0.700 | 0.700 |
| **Sparse Forest (10<50%)** | 32 | 56 | 71 | 78 | 0.840 | 0.840 | 0.840 | 0.840 | 1.200 | 1.200 | 1.200 | 1.200 | 1.200 | 0.850 | 0.840 | 0.840 |
| **Forest (>50%)** | 37 | 57 | 71 | 78 | 0.670 | 0.670 | 0.670 | 0.670 | 0.960 | 0.960 | 0.960 | 0.960 | 0.960 | 0.680 | 0.670 | 0.670 |
| **Shrubland** | 79 | 87 | 92 | 95 | 0.500 | 0.500 | 0.500 | 0.500 | 0.490 | 0.490 | 0.490 | 0.490 | 0.490 | 0.500 | 0.500 | 0.500 |
| **Barren** | 69 | 79 | 86 | 90 | 0.440 | 0.440 | 0.440 | 0.440 | 0.430 | 0.870 | 1.660 | 1.800 | 1.710 | 0.440 | 0.440 | 0.440 |
| **Agriculture** | 34 | 59 | 73 | 80 | 0.610 | 0.610 | 0.610 | 0.610 | 0.910 | 1.210 | 1.210 | 1.340 | 1.340 | 1.050 | 0.610 | 0.610 |
| **Orchard** | 61 | 75 | 83 | 87 | 0.800 | 0.800 | 0.800 | 0.800 | 0.790 | 0.790 | 0.790 | 0.790 | 0.790 | 0.800 | 0.800 | 0.800 |
| **Feedlot** | 98 | 98 | 98 | 98 | 0.840 | 0.840 | 0.840 | 0.840 | 0.830 | 0.830 | 0.830 | 0.830 | 0.830 | 0.840 | 0.840 | 0.840 |

*Table 35: Biophysical Table Values for InVEST Parameterization for Seasonal Water Yield when the condition is barren and the Forest loss is 0.75%. Curve Numbers A-D refer to soil types and Kc 1-12 refers to the monthly cover factors for each site.*

| Land Use | Curve Number A | Curve Number B | Curve Number C | Curve Number D | $K_c$_1 | $K_c$_2 | $K_c$_3 | $K_c$_4 | $K_c$_5 | $K_c$_6 | $K_c$_7 | $K_c$_8 | $K_c$_9 | $K_c$_10 | $K_c$_11 | $K_c$_12 |
|---|---|---|---|---|---|---|---|---|---|---|---|---|---|---|---|---|
| **Null** | 98 | 98 | 98 | 98 | 0.840 | 0.840 | 0.840 | 0.840 | 0.840 | 0.840 | 0.840 | 0.840 | 0.840 | 0.840 | 0.840 | 0.840 |
| **Urban** | 47 | 66 | 78 | 83 | 0.900 | 0.900 | 0.900 | 0.900 | 0.900 | 0.900 | 0.900 | 0.900 | 0.900 | 0.900 | 0.900 | 0.900 |
| **Rural** | 98 | 98 | 98 | 98 | 1.250 | 1.250 | 1.250 | 1.250 | 1.250 | 1.250 | 1.250 | 1.250 | 1.250 | 1.250 | 1.250 | 1.250 |
| **Water** | 98 | 98 | 98 | 98 | 0.140 | 0.140 | 0.140 | 0.140 | 0.530 | 0.530 | 0.530 | 0.530 | 0.530 | 0.140 | 0.140 | 0.140 |
| **Wetland** | 83 | 83 | 83 | 87 | 0.790 | 0.790 | 0.790 | 0.790 | 1.300 | 1.300 | 1.300 | 1.300 | 1.300 | 0.790 | 0.790 | 0.790 |
| **Forested Wetland** | 46 | 67 | 78 | 84 | 0.710 | 0.710 | 0.710 | 0.710 | 1.170 | 1.170 | 1.170 | 1.170 | 1.170 | 0.710 | 0.710 | 0.710 |
| **Sparse Forest (10<50%)** | 31 | 56 | 71 | 78 | 0.850 | 0.850 | 0.850 | 0.850 | 1.220 | 1.220 | 1.220 | 1.220 | 1.220 | 0.850 | 0.850 | 0.850 |
| **Forest (>50%)** | 36 | 57 | 71 | 78 | 0.680 | 0.680 | 0.680 | 0.680 | 0.970 | 0.970 | 0.970 | 0.970 | 0.970 | 0.680 | 0.680 | 0.680 |
| **Shrubland** | 78 | 87 | 92 | 95 | 0.500 | 0.500 | 0.500 | 0.500 | 0.500 | 0.500 | 0.500 | 0.500 | 0.500 | 0.500 | 0.500 | 0.500 |
| **Barren** | 68 | 79 | 86 | 90 | 0.440 | 0.440 | 0.440 | 0.440 | 0.440 | 0.880 | 1.670 | 1.810 | 1.720 | 0.440 | 0.440 | 0.440 |
| **Agriculture** | 33 | 59 | 73 | 80 | 0.620 | 0.620 | 0.620 | 0.620 | 0.920 | 1.230 | 1.230 | 1.350 | 1.350 | 1.050 | 0.620 | 0.620 |
| **Orchard** | 60 | 75 | 83 | 87 | 0.800 | 0.800 | 0.800 | 0.800 | 0.800 | 0.800 | 0.800 | 0.800 | 0.800 | 0.800 | 0.800 | 0.800 |
| **Feedlot** | 98 | 98 | 98 | 98 | 0.840 | 0.840 | 0.840 | 0.840 | 0.840 | 0.840 | 0.840 | 0.840 | 0.840 | 0.840 | 0.840 | 0.840 |

## Appendix 4: Model Repository

A repository of the model structures described in the above dissertation is available at (https://github.com/EWLyttek/EAB_MODEL_ARCHIVE) as an archive for further detail, transparency and replicability.